Motor-driven transport of RNA cargoes in *Drosophila melanogaster*

Georgia Vendra

PhD Thesis
The University of Edinburgh
2006

EX LIBRIS UNIV. EDINBURGH

I hereby declare that this thesis is my own work, unless otherwise stated. The experiments were performed in the Wellcome Trust Centre for Cell Biology, University of Edinburgh.

Georgia Vendra

Acknowledgements

This work was performed in the Wellcome Trust Centre for Cell Biology, under the supervision of Ilan Davis. I would like to thank Ilan for all his enthusiastic support, encouragement and help during the last four years.

I am indebted to Ilan and members of the Davis and Finnegan labs for scientific advice, fruitful discussions and technical help, for their comments on parts of the thesis and for making the lab such a stimulating, homely and fun place to work in. Special thanks to Ale for endless scientific (and not only) discussions, encouragement and for her friendship, Carine for a lot of advice and support, for help with genetics and her jokes, Vero and Renald for invaluable help and suggestions and Russell for help with computers and statistics.

I would like to thank Dimitris for help with statistics and Illustrator and Ale, Sebastian, Jan and Kostas for helping me submit this thesis on time.

I am indebted to the State Scholarship Foundation of Greece and the Wellcome Trust for funding.

Finally, I would like to thank my parents for keeping our family together, under very difficult circumstances since I left Greece and all my friends in Edinburgh for their love, patience and cooking during difficult times.

ABBREVIATIONS

AAA	ATPases Associated with diverse cellular Activities
Arp	actin related protein
bcd	*bicoid*
BicD	Bicaudal D
bp	base pair
BLE	Bicoid localisation element
cAMP	cyclic AMP
cDNA	complementary deoxyribonucleic acid
CNS	Central Nervous System
DAPI	4, 6-diamidino-2-phenylindole
Dcp	Death caspase
DGC	Drosophila Gene Collection
DIC	Diffraction interference contrast
DIG	Digoxygenin
Dhc	Dynein heavy chain
Dic	Dynein intermediate chain
Dlc	Dynein light chain
DNA	Deoxyribonucleic acid
ds	double stranded
Dpp	*decapendaplegic*
EDTA	Ethylenediaminetetraacetic acid
Egl	Egalitarian
EJC	Exon-exon junction complex
EMS	ethyl methane sulphate
Exu	Exuperantia
Flp	Flipase
FRT	Flipase-recognition target sequence
fs	female sterile
ftz	*fushi tarazu*
GFP	Green fluorescent protein
GLS	*gurken* localisation signal
grk	*gurken*
GUK-h	*GUK-holder*
hnRNP	heterogeneous nuclear ribonucleoprotein
hb	*hunchback*
HRP	Horse radish peroxidase
Hsp	heat shock protein
ILS	*I* factor localisation signal
Kb	kilobase(s)
KDa	kilo Daltons
khc	Kinesin heavy chain
klc	Kinesin light chain
LSD2	lipid storage droplet-2

LTR	Long Terminal Repeats
MBP	Myelin Basic Protein
mRNA	messenger ribonucleic acid
MT	Microtubule
MTOC	Microtubule organising centre
mm	millimetre
mM	milliMol
mm	micrometre
ml	millilitre
ml	microlitre
NGS	normal goat serum
nls	nuclear localisation signal
osk	*oskar*
PBS	phosphate buffered saline
PBT	PBS/0.1% Tween 20
PBTrx	PBS/0.3% Triton-X 100
PCR	Polymerase chain reaction
PDZ	PSD-95 (postsynaptic density protein)-Dlg (Disks large) ZO1 (zonula occludens 1)
PI-3	phosphatidyl inositol 3
PKA	Protein kinase A
RNA	Ribonucleic acid
RNAi	RNA interference
RNAse	Ribonuclease
RNP	Ribonucleoprotein
rpm	Revolutions per minute
SCF	Skp1/Cul1/F-box protein
slmb	supernumerary limbs
SOE-PCR	single overlapping extension PCR
TSA	tyramide signal amplification
TGF-α	Transforming-growth factor alpha
Tris	Tris(hydroxymethyl)-amino-methane
Triton-X 100	Octylphenoxypolyethoxyethanol
Tween 20	Polyoxyethylene sorbitan monolaurate
wg	*wingless*
3'UTR	3' untranslated region
5'UTR	5' untranslated region

FIGURES AND TABLES **following page**

Figure 1.1: Examples of localising RNAs 2

Figure 1.2: Patterning of the *Drosophila* oocyte 6

Figure 1.3: Establishment of the body plan of Drosophila larva and distribution of key transcripts during this process

Figure 1.4: Cargo transporting motors 21

Figure 1.5: Trans-acting factors recognise the cis-acting signals and link the RNA to the motor machinery

Figure 3.1.1: The coordination complex 37

Figure 3.1.2: Dynein and its accessory complex, dynactin 39

Figure 3.2.1: Bidirectional RNA motility in *Drosophila* embryos 42

Figure 3.2.2: The DFS technique for selecting homozygous germ-line clones 50

Figure 3.2.3: Khc^{27} mutant oocytes and embryos

Figure 3.2.4: $KLP64D^{k1}$ and $KLP64D^{n123}$ egg chambers

Figure 3.2.5: Wild type localisation of endogenous and injected *ftz* RNA in *KLP64D* embryos

Figure 3.2.6: Bidirectional RNA motility in Khc^{27} and $KLP64D^{k1}$ mutant embryos

Figure 3.2.7: *ftz* RNA does not recruit Kinesin I

Figure 3.2.8: *ftz* RNA particle runs in wild type embryos 58

Figure 3.2.9: *ftz* RNA particle runs in $Glued^{1}$ embryos

Figure 3.2.10: Glued suppresses bidirectional RNA motility

Figure 3.2.11: Wild type localisation of endogenous and injected *ftz* RNA in *Klar* mutant embryos 65

Figure 3.3.1: Dynactin could suppress dynein's backward slippage by various means 72

Figure 4.1.1: *GLS* and *ILS* share a similar predicted secondary structure 76

Figure 4.1.2: An outline of the bioinformatics approach 78

Figure 4.1.3: A detailed description of the bioinformatics tool 79

Figure 4.2.1: Apical localisation of *slmb/CG3412/LD08669* in blastoderm embryos 86

Figure 4.2.2: Apical localisation of *CG1962/LD41224* in *Drosophila* embryos

Figure 4.2.3: Apical targeting of *CG1841/HL07962* in blastoderm embryos 91

Figure 4.2.3: Apical accumulation of *CG5876/LD08295* in blastoderm embryos 95

Figure 4.2.5: Localisation of *CG11448/GH23835* in blastoderm embryos

Table 4.2.1: A list of the tested bioinformatics candidates and random transcripts 99

Table 4.2.2: Localisation success of random transcripts and RNAdistance or RNAMotif candidates

Figure 4.2.6: Apical targeting of *G2* retrotransposon in blastoderm embryos 104

Figure 4.2.7: Novel patterns of transport and localisation 105

Figure 4.2.8: Asymmetric distribution of GUK-h RNA during oogenesis 107

Figure 5.2.1: Morphology and microtubule organisation of S2 cells spread on ConA 121

Figure 5.2.2: RNA distribution of S2 cells spread on ConA

Figure 5.2.3: Morphology and microtubule organisation of Kc cells treated with HE 124

Figure 5.2.4: Morphology and microtubule organisation of Clone 8 cells 126

Figure 5.2.5: Distribution of *wingless* RNA in Clone 8 cells

Figure 5.2.6: Morphology and microtubule organisation of SR+ cells 130

Figure 5.2.7: Morphology and microtubule organisation of MBN2 and UC88 cells

Figure 5.2.8: Morphology and microtubule organisation of BG2-C2 and BG2 cells

Figure 5.2.9: Morphology and microtubule organisation of BG2 cells

TABLE OF CONTENTS

Introduction **1**

Introduction to RNA localisation *2*

Key examples of RNA localisation during early Drosophila patterning *4*

Functions of RNA localisation *9*

Mechanisms of RNA localisation *11*

Active transport of RNA by molecular motors along cytoskeletal tracks *12*

Components of transport machinery-key players/determinants of localisation .....

Molecular motors *14*

Cis-acting elements *17*

Trans-acting factors *18*

Aims *24*

Materials and Methods **25**

Solutions and reagents *26*

Purification of Plasmid DNA *26*

DNA precipitation *26*

RNA in vitro transcription and labelling *26*

Synthesis of fluorescently labelled RNAs *27*

Synthesis of Biotin labelled RNAs *27*

Synthesis of Dig labelled RNAs *27*

RNA precipitation *28*

RNA precipitation *28*

Preparation and microinjection of Drosophila embryos *28*

Dissection and fixation of Drosophila ovaries for staining procedures *29*

RNA in situ hybridisation of Drosophila ovaries *29*

RNA in situ hybridisation in Drosophila embryos *30*

Immunofluorescence on Drosophila ovaries *30*

3-D microscopy and data analysis 30
GST-dynamitin bacterial expression and purification 31
Expression and purification of $(His)_6$ tagged dynamitin 32
Flystock and crosses 32
Particle tracking and analysis 33

Investigating the role of motors and their cofactors in bidirectional RNA motility in *Drosophila* embryos **34**

Introduction 35

Bidirectional transport 35
Dynactin as a processivity factor for dynein 39
Aims-Introduction to the experimental assay used in this chapter 41

Results 42

ftz RNA particles move bidirectionally along MTs 42
Significance of RNA backward motility in Drosophila embryos 44
Physical properties of plus end directed runs suggest that the RNA is driven towards the plus ends by molecular motors 45

Plus end motility is not mediated by Kinesin-1 46
Plus end motility is not mediated by Kinesin-2 49
Interference with dynactin's activity increases the frequency of plus runs and decreases the velocity and the average length of minus ends runs 57
Studying the potential role of Lissencephaly-1 in plus motility in Drosophila embryos 62
The regulators of bidirectional motility Klarschict and Halo are not involved in RNA motility 64

Discussion 67

Identification of novel localising transcripts during *Drosophila* oogenesis and embryogenesis: Experimental validation of novel bioinformatics approaches for the identification genes containing RNA localisation signals **75**

Introduction 76

Gurken and the I factor transcripts share a consensus localisation signal 76
Genome-wide searches for RNA localisation motifs similar to GLS and ILS 78
Aims 81

Results 83

Experimental assay 83
Pilot screen-Determination of the localisation potential of transripts that contain RNAdistance hits and are known to localise during embryogenesis 85
Assessing the localisation potential of transcripts containing putative localisation signals predicted by RNAdistance 89
Assesing the localisation potentials of transcripts containing putative localisation signals predicted by RNAMotif 93
slmb/CG3412, CG1962, CG1841, CG15095, CG11448 and CG5876 are homogenouesly distributed in oocytes 98
Testing the localisation potential of a random pool of transcripts 98
Assessing the localisation potential of transposable elements that contain bioinformatics hits 104
Some transcripts accumulate basally upon injection into blastoderm embryos 105
Some non-localising transcripts form particles and move directionally 105
Endogenous CG31043 is asymmetrically distributed in oocytes 107

Discussion 109

Development of an RNA localisation assay in cultured *Drosophila* cells with a view to perform genome-wide screens for factors required for RNA localisation **115**

Introduction 116

Trans-acting factors involved in RNA localisation 116
Aims 118

Results 120

Morphology and microtubule organisation in S2 cells 120
RNA distribution in S2 cells 121
Morphology and microtubule organisation in Kc cells 124
Morphology, microtubule organisation and RNA distribution of Clone 8 cells 126
Morphology and microtubule organisation of SR+, BG2, BG2-C2, MBN1 and UC88 cells 129

Discussion 135

Discussion and future perspectives **138**

References **145**

ABSTRACT

RNA localisation is a post-transcriptional mode of regulation of gene expression, acting in a diverse range of organisms and in most cell types, to target proteins to their site of function. The restriction of RNAs in specific regions of the cytoplasm is often mediated by motor-driven transport along cytoskeletal filaments. The cytoplasmic destination of transcripts is thought to be determined by the cis-acting sequences that usually lie in its 3'UTR and act as zipcodes, by the trans-acting factors that interpret the localisation signals and by the type of motors that are engaged to transport the RNP (Ribonucleoprotein) particles. The molecular motors Dynein and Kinesin transport their RNA cargoes over long distances towards the minus or plus ends of microtubule tracks respectively, whereas myosin mediates short-distance transport along actin microfilaments.

Although many cargoes undergo net displacement and achieve asymmetric subcellular distribution over time, their motion is not always highly unidirectional and is often interrupted by pauses and switches in direction. In Chapter 3 of this thesis, we investigate in detail the role of motors and their cofactors in bidirectional RNA motility in *Drosophila* embryos. We show that Kinesin-1 and Kinesin-2 are not involved in the reverse motion of dynein-driven RNA cargoes and we suggest that dynein moves bidirectionally in vivo. Furthermore, we demonstrate that dynactin, dynein's accessory factor, is required to reduce backwards motility. We suggest that dynactin mediates suppression of reversals by stabilising dynein on the microtubule or by assembling and coordinating multiple dyneins together.

In Chapter 4, we explore novel genome-wide bioinformatics approaches for the identification of localisation signals and localising transcripts in *Drosophila* embryos and oocytes and we show that the method successfully predicts localisation signals in transposable elements and in the 3'UTR of endogenous *Drosophila* genes.

Finally, in Chapter 5, we address the suitability of various *Drosophila* cell lines for the establishment of an RNA localisation assay, with the aim of using the assay for a genome-wide RNAi screen for novel RNA localisation factors.

CHAPTER 1

INTRODUCTION

1.1 INTRODUCTION TO RNA LOCALISATION

RNA localisation is a universal post-transcriptional mode of regulation of gene expression and acts in most cell types, to target proteins to their site of function and establish or maintain polarity. RNA sorting plays a key role in diverse cellular functions, such as cell motility, myelination of nerve cells' axons, synaptic activity of neurons and transposition of retrotransposons and is also fundamental for developmental processes, as it is involved in oogenesis, axis specification, body plan formation and cell fate determination.

Although RNA localisation is best understood in oocytes and early embryos of *Drosophila melanogaster* and in yeast, there are numerous reported examples (some shown in Figure 1.1) of localising transcripts in many other systems. RNA is asymmetrically distributed in protozoa (Han *et al*, 1997, Suh *et al*, 2002), mollusc embryos (Lambert and Nagy, 2002), *Drosophila* neuroblasts (Li *et al*, 1997, Broadus *et al*, 1998), *Drosophila* epithelials (Matsuzaki *et al*, 1998) and embryos of various diptera (Bullock *et al*, 2004). Various transcripts are segregated in distinct regions of chicken fibroblasts (Kislauskis *et al*, 1994, Mingle *et al*, 2005), mouse oligodendrocytes (Trapp *et al*, 1987), mammalian hippocampal and sympathetic neurons (Tiedge *et al*, 1991, Chicurel *et al*, 1993, Cristofanilli *et al*, 2006) and frog oocytes (Mosquera *et al*, 1993, Zhang *et al*, 1998). Plants, also, transfer RNAs over long distances, through their vascular system (Okita and Choi, 2002 review and references therein, Haywood *et al*, 2005).

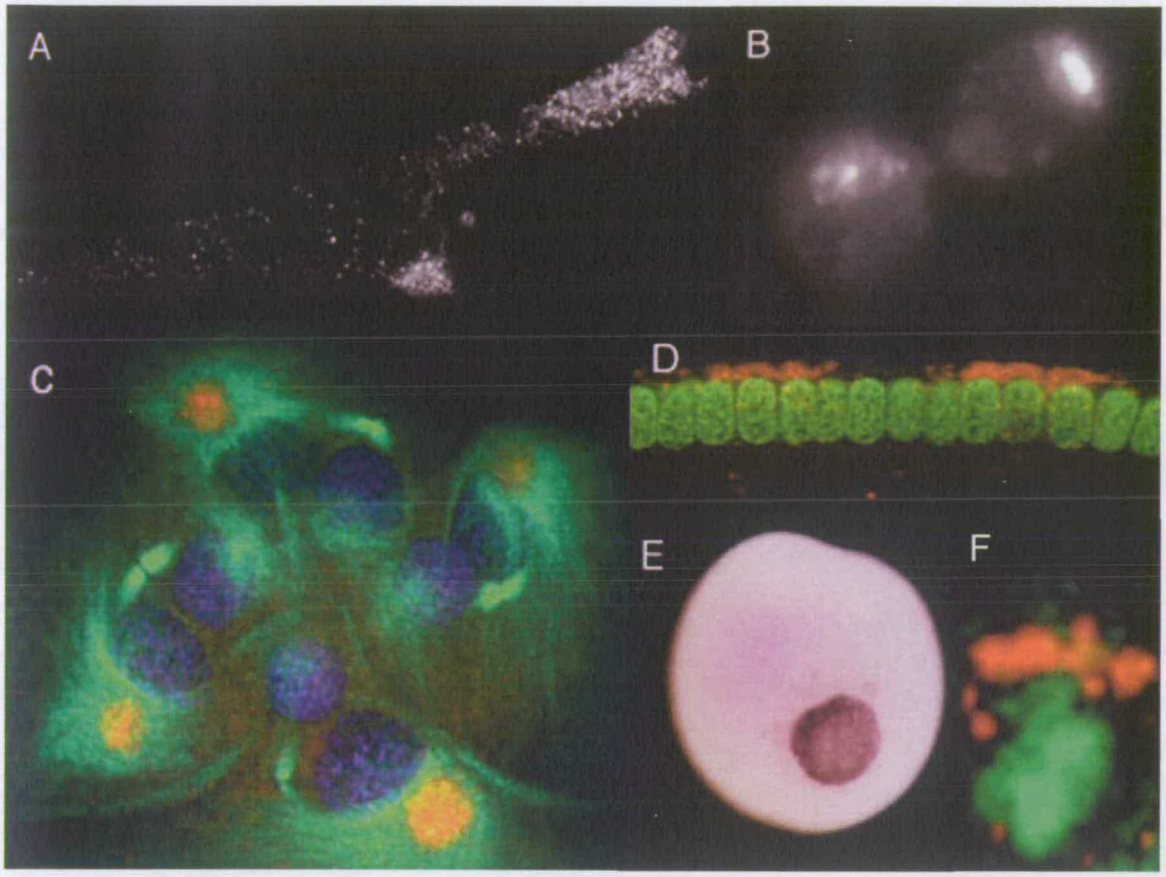


Figure 1.1: Examples of localising RNAs

A) *β-actin* mRNA localised at the protrusions of chicken fibroblasts (from Mingle *et al*, 2005). B) *ASH1* mRNA in the budding tip of *S. cerevisiae* (Long *et al*, 1997). C) *Dpp* mRNA localised near the centromere in 8-cell embryos of *Ilyanassa obsoleta*. RNA is shown in red, DNA in blue and MTs in green (Lambert and Nagy, 2002). D) apical localisation of *hairy* mRNA in *Megaselia abdita* syncytial embryos. RNA is shown in red and nuclei in green (Bullock *et al*, 2004). E) *Xlsirt* RNA localised at the vegetal cortex of *Xenopus* oocytes (from Kloc and Etkin, 1995). F) *prospero* mRNA localised at the apical side of *Drosophila* neuroblasts (from Schuldt *et al*, 1998).

1.2 KEY EXAMPLES OF RNA LOCALISATION DURING EARLY *DROSOPHILA* PATTERNING

The basic body plan of the *Drosophila* larva is set up very early, during oogenesis, when maternal genes establish the antero-posterior and dorso-ventral axis of the future organism (Figure 1.2) and provide a framework, upon which later metameric patterning is built (Figure 1.3). The *Drosophila* egg chamber consists of 16 germ cells, the oocyte and 15 nurse cells, all interconnected with cytoplasmic bridges, named ring canals and surrounded by a layer of somatic, epithelial cells, known as follicle cells. The nurse cells provide the oocyte with most of the material required for its growth and maturation. The follicle cells have a key role in patterning and also secrete the materials needed for the vitelline membrane and the eggshell of the mature egg.

During *Drosophila* oogenesis, various RNAs are distributed asymmetrically in the developing oocyte. The most extensively studied ones are the key axis determinants *gurken, bicoid* and *oskar*. *Grk* localises first at the posterior, as a crescent (Gonzalez-Reyes, 1995, Roth *et al*, 1995), to initiate the rearrangement of the microtubule cytoskeleton (Figure 1.2a). Grk protein induces its adjacent follicle cells to adopt posterior fate. These cells send a signal back to the oocyte that leads to the disassembly of the previoulsy posterior (Clark *et al*, 1994, Theurkauf *et al*, 1992) microtubule organising centre (MTOC) and the nucleation of MTs from its anterior margin (Clark *et al*, 1997). The reorganisation of the MTs by Grk is crucial for the localisation of the oocyte nucleus (Figure 1.2a) and key cytoplasmic components and the establishment of the antero-posterior axis. As oogenesis proceeds, *grk* localises as a cap around the nucleus (Figure 1.2c) at the dorso-anterior corner of the oocyte (Gonzalez-Reyes, 1995, Roth *et al*, 1995), where Grk protein now induces dorsal cell fates (Gonzalez-Reyes *et al*, 1995, Neuman-Silberberg *et al*, 1993) and eggshell structures and specifies the dorso-ventral axis (Figure 1.2c and 1.2d). First, together with the Decapendaplegic signal sent from anterior follicle cells, it defines the formation of the dorsal appendages (Peri and Roth, 2000). The Grk signal also

attracts the border cells dorsally (Duchek and Rorth, 2001), to form the micropyle, a dorsal chorion structure required for sperm entry. It finally represses the initiation of a ventralising signal cascade at the dorsal side (Sen *et al*, 1998), restricting it to the ventral half of the follicular epithelium, ensuring dorso-ventral asymmetry in the future egg.

Osk localises at the posterior of the oocyte (Ephrussi *et al*, 1991), to recruit *nanos* RNA and other pole plasm components (Figure 1.2b and 1.2d) and induce the formation of the abdomen and the germ cells. *Bcd* localises at the anterior cortex of the oocyte, where it defines anterior structures (Figure 1.2b). Bcd is translated later, upon egg activation and forms an anterior morphogen gradient (Berleth *et al*, 1988), which together with the Nanos gradient from the posterior, will regulate other maternal transcripts, such as *caudal* and *hunchback* (Barker *et al*, 1992, Murata and Wharton, 1995, Wharton and Struhl, 1991, Dubnau and Struhl, 1996) and initiate a cascade of zygotic activities that will finally divide the larval body into a series of segments and anatomical regions (Figure 1.3).

The first embryonic genes to be activated along the AP axis, each at a different threshold concentration of the maternal sources, are the gap genes. The gap genes are expressed in broad regions (Figure 1.3B) and code for transcription factors that switch on the expression of different pair rule genes in different groups of nuclei, according to their position along the embryo. Up to this stage, the embryo is still a syncytium, formed by 14 rounds of nuclear divisions that are not followed by cytoplasmic divisions. All its 6000 nuclei form a single layer around the periphery, underneath the membrane and share a common cytoplasm.

Pair rule genes, such as *fushi tarazu, hairy, runt* and *even-skipped* are expressed in seven narrow stripes. RNA localisation plays a fundamental role in the fidelity of this expression pattern. It restricts the RNA at the apical side of the embryo (Ingham *et al*, 1985), where cellularisation has begun (Figure 1.3C), and augments gene

activity by ensuring that the translated transcription factor will not diffuse laterally, towards neighbouring nuclei (Bullock *et al*, 2004).

The pair rule proteins delimit the parasegments, visible as grooves on the surface of the gastrulating embryo and activate the segment polarity genes, which are expressed in 14 narrow stripes. Segment polarity proteins further elaborate segmentation, by patterning the segments and defining the boundaries between segments and parasegments, before homeotic genes take action, to specify the unique identity of each segment and set up their future developmental pathway. Some segment polarity genes code for cell-cell signalling molecules. Although their membrane targeting generally involves protein trafficking, RNA localisation has also been implicated in the process. Wingless morphogen, for instance, is a secreted protein that regulates gene expression in adjacent cells. *Wingless* RNA is asymmetrically distributed, to target its protein product apically, to its site of secretion (Figure 1.3D). When the localisation of the RNA is inhibited, the intracellular and extracellular distribution of the protein is disturbed and its activity is reduced (Simmonds *et al*, 2001).

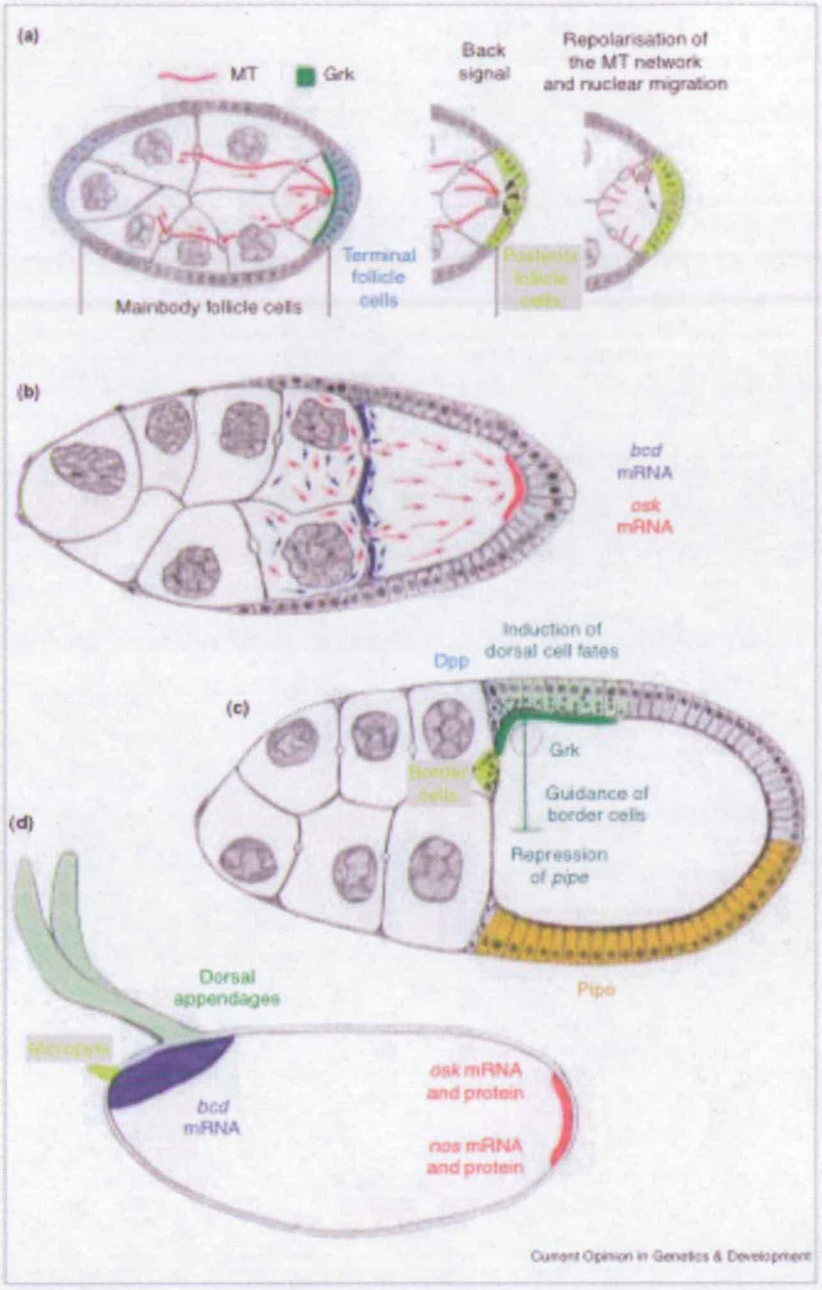


Figure 1.2: Patterning of the *Drosophila* oocyte

(a) repolarisation of the MT cytoskeleton by Grk signalling at the posterior of the oocyte, at stage 6-7 of oogenesis. (b) posterior localisation of *osk* and anterior localisation of *bcd*. (c) patterning of the egg by the second Grk signal. Grk induces dorsal cell fates and represses ventralising signals at the antero-dorsal corner of the oocyte. It also specifies eggshell structures. (d) localisation of anterior and posterior determinants in the egg. (Picture from Riechmann and Ephrussi, 2001).

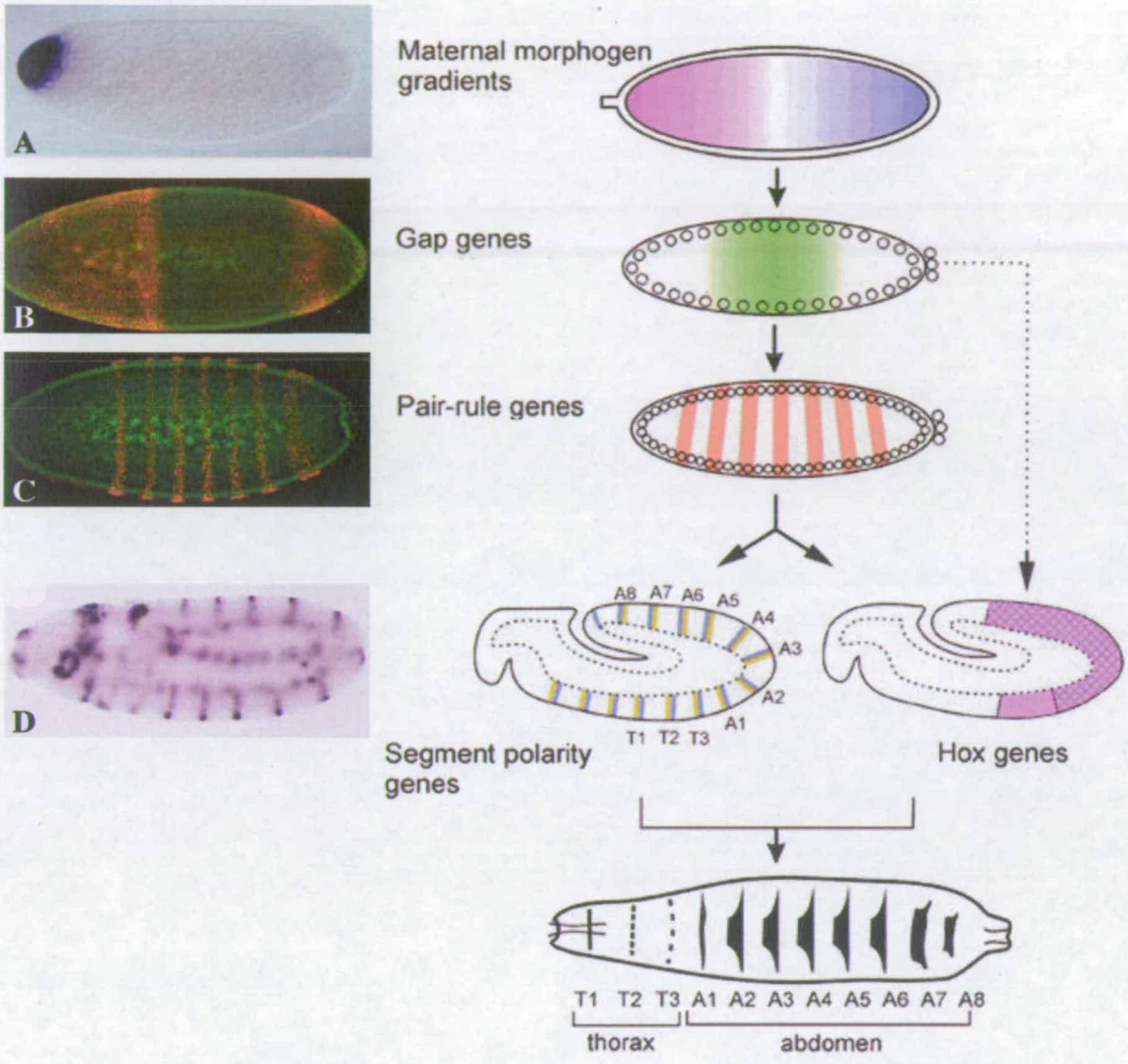


Figure 1.3: Establishment of the body plan of the *Drosophila* larva (cartoon from Benedicte Sanson, 2001) and distribution of key transcripts during this process.

A) *bcd* mRNA at the anterior of the embryo as a source of diffusible gradient (picture from Ephrussi and St Johnston, 2004). B) unlocalised *hunchback* mRNA in syncytial embryos (picture from Wilkie and Davis, 2001). C) Apically localised *runt* mRNA in syncytial embryos. RNA is shown in red, nuclei in green (picture from Wilkie and Davis, 2001). D) *wingless* mRNA localised at the apical side of epithelial cells (picture from Bullock *et al*, 2004).

1.3 FUNCTIONS OF RNA LOCALISATION

There are several proposed functions for localising mRNA molecules instead of the proteins they encode. For instance, the transport of the proteins themselves is not always feasible and protein localisation can be achieved only through the transport of the corresponding RNAs. Even in cases when protein transport is possible, RNA transport is generally preferable. Targeting an RNA molecule that can be translated multiple times and produce high levels of protein, requires less energy than localising many protein molecules (e.g accumulation of *β-actin* mRNA in the leading edge of a fibroblast, Kislauskis *et al*, 1994). Association of the RNA with components of the translation machinery is important, in this case, to ensure the efficiency of localised translation.

Localisation of a transcript can also regulate its translation, provided that the translation will get activated at the site of localisation. This has been suggested for *nanos* RNA (Bergsten and Gavis, 1999). Coupling RNA transport with translational repression and subsequent derepression of translation when the RNA reaches its final destination, ensure that no protein is expressed at the wrong location. This is probably the case for Myelin Basic Protein (MBP), a component of the myelin sheath of oligodendrocytes' axons. MBP interacts with membranes and causes them to compact. If it were transported from the cell body to the site of myelin formation, it would stick to any membrane found along its way. The cell overcomes this problem by accumulating *MBP* RNA at the cell processes and synthesising the protein locally (Carson *et al*, 1997).

Colocalisation of different RNAs might be involved in facilitating the cotranslational assembly of supermolecular structures, such as the formation of the basal body and flagella of *Naegleria gruberi* (Han *et al*, 1997). It has been suggested that coassembly of different mRNAs in the same RNP particle may be a mechanism of coordinated regulation of multiple functionally related genes in higher eukaryotes. The particles may represent posttranscriptional operons that substitute for the polycistronic mRNAs of prokaryotes (Keene and Tetenbaum, 2002). This hypothesis

is based on genome array data in mammals, which revealed that RNA binding proteins recognise and associate with unique subpopulations of messages (Keene and Tetenbaum, 2002).

Another function of RNA localisation is the production of a gradient of a morphogen, by diffusion of the protein translated from the localised RNA source. As mentioned above, *bicoid* mRNA localises at the anterior within the *Drosophila* oocyte and acts later, in early embryogenesis, as a source of diffusible protein that will spread from the anterior towards the centre of the embryo (Berleth *et al.* 1988).

Sorting of a transcript to a distinct region of a cell can segregate the protein product into only one of its daughter cells and determine their fate. *ASH1* mRNA in budding cells of *S.cerevisiae* localises in the daughter cell, where it is required for repression of the mating type switching, exclusively in this cell (Takizawa *et al*, 1997, Long *et al*, 1997). In the *Drosophila* embryonic CNS, neuroblasts undergo an asymmetric cell division, which gives rise to another neuroblast and a ganglion mother cell (GMC). *Prospero* mRNA and Prospero protein localise in the GMC and their localisation is a key event in this cell fate decision (Broadus *et al*, 1998).

Although research in the field initially focused on functional studies, recently there is an increasing interest and exciting progress in elucidating the mechanism of RNA localisation.

1.4 MECHANISMS OF mRNA LOCALISATION

RNA sorting can arise from selective stability of the transcript at the site of localisation. *hsp83* mRNA, for instance is distributed uniformly in early *Drosophila* embryos, but after cycle 10 it becomes restricted to the pole cells (Ding *et al*, 1993). This occurs by recruitment of a deadenylase complex (Semotok *et al*, 2005) and general degradation of RNA in all parts of the embryo except from the posterior pole, where *hsp83* is protected from degradation (Bashirullah *et al*, 1999). Degradation is also responsible for the gradient of maternal *hunchback* and *caudal* mRNAs in the embryo, but it is the instability of the transcripts at the poles and not their protection that creates the gradient (Wharton and Struhl, 1991, Dubnau and Struhl, 1996).

Vectorial nuclear export is another possible mechanism, but no examples have been found so far. General diffusion and local docking by already localised anchors has been described in *Drosophila* for *cyclin B* (Raff *et al*, 1990) and *nanos* mRNAs (Forrest and Gavis, 2002) and at least in some stages of oogenesis for *oskar* mRNA (Glotzer *et al*, 1997). In the case of *osk* and *nanos*, it has been shown that the RNA does not diffuse passively, but it rather circulates and reaches the posterior facilitated by the ooplasmic streaming.

It is also possible that at least some RNAs hitchhike on organelles, such as ribosomes or ER cysts and this might be the case for *Vg*1 RNA, which is thought to be transported on the rough ER (Deshler *et al*, 1997). Murine leukemia virus (MLV) RNAs have also been shown to be tethered onto lysosomes and endosomes (Basyuk *et al*, 2003).

1.4.1 Active transport of RNA by molecular motors along cytoskeletal tracks

Active transport along microtubule tracks, using dynein and/or kinesin motors and along actin microfilaments, using myosin V motors has been proposed for many RNAs. The actin network has been implicated in short distance travel, whereas the MTs in long distance travel. Active transport is difficult to prove and it is, in most of the cases, only the cytoskeleton involvement and not the motor dependence that has been reported conclusively. Motor mediated transport has been demonstrated in only a few cases.

ASH1 mRNA is transported along actin by She1/Myo4p, an unconventional class V myosin motor (Bobola *et al*, 1996, Munchow *et al*, 1999). *oskar* mRNA is transferred towards the plus ends of MTs, at the posterior pole of the *Drosophila* oocyte by Kinesin-1. Brendza *et al*, 2000 first demonstrated that in Kinesin heavy chain mutants, posterior localisation of *osk* is abolished. It was debatable, though, if this was a secondary effect of the disturbance of ooplasmic streaming in these mutants. It was recently shown that certain mutations that block streaming do not inhibit *osk* localisation (Serbus *et al*, 2005), suggesting a direct role for Kinesin-1 in its transport. Kinesin-1 is also involved in the movement of *MBP* mRNA along MTs in oligodendrocytes. It has been reported that injected RNA forms particles that move from the main cell body to the peripheral processes. The direction and speed of movement suggested motor dependent transport towards the plus ends of MTs. Indeed, the movement is abolished by drugs that disrupt microtubules and by antisense oligonucleotides against Kinesin-1 (Carson *et al*, 1997, Ainger *et al*, 1997).

There is strong evidence that *wingless* and pair rule mRNAs are transported by dynein. It has been demonstrated that injected transcripts are directed towards the minus ends of MTs and localise at the apical cytoplasm (Wilkie and Davis, 2001). Their movement requires intact microtubules, as injection of colcemid disrupts localisation. Moreover, apical transport is dynein/dynactin dependent. Injection of dynein antibodies inhibits localisation, whereas RNA moves with 70% reduced

speed in dynein mutants. Disruption of the dynactin complex, which is thought to regulate dynein's activity, also decreased the speed of transport, confirming the requirement for cytoplasmic dynein. It has been shown (MacDougall *et al*, 2003) that *gurken* mRNA also localises in a MT and dynein dependent manner. Injected RNA forms particles that move first to the anterior and then towards the dorso-anterior corner of the oocyte, above the nucleus, mimicking the localisation pattern of the endogenous transcript. Both steps of localisation are abolished by injection of colcemid and antibodies against Dynein heavy chain. The dynein transport complex is also required for the localisation of *inscuteable* mRNA in *Drosophila* neuroblasts (Hughes *et al*, 2004).

1.5 COMPONENTS OF TRANSPORT MACHINERY-KEY PLAYERS/ DETERMINANTS OF LOCALISATION

1.5.1 Molecular motors

Molecular motors are nanomachines that convert chemical energy to mechanical work and take nanometer steps along cytoskeletal elements. Movement results from force generation by conformational changes induced in the motor domain by ATP hydrolysis. Here I focus on cytoplasmic motors implicated in the intracellular transport of molecules, organelles and vesicles. Motors with other specialised functions, such as Kinesins or kinesin related proteins involved in chromosome and spindle motility or MT depolymerisation, axonemal dyneins for ciliary or flagellar beating and myosins responsible for actin retraction in muscles and other structures, are not introduced. Aspects of motor processivity, efficiency and directionality are also not mentioned here, as they are discussed in detail in Chapter 3.

1.5.1.1 Cytoplasmic dynein

Dynein is composed of multiple types of tightly associated subunits: two heavy chains (DHC), two intermediate chains (DIC), two light intermediate chains (DLIC) and several light chains (DLC), shown in Figure 1.4A. Dynein heavy chains contain a large motor domain, a coiled coil region that mediates dimerisation and provides binding sites for the smaller accessory subunits and a small globular tail for MT attachment (Vale, 2003). Conformational changes of the motor domain are transmitted to a stalk, which swings position and leads to a displacement of its tail along the microtubule (Schliwa and Woehlke, 2003).

The large size of the motor domain results mainly from the multiplicity of ATPase-like units (domains AAA1-6) that are arranged in an hexameric ring (Vallee *et al*, 2004), giving dynein an architecture fundamentally different from the design of other motors. AAA1 is the domain responsible for ATPase activity (Gibbons *et al*, 1987).

Nevertheless, all first four domains can bind ATP and the AAA ring must be intact for the motor to function properly (Vallee *et al*, 2003). Moreover, binding of ATP at the secondary sites compacts the ring comformation and enables dynein to "shift gears" and take smaller but more powerful steps (Mallik *et al*, 2004).

The intermediate chains can bind the heavy and light chains and act as scaffolds for the assembly of the whole complex. They also bind dynactin, dynein's accessory complex. The role of dynactin as a co-factor for dynein is discussed in Chapter 3. The light chains are involved in cargo recognition and specificity directly or indirectly, by binding to cargo partners-adaptors (Vale, 2003).

Dynein drives a huge repertoire of cargoes, from single RNA and protein molecules to membranes, organelles and nuclei, towards the minus ends of microtubules.

1.5.1.2 Kinesins

Kinesin motors move towards the plus ends of microtubule tracks. The major cargo transporters in the cell are members of the Kinesin-1, Kinesin-2 and Kinesin-3 families.

Kinesin-1, also known as Kinesin I or conventional Kinesin, (Figure 1.4B) was the first one to be identified and is composed of two heavy chains (KHC) and two light chains (KLC). KHCs consist of a NH2-terminal motor domain with the MT and ATP binding sites, a central coiled-coil domain that dimerises to form a stalk and a COOH-terminal globular tail. KLCs interact with the tail of KHCs and link them to the cargoes. Kinesin-1 mediates the transport of vehicles, mitochondria, lysosomes, ER cysts, pigment granules, intermediate filaments and mRNAs in diverse systems (Brendza *et al*, 2000, Hurd and Saxton, 1996, Kanai *et al*, 2004, Tanaka *et al*, 1998, Pilling *et al*, 2006, Kamal *et al*, 2004).

The Kinesin-2 (Figure 1.4C) family, also known as Kinesin II or KIF3 consists of

heterotrimeric complexes with two different motor subunits, responsible for force generation and a third polypeptide, known as kinesin associated protein or KAP, with homology to KLC, thought to interact with the cargo (Takeda, *et al*, 2000). Kinesin-2 has been demonstrated to drive a wide range of cargoes and mediate diverse transport processes. It is implicated in the transport of melanosomes in melanophores (Rogers *et al*, 1997), membranes between the ER and Golgi in the secretory pathway (Le Bot *et al*, 1998) and flagellar and ciliary components in *C. elegans* and urchins (Morris and Scholey, 1997, Shakir *et al*, 1993). It is also involved in the trafficking of vesicles in mice, *tau* mRNA in neurons and *Vg1* mRNA towards the vegetal cortex of frog oocytes (Betley *et al*, 2004). The *Drosophila* homolog transports choline acetyltransferase in axons (Ray *et al*, 1999) and its subunits are referred to as KLP64D, KLP68D and KAP3.

Kinesin-3, also known as Unc104/KIF1, (Figure 1.4D) acts as a homodimer (Tomishige *et al*, 2002) and is responsible for membrane transport in *Dictyostelium* (Pollock *et al*, 1999) and other lower eukaryotes, as well as the transport of synaptic vesicle precursors in *C. elegans* and mice neurons (Hall and Hedgecock, 1991). The *Drosophila* homolog is known as Kinesin-73 or Khc-73.

1.5.1.3 Myosin V

Myosin V is the class of myosin motors that have been implicated in cargo transport along actin microfilaments. It consists of two heavy chains and one light chain (Figure 1.4E). The heavy chain is composed of the amino-terminal motor domain with binding sites for actin and ATP, a neck with binding sites for calmodulin, a coiled coil region responsible for dimerisation and a carboxyl-terminal region implicated in cargo binding (Reck-Peterson *et al*, 2000). Members of the Myosin V family have been reported to transport mRNAs, proteins and vesicles from the mother to the bud in yeast, ER cysts in squid and melanosomes in *Xenopus* (reviewed in Vale, 2003).

1.5.2 Cis-acting elements

The destination of an RNA is determined by cis-acting sequences which, in most of the cases, lie within its 3'UTR. These sequences, often called zip codes, are essential for localisation, as their removal or mutation inhibits it. They are usually also sufficient, as they are able to target themselves or non-localising transcripts towards the localisation site.

The identification of localisation elements has not been straightforward. Even transcripts that utilise the same motors and share common localisation sites, usually lack any obvious homology or secondary structure similarity, making mapping experiments absolutely necessary for the identification of their zip codes. The generation of transgenics bearing deletion and fusion constructs, as well as the injection of truncated RNAs have revealed the minimal sequences that are responsible for localisation of various messages.

The localisation signal of *hairy* is bipartite and comprises of two stem-loop structures, named SL1 and SL2, residing in a 121nt region within its 3'UTR. This element is sufficient to recruit components of the transport machinery and necessary for apical transport of the RNA (Bullock *et al*, 2003). Simmonds *et al*, 2001, mapped down *wingless* RNA to two minimal elements in its 3'UTR, WLE1 and WLE2, each sufficient for localisation.

BLE1, a 50nt segment in *bcd* 3'UTR, when dimerized, is essential and sufficient for its transport towards and within the oocyte (MacDonald *et al*, 1993). The anterior localisation of *K10* transcript in the *Drosophila* oocyte (Serano and Cohen, 1995), as well as the apical localisation of ectopic *K10* in follicle cells (Karlin-McGinnes *et al*, 1996) or blastoderm embryos (Bullock and Ish-Horowicz, 2001) is mediated by a 44nt element, the TLS. TLS drives localisation regardless of its position in the transcript or the sequence context. A TLS-like motif is responsible for the localisation of another maternal transcript, *Orb*, which is also found at the anterior

cortex of oocytes (Cohen *et al*, 2005). A 64nt element in the coding region of *grk*, named GLS, is the signal that directs its localisation in the oocyte (Van de Bor *et al*, 2005). A similar motif, ILS, targets the *I* factor retrotransposon towards the oocyte nucleus (Van de Bor *et al*, 2005).

Vg1, *VegT* and *Xlsirt* localisation elements, all containing sub-elements/redundant repeats, direct the respective RNAs towards the vegetal cortex of *Xenopus* oocytes (Gautreau *et al*, 1997, Mowry and Melton, 1992, Allen *et al*, 2003). The perinuclear accumulation of *metallothionein-1* mRNA in rat cells is mediated by a motif of bipartite nature, present in its 3'UTR (Chabanon *et al*, 2004). *ASH1* RNA contains four localisation sequences, E1, E2A, E2B and E3, three of them residing in the coding region and one extending towards the 3'UTR. Each element is essential for recognition by the transport machinery and sufficient to direct an heterologous RNA to the bud (Long *et al*, 1997, Chartrand *et al*, 1999, Gonzalez *et al*, 1999).

1.5.3 Trans-acting factors

The primary RNA sequence and the secondary or tertiary structure of the RNA are recognised by RNA-binding proteins. The interaction of these proteins with the transcript possibly promotes the recruitment and association of a series of other factors, thus initiating the assembly of the "locasome". Although these factors could simply act as physical linkers between the RNA and the motor, it is thought that at least some of them might provide cargo specificity, or regulate the activity of the motor and consequently the efficiency of the transport. However, little information is available about the composition and function of the "locasome" and only a few trans-acting factors have been identified (reviewed in detail in Palacios and St Johnston, 2001, Tekotte and Davis, 2002), using biochemical, cell biology and genetic approaches.

She2 and She3 are involved in actin dependent transport of *ASH1* mRNA from the mother cell to the bud in yeast. She2 is a dsRNA-binding protein that binds *ASH1*,

whereas She3 links the complex to the myosin heavy chain (Long *et al*, 2000, Bohl *et al*, 2000). Bicaudal D and Egalitarian are recruited by injected pair rule RNAs and are required for the apical localisation of the injected and endogenous pair rule transcripts in *Drosophila* blastoderm embryos (Bullock and Ish-Horowicz, 2001) and *inscuteable* RNA in *Drosophila* neuroblasts (Hughes *et al*, 2004). It has been shown that Egl can bind dynein light chain (Navarro *et al*, 2004). There is evidence that the mammalian BicD recruits dynein and controls ER-Golgi transport (Matanis *et al*, 2002).

Vera is required for the microtubule dependent localisation of *Vg*1 mRNA to the vegetal pole in *Xenopus* oocytes (Cote *et al*, 1999). It contains five RNA binding motifs and has been reported to bind to the *Vg*1 mRNA localisation signal. Vera colocalises with *Vg*1 and associates with MTs. ZBP-1, the chicken homologue of Vera, is involved in the actin dependent localisation of *β-actin* mRNA and can bind the *β-actin* localisation element (Ross *et al*, 1997). Exuperantia is implicated in some MT dependent steps of *bicoid* mRNA localisation in early *Drosophila* oocytes (reviewed in detail in Palacios and St Johnston, 2001). Exu mutants disrupt *bcd* mRNA localisation, whereas both endogenous and fused with GFP Exu protein colocalises with the transcript. Exu-GFP forms particles that move along MTs, following the same path as *bcd,* but the RNA has not been shown yet to associate with these particles. Swallow protein is required for the maintenance of *bcd* mRNA at the anterior of the oocyte, later in oogenesis. It binds dynein light chain and it could link the *bcd* to the dynein machinery. However, *bcd* mRNA is not a component of Swallow/dynein complexes, raising the possibility that Swallow functions as an anchor, rather than being actively involved in the actual transport process.

Staufen was the first RNA binding protein that was found to mediate RNA localisation and it probably represents the most thoroughly studied trans-acting factor. It plays an important role in the MT dependent localisation, anchoring and translation of *oskar* mRNA (St Johnston *et al*, 1991, Micklem *et al*, 2000), in the anchoring and translation of *bcd* mRNA (St Johnston *et al*, 1991, Ferrandon *et al*,

1994) and in the actin mediated transport of *prospero* RNA and protein in *Drosophila* neuroblasts. Staufen contains five dsRNA binding domains, three of which have been shown to bind dsRNA in vitro. There is evidence that it can bind directly to *osk*, *bcd* (Ferrandon *et al*, 1994) and *pros* (Broadus *et al*, 1998) mRNAs zip codes. The rat homologue of Staufen has been identified in RNP particles that associate with microtubules and move along dendrites, in hippocampal neurons (Kohrmann *et al*, 1999). Miranda binds one of the dsRBD of Staufen. It colocalises with Staufen protein and *prospero* RNA and is required for their localisation (Shen *et al*, 1997, Shen *et al*, 1998, Matsuzaki *et al*, 1998). It acts probably as an adaptor between the Staufen/*prospero* complex and the actin cytoskeleton. Modulo, PABP, Smooth and Nod were identified by biochemical purification, as a complex, also including Swallow, that specifically binds the *bcd* localisation signal (Arn *et al*, 2003).

Heterogeneous nuclear RNPs (HnRNPs) are nuclear nucleic acid-binding proteins. These proteins may affect the cytoplasmic sorting of an mRNA by different ways. The assembly of RNP complexes in the nucleus may deposit a landmark on the RNA, which will determine its cytoplasmic fate. Alternatively, the proteins may be loaded on the RNA during its export from the nucleus and target it in the cytoplasm. Finally, a subset of the hnRNPs shuttle between the nucleus and the cytoplasm and can therefore direct the RNAs in the cytoplasm like any other cytoplasmic factor. For example, hnRNPA2 is detected in the nucleus and in the cell body and axons of rat neurons (Hoek *et al*, 1998). It colocalises with *MBP* RNA and it is required for its transport, as it has been demonstrated by RNAi experiments. Squid or hrp40 is involved in *gurken* mRNA localisation and translational control in *Drosophila* (Norvell *et al*, 1999). In *squid* mutant oocytes, *gurken* remains at the anterior cortex and does not form a dorso-anterior cap. There are three isoforms of Squid, two nuclear and one cytoplasmic, which act in different steps of *grk*'s metabolism. Mago nashi, Y14 and Barentz are components of the exon-exon junction complex of the spliceosome and are required for *osk* mRNA localisation at the posterior of the

Drosophila oocyte. Splicing is indeed essential for the localisation of *oskar* (Hachet and Ephrussi, 2004) and might regulate the assembly of various RNP complexes.

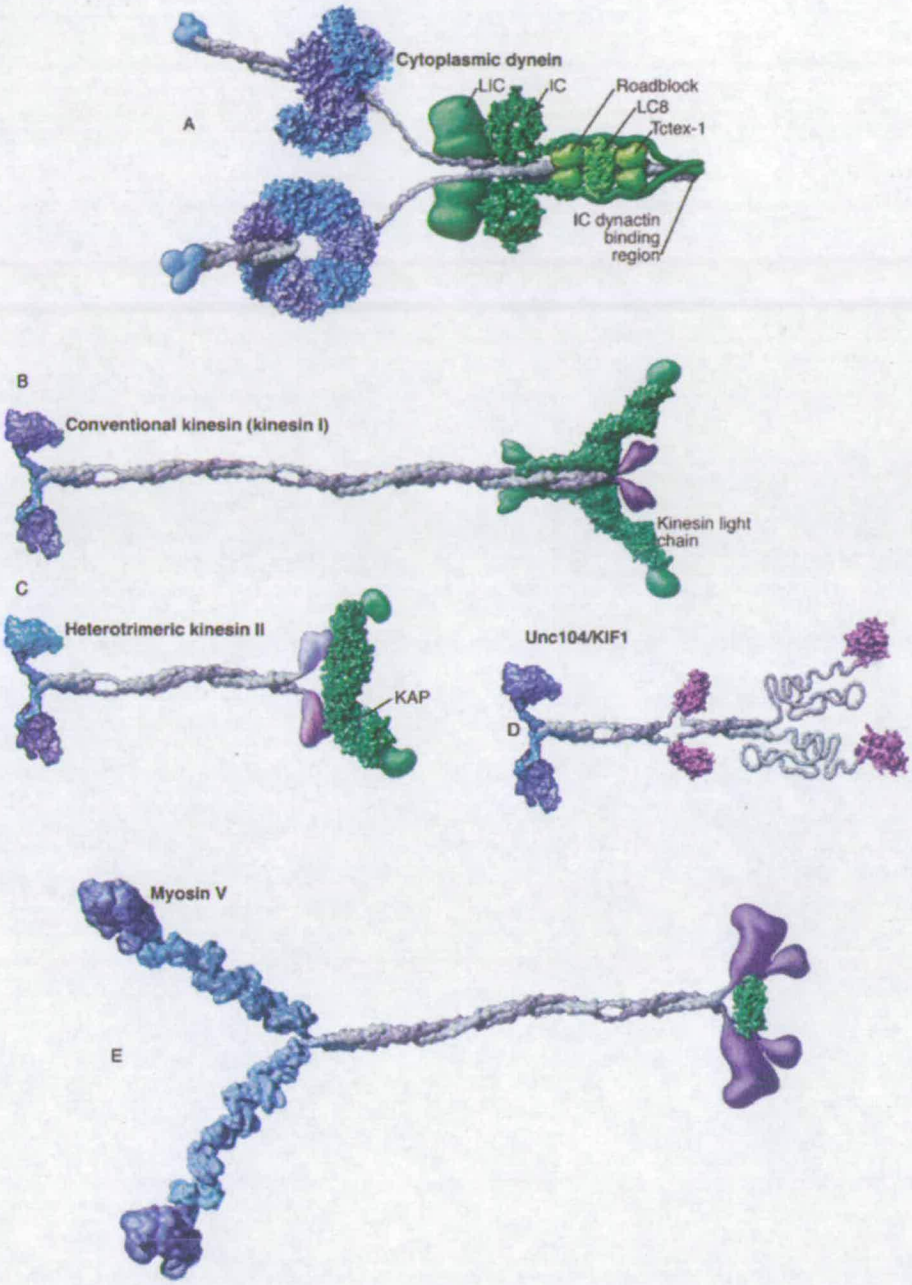


Figure 1.4: Cargo-transporting motors
Dynein (A) is composed of two heavy chains (DHC), two intermediate chains (DIC), two light intermediate chains (DLIC) and several light chains (DLC). Kinesin-1 or Kinesin I (B) is composed of two heavy chains (KHC) and two light chains (KLC). Kinesin-2 or Kinesin II (C) is a heterotrimeric complex with two different motor subunits, and a third accessory polypeptide. Kinesin-3 or Unc104/KIF1 (D) acts as a homodimer. Myosin V (E) consists of two heavy chains and one light chain. The motor catalytic domains of the heavy chains are displayed in blue, mechanical amplifiers in light blue and tail domains in purple. Light chains are shown in green (picture from Vale, 2003).

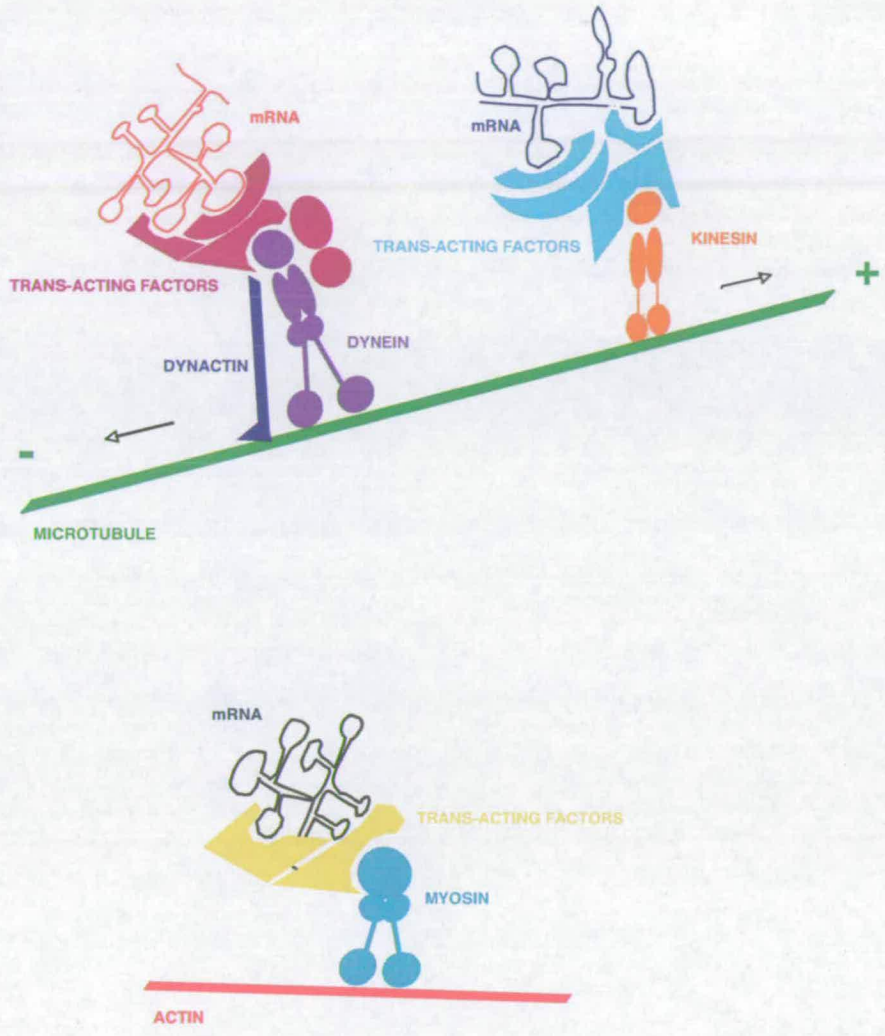


Figure 1.5: Trans-acting factors recognise the cis-acting signals and link the RNA to the motor machinery.

AIMS

Chapter 3

Investigation of the role of motors and their co-factors in bidirectional RNA motility in *Drosophila* syncytial blastoderm embryos.

Chapter 4

Identification of novel localising transcripts during *Drosophila* oogenesis and embryogenesis - Experimental validation of novel bioinformatics approaches for the identification of RNA localisation signals and localising transcripts in *Drosophila*.

Chapter 5

Development of an RNA localisation assay in *Drosophila* cultured cells, with the aim to use it for an RNAi screen for novel trans-acting factors involved in RNA localisation.

CHAPTER 2

MATERIALS AND METHODS

Solutions and reagents

All solutions used were prepared as described in Molecular Cloning-A Laboratory Manual (Sambrook *et al*, 1989). Chemicals used to prepare buffers and solutions were from SIGMA, BDH and Fisher. Restriction enzymes, Taq polymerase, T7, T3 and SP6 polymerases, ligases and phosphatases were obtained from Roche, New England Biolabs (NEB), Promega and Stratagene and were used according to manufacturers instructions. Phosphate buffers Saline (PBS) and Luria Betani mediums (LB) and LB-agar plates with Ampicillin or Kanamycin were prepared and autoclaved by the Swann building media kitchen. LB/Chloramphenicol plates were prepared by spreading 25ul of 34mg/ml Chloramphenicol solution onto agar plates.

Purification of Plasmid DNA

Qiagen mini, midi or maxi-prep kits were used according to Qiagen's protocols.

DNA precipitation

DNA was precipitated after restriction digest and PCR reactions as described in Sambrook *et al*, 1989. 1/10 volume of 5M Sodium Acetate pH5.2 plus 2.5x volume of 100% Ethanol was added the DNA sample, incubated at -20°C for 15mins and later centrifuged for 20mins at 14,000g. The pellet was washed in 70% Ethanol and resuspended in DEPC dH_2O. Alternatively, DNA was cleaned after PCR using the QIAquick PCR purification kit.

RNA in vitro transcription and labelling

Alexa-546, Dig and Biotin labelled RNAs were in vitro transcribed using Molecular Probes (Alexa) and Roche (Dig and Biotin) labelling kits. RNAs were synthesised from cDNA templates. *gurken* was a gift from T.Shupbach, *bicoid*, *fushi-tarazu* and *hairy* gifts from D.Ish-Horowicz, *oskar* a gift from A.Ephrussi and *runt* a gift from Peter Gergen. cDNAs have been cloned into pBS, pGEM or PCTopoII containing T3, T7 or SP6 promoters. cDNAs of the GOLD, DGC1 and DGC2 collections are cloned into pBS, pFLC-1, pOT2 and pOTB7 vectors, containing T3, T7 and SP6 promoters.

Synthesis of fluorescently labelled RNAs

Fluorescently labelled, capped RNAs were in vitro transcribed for injection into living embryos. RNAs were transcribed in 50ml volumes of DEPC treated dH20, including 1-2mg linearised DNA as a template, 0.4mM ATP, 0.4mM CTP, 0.36mM UTP and 0.04 mM AlexaFluor 546-UTP or AlexaFluor488-UTP, 0.12mM GTP, 0.3mM 7mG('5)ppp(5') CAP analogue and 40Units of RNAse inhibitor (Promega) and either T3, T7, SP6 polymerases (20U/ml) (Roche and Promega) with the corresponding transcription buffers. The transcription reaction was incubated at 37°C for 2 hours. The DNA template was digested with DNaseI (Promega, 2 Units) for 10 mins at 37°C. Unincorporated nucleotides were removed by using a G50 RNA spin column (Roche) according to manufacturers instruction. Cleaned RNA was precipitated by adding 1/5 volume of 3M Ammonium Acetate pH5.2 and 2.5x volume of 100% ethanol, incubated at -20°C for 15mins and spun at 4°C, at 14.000g for 30mins. The RNA precipitate was washed with 70% ethanol RNA was resuspended in 5-10μl of DEPC treated water depending on the size of the pellet. Final concentration of RNA was 200-500ng/μl.

Synthesis of Biotin labelled RNAs

Biotin labelled RNAs for injection int embryos were in vitro transcribed using a similar protocol to that described for Alexa-UTP labelling, but 0.5x Biotin labelling mix (containing all four GTP, ATP, CTP and Biotin-UTP) was used, instead of Alexa UTP All subsequent steps are identical to the protocol described above for RNA Alexa labelling.

Synthesis of Dig labelled RNAs

Sense and anti-sense RNA probes were synthesised for RNA in situ hybridisation. Dig labelled RNA was in vitro transcribed from 1-2ug of linearised DNA in a 20ml reaction volume. Dig labelling mix (10x) contains 10mM ATP, 10mM CTP, 10mM GTP, 6.5mM UTP, 3.5mM DIG-11-UTP, pH7.5. 20ml reaction contained 1x (2ul) of Dig labelling mix, 1-2ug of linearised DNA, transcription buffer and T3, T6 or SP6 polymerase (20U/ml). The reaction was incubated at 37°C for 2 hours. All

subsequent steps are identical to previous RNA labelling protocols. For in situ hybridisation RNA probes were diluted in hybridisation buffer at 1/200-1/1000 depending on the efficiency of the transcription reaction to achieve a final concentration of approximately 0.3ng/ml.

RNA precipitation

After in vitro transcription RNA was cleaned from unincorporated nucleotides using Roche G50 columns according to the manufacturer instruction. It was then precipitated by adding 1/5 volume 3M Ammonium Acetate plus 2.5x volume of 100% Ethanol. The sample was incubated at -20°C for 15mins and later centrifuged for 20mins at 14,000g. The pellet was washed in 70% Ethanol and resuspended in DEPC dH_2O.

PCR

Standard conditions for a 50ml reaction were: 50ng template DNA, 1XPCR buffer containing 15mM MgCl2 (Roche), 0.2mM Ultrapure dNTPs (Roche), 1mM primer each (Sigma) and 2.5 Units Taq polymerase (Roche).The standard program used was 95°C hot start for 5 minutes, 35 cycles of melting at 95°C for 30 seconds, annealing at 50-60°C for 30 seconds and elongation at 68-72°C for 1-3 min. A final elongation step was carried out at 68-72°C for 10 minutes.

Preparation and microinjection of Drosophila embryos

Fly cages were set up and embryos from 2h collections were used for microinjection. Embryos were collected from fruit juice-agar plates, placed in a sieve and dechorionated for 90sec at room temperature, using 50% household bleach. Embryos were washed with plenty of dH_2O and transferred to a piece of agar placed over a coverslip. Using tweezers, embryos were aligned to allow rapid injection. Glue made by sticky tape dissolved in heptane was spread onto a coverslip thickness no1 was used to lift the aligned embryos from the agar and stick them to the surface of the coverslip. Embryos were then dehydrated in silica gel for 10-15 mins at room

temperature and subsequently covered with halocarbon oil series 700 (KMZ Chemicals Ltd). Embryos were injected with eppendorf femtotip needles.

Dissection and fixation of *Drosophila* ovaries for staining procedures

Fly ovaries of 2 days old females were dissected in PBS and then transferred to 3.7% (w/v) formaldehyde/PBS for 20mins. After fixation, ovaries were washed 3x5mins in PBS/0.1% (v/v) Tween. Ovaries were some times stored for at least two hours in 100% Methanol at –20°C prior to in situ hybridisation. Visualisation of DNA was performed through staining of ovaries with 4", 6-diamidio-2-phenolyndole (DAPI) for 2 minutes, following two washes with PBT. Ovaries were mounted in Vectashield medium containing anti-photobleaching reagents.

RNA in situ hybridisation of *Drosophila* ovaries

In situ hybridisation was performed as previously described by Tautz and Pfeifle, 1989 and (Wilkie and Davis, 1999) by fluorescent tyramide detection (NEN LifeSciences or Molecular Probes) and according to the manufacturer's instructions. Ovaries were rehydrated through a series of methanol/PBT (1:1) into PBT for at least five minutes each. Ovaries were then postfixed for 15 minutes in 3.7% formaldehyde/PBT and washed 5 x 5 minutes in PBT to remove all traces of fix. Ovaries were then washed in hybridisation mix/PBT (1:1) for 10min and transferred into hybridisation mix for another 10min. Prehybridisation was carried in hybridisation buffer with added tRNA and Heparin at 70°C for at least 2h. Hybridisation was carried out overnight at 70°C. Two washes were performed in hybridisation solution for 30mins, one in PBT/hybridisation solution for 30mins and for washes were performed at RT for 30min each. Dig labelled probes were detected by incubation with anti-DIG antibody conjugated to horseradish peroxidase (sheep anti-DIG-POD Fab fragment, Roche) for 2 hours at room temperature (1:1000 in PBT). Egg chambers were washed 2x30mins and the HRP coupled antibody was visualised incubation of tyramide-Cyanine-3 (Cy3) 1:50 in amplification buffer (TSA Direct, NEN Life Sciences, UK or Molecular Probes). The reaction was allowed to proceed for 5 minutes before washing with PBT (3x10min). Egg

chambers were then stained with DAPI and mounted with Vectashield as previously described.

RNA in situ hybridisation in *Drosophila* embryos

Embryos were collected from fly cages and dechorionated as described above. They were fixed rapidly in a two phase mixture of 37% formaldehyde and heptane (Wilkie and Davis, 1998, Wilkie et al, 1999). Fixed embryos were devitellinised in methanol and stored in methanol at -20°C. In situ hybridisation to detect mRNA with fluorescent tyramides (NEN LifeSciences or Molecular Probes) was performed as described in Wilkie and Davis, 1998, Wilkie et al, 1999). Embryos were rehydrated, then post-fixed and rinsed five times in 1x PBT and prehybridized for at least one hour at 70°C in mRNA hybridisation buffer. DIG labelled antisense and sense RNA probes were hybridised to embryos overnight at 70°C and embryos were washed after hybridisation as described before for ovaries. Dig labelled probes were detected as previously described for egg chambers. Embryos were stained with DAPI as described above for egg chambers and then mounted in Vectashield.

Immunofluorescence on *Drosophila* ovaries

Drosophila ovaries were dissected and fixed as described above. Three washes were performed in PBS/TritonX100 (PBTrx) for five minutes each. Ovaries were blocked in 10% NGS in PBTrx for two hours. Incubation with the primary antibody was carried out overnight at 4°C. After three 20mins washes, ovaries were incubated with a secondary antibody coupled to Alexa 546 fluorochrome (Molecular probes). Incubation with the secondary antibody was carried out at room temperature for two hours. Ovaries were mounted in Vectashield mediumand stained for DNA as described above.

Microscopy and data analysis

A Sedat/Agard DeltaVision widefield microscope from Applied Precision Inc. was used. The microscope consists of an Olympus IX70 inverted microscope with a 12 bit cooled CCD camera (Photometrics). Immersion oil with the appropriate refractive

index was used to minimise spherical aberration when 100x oil and 40x oil lenses were used. SoftWoRx was used to control the 3D movement of the stage, the filter wheels and the shutter. Out-of- focus light was reassigned to its original source using deconvolution algorithms (Parton and Davis, 2004). Analysis of images and movies was carried out using SoftWoRx on Silicon Graphics workstations or ImageJ on Macs. Tracking was performed with Metamorph, manually or semi-automatically.

GST-dynamitin Bacterial Expression and Purification

BL21(DE3) bacteria transformed with GST-dynamitin were grown in a 50ml culture of LB broth overnight at 37°C with 100mg/ml of ampicillin. 10mls of the culture were added 1L of LB medium with 100μg/ml ampicillin and incubated at 37°C to an O.D.$_{600}$=0.6-0.8. Induction with 0.1mM IPTG and incubation at 18°C for 3 hours followed and bacteria were pelleted at 4 °C. The pellet was washed with cold Wash Buffer 1 (Kasp buffer = 150mM L-Aspartic acid (monopotassium salt), 10mM KH_2PO_4, 1mM $MgSO_4$, pH7.4 + 1mM DTT) and then resuspended in cold Lysis buffer (Kasp buffer + 0.1mM PMSF, 1mM ATP, 1mM EGTA, 2mM $MgSO_4$, 1% TritonX-100, and all protease inhibitors, pH7.4) at 5mls/1g of wet pelleted cells. The lysate was spun for 20min at 15.000g at 4°C and the supernatant was collected and kept on ice.

Glutathione-agarose beads (Sigma) were resuspended in Wash Buffer 1 and rocked for 2 hours at 4°C, then washed twice with cold Asp buffer and finally resuspended in Wash Buffer 1 and stored at 4°C with 1mM NaN_3. The beads were equilibrated in the cold room by pouingr 0.3 ml of beads into a 20ml Biorad column and washing the column with 20mls of cold Wash buffer 1 and then 2mls of cold Lysis Buffer (that includes the protease inhibitors, DTT, MgATP, EGTA, and TritonX-100, pH7.4).

The bacterial lysate was put over the column at a flow rate of 1ml/min and the flow through was collected for Bradford and gel samples. The column was washed with 50mls of cold Wash Buffer 2 (Kasp buffer + 1mM $MgSO_4$, 0.1 mM ATP, all protease inhibitors, 1mM EGTA, but no TritonX-100, pH7.4), with 5mls of cold High Salt Buffer (Kasp buffer, including 1mM $MgSO_4$, 1mM ATP, all protease

inhibitors, plus an additional 300mM KGlutamate, pH7.4). and 50mls of cold Wash buffer 1. Elution of bound GST-dynamitin was performed at RT with Elution buffer (Kasp buffer, 10mM Glutathione, pH 7.0-7.5).

Expression and purification of $(His)_6$-tagged dynamitin

pET28c-transformed BL21(DE3) bacteria were grown shaking overnight in 50mls of LB at 37°C with 50mg/ml of kanamycin. 10mls of the culture was added to 1L of LB(+) media (10g Bactotryptone, 5g yeast extract, 5g NaCl, 2g $MgSO_47H_2O$, and 1g Casamino acids, pH7.5) plus 50μg/ml kanamycin and was incubated at 37°C to an $O.D._{600}$=0.6-0.8. Expression was induced with 0.1mM IPTG and shaking at 16°C for 3 hours. The culture was spun at 3,000xg for 20min at 4°C and the pellet was washed with cold Wash Buffer (K/Asp buffer - 150mM L-Aspartic acid 10mM potassium phosphate, pH7.2). Cold Lysis buffer (K/Asp buffer, pH7.2 plus 1mM ATP, 1mM EGTA, 2mM $MgSO_4$, 1% TritonX-100 and protease inhibitors cocktail from Roche) was added at 5mls/1g of wet pelleted cells. The lysate was spun for 20min at 25,000g at 4°C. The supernatant was collected and kept on ice.

0.5mls of Qiagen Ni-NTA Agarose beads were poured into a 20ml Biorad plastic disposable column and washed with 40mls of cold Wash buffer and 5mls of cold Lysis Buffer. The beads were mixed with the bacterial lysate for 30 minutes at 4°C and poured into a 20ml Biorad column and then washed with 50mls of cold Lysis buffer (that includes the 2.5mM $MgSO_4$, 0.1mM ATP, all protease inhibitors, 1mM EGTA, but no TritonX-100 and only 0.1mM ATP, pH7.2). The column was washed with 5mls of cold Lysis buffer with high salt (including 1mM $MgSO_4$, 1mM ATP, all protease inhibitors, plus an additional 300mM KGlutamate; this time no EGTA no TritonX-100, pH7.2), 100mls of cold Wash buffer 2 (with 1mM $MgSO_4$ but no ATP or protease inhibitors, pH7.2). The bound protein was eluted with 10mls of cold wash buffer containing 175 mM Imidazole, pH7.2.

Flystocks and crosses

All flystrains were raised on standard yeasted cornmeal-agar medium at 25°C. The stocks used are mentioned in the results chapters.

Particle tracking and analysis

RNA particles were tracked using Metamorph. Tracking was performed in a semi-automated manner. The X,Y coordinates were logged directly on Excel files. Excel files were loaded on ParticalStats, which displayed graphs and physical parameters of runs (run length, speed, frequency of reversals).

CHAPTER 3

Investigating the role of motors and their cofactors in bidirectional RNA motility in *Drosophila* embryos

3.1 INTRODUCTION

3.1.1 BIDIRECTIONAL TRANSPORT

3.1.1.1 EXAMPLES OF BIDIRECTIONAL CARGOES

Many cargoes of molecular motors have been demonstrated to exhibit bidirectional saltatory motion along microtubules. They move towards one direction, pause or undergo Brownian motion and frequently reverse course and run towards the opposite direction. Cargoes that move in this manner include mitochondria in axons (Morris and Hollenbeck, 1993), lipid droplets in *Drosophila* embryos (Welte *et al*, 1998) and mammalian cells (Valetti *et al*, 1999), pigment granules in mice melanocytes (Wu and Hammer, 2000), frog and fish melanosomes (Nascimento *et al*, 2003), neuronal (Leopold *et al*, 1990) and secretory (Wacker *et al*, 1997) vesicles, HIV particles (Macdonald *et al*, 2002), herpes viruses in sensory neurons (Smith *et al*, 2001), influenza viruses (Lakadamyali *et al*, 2003), adenovirus particles (Suomalainen *et al*, 1999), vimentin intermediate filaments in fibroblasts (Prahlad *et al*, 1998), neurofilaments in squid axoplasm (Prahlad *et al*, 2000) and mRNPs in rat hippocampal neurons (Kohrmann *et al*, 1999).

It is highly likely that there is a large number of bidirectionally moving cargoes that are still unidentified, because of the low frequency or duration and run length of the reversals and the limited time and spatial resolution of the sampling. Various advancements like improved camera sensitivity and scanning speed, brighter and more stable fluorescent dyes, as well as centroid analysis coupled with subpixel resolution are improving the rate of acquisition of fluorescent images and the tracking of motion and are revealing more and more switches in direction.

3.1.1.2 BIDIRECTIONAL TRANSPORT WITH UNIDIRECTIONAL MOTORS

Cytoskeletal tracks are polar and motors recognise this polarity and move in a uni-directional manner. A couple of exceptions to this rule are discussed later. Actin filaments, for instance, have distinct barbed and pointed ends and myosins move towards the polymerizing ends. The plus and minus ends of microtubules are different morphologically and chemically (Welte, 2004) and have distinct dynamics and position in the cell. The organisation of the cytoskeletal elements determines the destination of the molecular motor and subsequently the cargo. Cytoplasmic and axonemal dynein power transport towards the minus ends of microtubules and most members of the superfamily of kinesin motors drive their cargoes towards the plus ends.

An important question is how bidirectional transport arises from the activity of specialised, exclusively unidirectional motors that travel on polarised cytoskeletal tracks.

3.1.1.3 MODELS OF BIDIRECTIONAL TRANSPORT

Three models have been suggested to explain bidirectional transport: The "tug of war" model, the "exclusionary-presence" model and the "coordination" model. Here I briefly introduce these models. The predictions they lead to and the tests done to evaluate them experimentally, are critically and thoroughly discussed in an excellent review on bidirectional motility, written by Steven Gross (Gross, 2004) and are thus not described in this chapter.

In the "tug of war" model, the cargo finds itself bound at the same time to functional, opposite polarity motors. The back and forth vibration or long reversals reflect a stochastic struggle between the two classes of motors. In this case, net transport could be controlled by determining how many active motors of each inclination are engaged on the cargo and fighting to transport it. This hypothesis predicts that impairment of the performance of one motor should improve the properties of transport towards the opposite direction. Experiments demonstrating instead that the

movements in opposite directions are mutually dependent (reviewed in Welte *et al*, 1998, Gross *et al*, 2002), argue against the "tug of war" model, which is not currently favored.

According to the second model, the two type of motors cannot attach the cargo simultaneously. They might share one binding site on the cargo or the attachment of one motor might change the conformation of the cargo, so that it cannot bind the opposing one. However, the colocalisation of kinesin, dynein and mRNP granules in oligodendrocytes (Carson *et al*, 2004), as well as other data (summarised in Gross, 2002), which show that the properties of opposite direction runs are not independent of each other, argue against this idea.

In the coordination model (Fig 3.1.1), both classes of motors can be engaged with the cargo at the same time, but they do not interfere with each-other's function. There is a switch that turns the plus-end motor off, when the minus-end motor is active and vice versa. The cargo is driven by the functional (at the time) type of motor and when this regulation fails, it pauses or displays short back and forth movements. The mechanism of regulation has not been completely dissected so far, but evidence from several systems fit the coordination model (Deacon *et al*, 2003, Welte *et al*, 1998, Watermann-Storer *et al*, 1997). In the *Drosophila* lipid droplet system, for example, in which bidirectional transport has been extensively studied, when you interfere with the activity of dynein, you impair both minus and plus end transport (Gross *et al*, 2002), which is the outcome you would expect if the opposite polarity motors are not competing.

3.1.1.4 REGULATION OF BIDIRECTIONAL TRANSPORT

In most cases studied, despite the frequent reversals, one direction tends to dominate and cargoes undergo net displacement over time. It is not known how motor coordination is achieved nor how net transport is determined. However, some of the

components of this -so called- "coordination complex" or "switch" have already been identified.

Halo is a directionality determinant for lipid droplets. It upregulates transport towards the plus ends of MTs (Gross *et al*, 2003). Klarsicht controls lipid droplets' motion (Welte *et al*, 1998), as well as photoreceptor nuclei migration (Fischer-Vize and Mosley, 1994) and is thought to be a core component of the coordination machinery. LSD2 is phosphorylated by Halo, physically interacts with Klar and alters the lipid droplet distribution (Welte *et al*, 2005). PI-3 kinase plays a role in the bidirectional motion of mitochondria (Chada *et al*, 2003). Net transport of fish melanosomes is controlled by the levels of cAMP. High cAMP levels activate PKA, which increases the length of the plus runs and shortens the minus runs. Low cAMP levels deactivate PKA, inducing an opposite effect (Rodionov *et al*, 2003). Rabs GTPases can interact with PKA, dynein light intermediate chains (Jordens *et al*, 2001, Bielli *et al*, 2001) and kinesin (Echard *et al*, 1998) and regulate the transport of endosomes, lysosomes, Golgi and mitochondria (Alto *et al*, 2002, Jordens *et al*, 2003, Short *et al*, 2002, Nielsen *et al*, 1999). Dynactin has been shown to regulate the activities of opposite polarity motors in diverse systems (discussed later in this chapter).

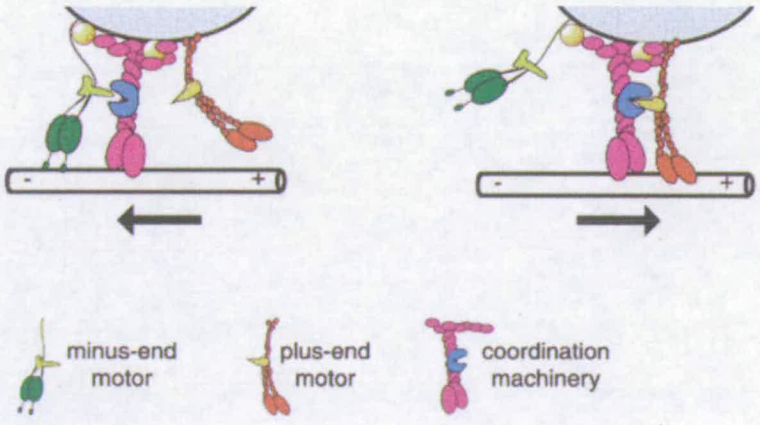


Figure 3.1.1: The coordination model (From Gross *et al*, 2003).

3.1.2 DYNACTIN AS A PROCESSIVITY FACTOR FOR DYNEIN

Motor complexes have to travel long distances of several micrometers, by taking nanometer steps. During each step, every single motor has a constant probability of dissociating from the cytoskeletal filament and diffusing away. Each class of motors overcomes this problem in different ways. Myosin II and axonemal dynein are organized in higher order complexes (Finer *et al*, 1994, Shingyoji *et al*, 1998). Multiple motors work synergistically and disengagement of one or some of them does not lead to detachment of the complex from their substrate. Motors that function individually or in small groups tend to employ other mechanisms to avoid detachment. Kinesin-1 coordinates its two motor heads to move hand-over-hand (Vale and Milligan, 2000) and is thus highly processive. Dynein is not as robust as kinesin in vitro. Single dynein molecules only travel short distances before dissociating from the track and exert limited force (Wang *et al*, 1995, Mallik *et al* 2004). Nevertheless, the average and maximum run length of dynein-driven cargoes in the cell and the force required to stall them are much higher (Preshley *et al*, 1997, Ashkin *et al*, 1990, Gross *et al*, 2000). This significant improvement in dynein's in vivo performance is thought to be accomplished by the use of 2-6 dynein motors (Gross *et al*, 2000, Mallik *et al*, 2005) and/or accessory proteins (Habermann *et al*, 2001, King and Schroer, 2000).

Dynactin is a cofactor of dynein, shown to be required for most dynein dependent motility (reviewed in Holleran *et al*, 1998). Although a large proportion of dynein and dynactin are not associated in vivo and dynein alone is sufficient to drive MT gliding in vitro, the two complexes do interact (both in vivo and in vitro) and dynactin increases dynein's processivity (King *et al*, 2000).

Dynactin is a multimeric complex, consisting of at least 7 subunits, ranging in size from 22-150KDa. These include p45/Arp-1/centractin, Arp-11 (actin related proteins), p150/Glued, p50/dynamitin, capping protein and several other less or no characterised polypeptides. Figure 3.1.2 shows a schematic of the organisation of the

different subunits in the complex. P50/dynamitin is positioned in the shoulder of dynactin and is crucial for dynactin's structure (Eckley *et al*, 1999). Overexpression of recombinant forms of dynamitin disrupts the complex and has been used as a tool to impair or abolish dynein's function in several cases (Wilkie and Davis, 2001, Echeverri *et al*, 1996). Arp-1 probably links the cargo to the dynein/dynactin complex (Muresan *et al*, 2001), through its interaction with the –COOH terminus of Glued (Waterman-Storer *et al*, 1995). P150/Glued binds microtubules and dynein intermediate chain (Karki and Holzbaur, 1995). It is thought to stabilise dynein's attachment to microtubules or to maintain dynein in close proximity to them, when it dissociates, thus promoting a more rapid reattachment.

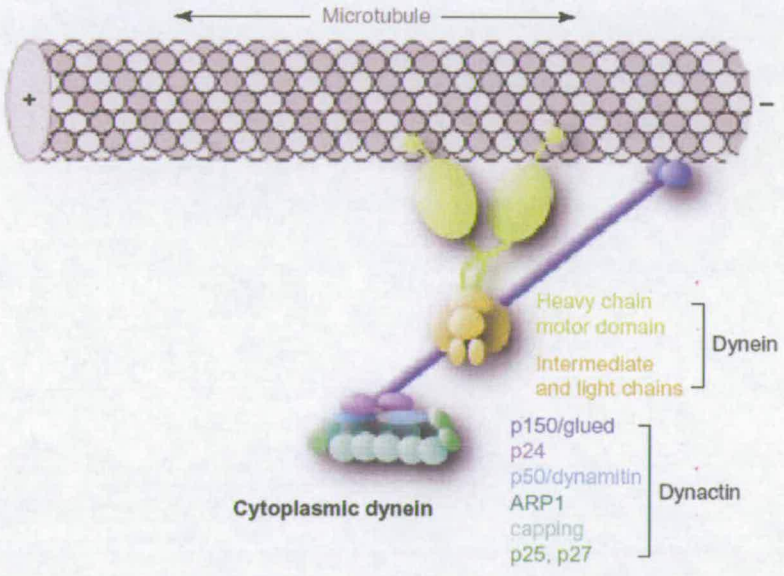


Figure 3.1.2: Dynein and its accessory complex, dynactin (Tekotte and Davis, 2003).

3.1.3 AIMS-INTRODUCTION TO THE EXPERIMENTAL ASSAY USED IN THIS CHAPTER

In this chapter, I am investigating the possible involvement of kinesin in RNA motility in *Drosophila* blastoderm embryos. I am also assessing the regulatory role of dynein cofactors in RNA transport. In order to address these questions, I mainly inject fluorescent pair rule RNA in *Drosophila* syncytial blastoderm embryos of various genetic backgrounds, I image the RNA in real time and analyse physical properties of its motion.

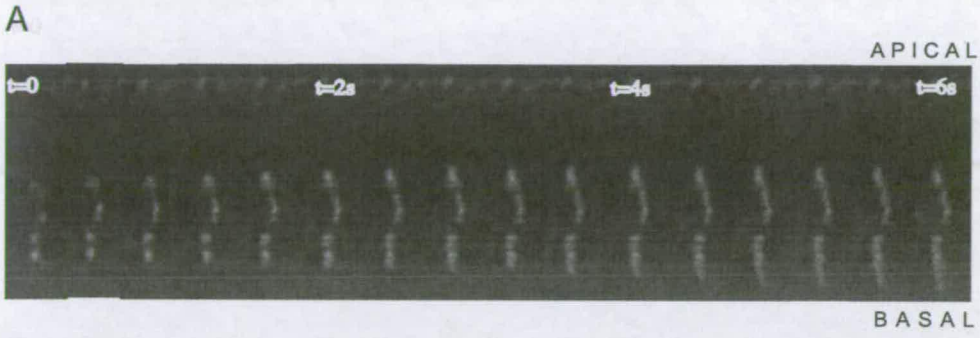
Microtubules are highly polarised at this stage and extend from their nucleating center that lies above the peripherally aligned nuclei, towards the basal cytoplasm of the embryo. Injected pair rule and *wingless* transcripts form particles, move from the site of injection towards the minus ends of MTs, driven by dynein/dynactin and localise apically, mimicking the endogenous RNA (Wilkie and Davis, 2002).

3.2 RESULTS

3.2.1. *FTZ* RNA PARTICLES MOVE BIDIRECTIONALLY ALONG MTs

In order to test whether pair-rule transcripts, like other dynein cargoes, move bidirectionally along microtubules, I improved the time resolution of the sampling up to 5 frames/second and the space resolution of the analysis, by using tracking methods that employ centroid analysis coupled with subpixel resolution. I also designed with Russell Hamilton ParticleStats, a programme that facilitates a more efficient and detailed analysis of the tracking data.

By improving the imaging and tracking of motion, I identified switches in direction that were previously unrevealed due to their low frequency, duration or length. I observed that pair rule RNA, although predominantly traveling towards the minus ends of MTs, also moves towards the opposite direction. Individual particles frequently pause or display back and forth vibration and occasionally backstep and display long runs towards the plus ends of MTs, before recapturing again in a new minus end run (movie 3.2.1, trail movie 3.2.2, movie 3.2.3, Figure 3.2.1).



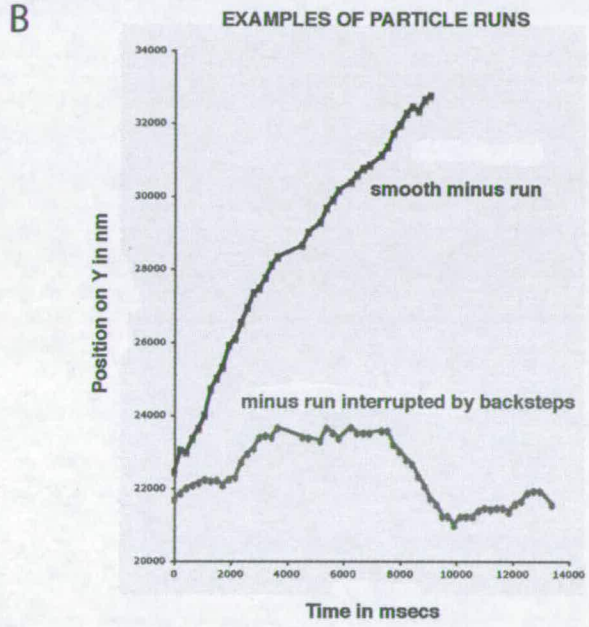


Figure 3.2.1: Bidirectional RNA motility in *Drosophila* embryos
(A) *ftz* RNA moving bidirectonally in wild type embryos. Time projection (1 frame/400 msec). (B) Examples of unidirectional and bidirectional runs.

3.2.2 SIGNIFICANCE OF RNA BACKWARD MOTILITY IN *DROSOPHILA* EMBRYOS

The plus motility of apical RNA particles is short and infrequent, and does not significantly perturb the overall progress towards the minus ends of MTs. What is then its significance? I frequently observe *ftz* RNA particles pausing in a given position, moving backwards for a short time, then reversing again and moving towards the apical cytoplasm. In such cases, interestingly, I occasionally observe, a little later, other particles pausing or reversing direction at the exact same position (movie 3.2.1).

We propose that through the reversals, the RNA particles are able to avoid "traffic jams" or obstacles, such as locked-up motors or paused organelles. It is likely that by stepping back, the particles explore the crowded cellular environment, switch MT tracks in order to bypass the other stuck motors/cargoes or take their time, until temporary obstructions are resolved.

3.2.3 PHYSICAL PROPERTIES OF PLUS END DIRECTED RUNS SUGGEST THAT THE RNA IS DRIVEN TOWARDS THE PLUS ENDS BY MOLECULAR MOTORS

Physical parameters of the observed backward motion, such as the run length, the directionality and the speed, indicate active transport, rather than diffusion. RNA particles can cover long distances, up to 2.2um, towards the plus ends. We believe that they travel along microtubules, because their paths are linear and frequently the same ones that these or other particles are running towards the opposite direction with dynein (movie 3.2.1). Finally, the mean and maximum velocities, 0.5μm/sec and 1.8μm/sec respectively, are of a magnitude that is generally thought to reflect motor activity.

3.2.4 PLUS END MOTILITY IS NOT MEDIATED BY KINESIN-1

Kinesin-1 is known to mediate the transport of membrane bound organelles in *Drosophila* larval axons, as well as lysosomes, Golgi vesicles, pigment granules, and intermediate filaments in various other systems (reviewed in Chapter 1). To test whether this motor is also involved in the plus end transport of RNA in *Drosophila* blastoderm embryos, we disrupted the function of Khc, which is the motor subunit of the tetrameric Kinesin-1 complex.

3.2.4a Generation of Khc germ-line clones

Out of the available *Khc* mutants, I chose Khc^{27}, which is a null allele with a stop codon in aa 65 (Brendza *et al*, 1999). Because of the essential role of motors in multiple developmental processes, loss of function alleles are recessive lethal at embryonic or early larval stages. Therefore, the study of their requirement for later events or their maternal effect phenotypes is not straightforward.

Khc is provided maternally and this contribution is necessary and sufficient for early embryogenesis. Because Khc^{27} homozygotes die as larvae, the generation of germ-line clones is the only way to completely remove the maternal supply. I used the Dominant Female Sterile technique (Chou *et al*, 1993) to make Khc^{27} germline clones. A short explanation of the DFS method is shown in Figure 3.2.2. Mitotic recombination was induced in the stem cells by heatshocking 1st instar larvae (60-72 hours) of the genotype hsFLP; FRT-Khc^{27}/FRT-$ovoD^{1}$. All the egg chambers that developed beyond stage 4 of oogenesis and therefore all the eggs that were laid were descendants of Khc^{27}/ Khc^{27} stem cells. Some of the mutant egg chambers had mispositioned oocyte nuclei (Figure 3.2.3A) and developed into dorsalised eggs with fused or no dorsal appendages. This phenotype has also been reported previously by Brendza *et al*, 2000 and Duncan and Warrior, 2004. For all the experiments described below, I collected eggs that were derived from mosaic females mated with wild type males.

The Khc^{27} mutant 65aa protein is not stable and thus not detectable by Western blots (Brendza *et al*, 1999). Therefore, I performed anti-KHC staining to confirm that I had removed the wild type protein. In wild type blastoderm embryos, Khc is distributed throughout the cytoplasm, but is slightly enriched in a layer of cytoplasm around the nuclei (Figure 3.2.3B,C). This pattern of staining was originally described by Saxton *et al*, 1991. In embryos laid by Khc^{27}/Khc^{27} clones, I do not detect any Khc in the cytoplasm (Figure 3.2.3D,E), which demonstrates that I have successfully depleted the wild type product. I observe a strong accumulation of the truncated product in the nuclei of these embryos (Figure 3.2.3D,E). The same phenomenon has been previously reported for egg chambers of other mutant backgrounds. Brendza *et al*, 2002 have detected Khc, as well as Dhc in the nucleus of Khc^{27}/Khc^{27} oocytes and Lei and Warrior, 2000 have detected Dhc in the nuclei of *Lissencephaly1* egg chambers. I cannot explain the nuclear accumulation of motors and I cannot rule out that anti-KHC and anti-DHC antibodies cross-react with a nuclear protein only in these mutant backgrounds and not in wild type egg chambers or embryos. Nevertheless, in our case, this striking difference in the staining pattern, between the wild type and the mutants, suggests that Khc is indeed disrupted and that I am not examining escapers.

3.2.4b Depletion of Kinesin-1 does not perturb the distribution of endogenous and injected *ftz*

If kinesin I is involved in RNA motility together with dynein and if the two motors are coordinated, we would expect that interfering with the activity of one would impair motion in both directions, as it has been shown for *grk* RNA in *Drosophila* oocytes and for lipid droplets in *Drosophila* blastoderms. In situ hybridisations against the endogenous *ftz* transcript and injections of in vitro transcribed *ftz* showed that this is not the case. The distribution of both endogenous and injected transcripts is normal in eggs laid from Khc^{27} clones (Figure 3.2.5B,E).

3.2.4c Depletion of Kinesin-1 does not alter the kinetics of transport of *ftz*

To examine if there are subtle effects that do not grossly perturb the dynein mediated transport and overall RNA distribution, but alter the kinetics of transport, I injected *ftz* RNA in mutant embryos and measured different parameters of motion. I observe that the mean velocity of the minus runs is not significantly affected in the mutants (Figure 3.2.6B). If Kinesin-1 were involved in the motility of the RNA, I would expect to detect an increase in the speed of the minus runs, if it competes with dynein, or a decrease of the minus speed if the two motors are coordinated. More importantly, I still observe backward episodes (movie 3.2.4, Figure 3.2.6A) in these embryos. Khc^{27} is a null allele and we would not expect to see any backward runs if Kinesin I is the motor that mediates them. Moreover, neither the frequency nor the average speed of the plus runs is reduced in the mutant embryos (Figure 3.2.6B, 3.2.6C).

3.2.4d Injected *ftz* RNA does not recruit Kinesin-1

To test if pair rule transcripts recruit Kinesin-1, I injected biotinylated *ftz* RNA and performed double staining against the injected transcript and endogenous Kinesin-1. I do not detect any enrichment of Kinesin-1 at the site of injection or localisation of the RNA (Figure 3.2.7). I conclude that *ftz* does not recruit Kinesin-1.

3.2.5 PLUS END MOTILITY IS NOT MEDIATED BY KINESIN -2

The Kinesin-2 superfamily consists of heterotrimeric complexes with two different motor subunits responsible for force generation and a third polypeptide, known as kinesin associated protein or KAP. Kinesin-2 has been demonstrated to mediate diverse transport processes, from axonemal to secretory pathway transport, and drive a wide range of cargoes, from RNA to melanosomes (reviewed in Chapter 1). The *Drosophila* homolog transports choline acetyltransferase in axons and its subunits are referred to as KLP64D, KLP68D and KAP3. To examine whether it is Kinesin-2 that is responsible for the backward motion in *Drosophila* embryos, I impaired the function of KLP64D.

3.2.5a Generation of KLP64D germ-line clones

I made germline clones of $KLP64D^{K1}$ and $KLP64D^{n123}$ recessive lethals (Ray *et al*, 1999), using the DFS technique, by inducing mitotic recombination in hsFLP; FRT-$KLP64D^{k1}$/FRT-$ovoD^{1}$ and hsFLP; FRT-$KLP64D^{n123}$/FRT-$ovoD^{1}$ 1st instar larvae. $KLP64D^{n123}$ is a deletion of the gene caused by the imprecise excision of a P element insertion (Perez and Steller, 1996). $KLP64D^{k1}$ is also most likely a null, since it bears an EMS induced point mutation that introduces a stop at codon 13 of the gene (Ray *et al*, 1999). $KLP64D^{n123}/KLP64D^{n123}$ clones have abnormal ovaries (Figure 3.2.4D) and do not lay eggs. $KLP64D^{k1}/KLP64D^{k1}$ clones have wild type ovaries, as shown by DAPI staining and *bicoid* RNA in situ hybridisation (Figure 3.2.4B). 1-2% of the egg chambers have a reduced number of nurse cells (Figure 3.2.4C). The females lay few eggs, most of which arrest in early embryogenesis.

3.2.5b Depletion of Kinesin-2 does not perturb the distribution of endogenous and injected *ftz*

In situ hybridisations against the endogenous *ftz* transcript and injections of in vitro transcribed *ftz* in embryos derived from $KLP64D^{k1}/KLP64D^{k1}$ clones showed that the

distribution of both endogenous and injected transcripts is indistinguishable form wild type (Figure 3.2.5C,F).

3.2.5c Depletion of Kinesin-2 does not alter the kinetics of transport of *ftz*

I injected *ftz* RNA in mutant embryos and measured different physical properties of RNA motion. Like in the Khc^{27} mutant embryos, the mean velocity of the minus runs is not significantly affected (Figure 3.2.6B). We also still observe backward movements (movie 3.2.5, Figure 3.2.6A) in these embryos. $KLP64D^{kl}$ is a null allele and I would not expect to see any backward runs if Kinesin-2 is the motor that mediates them. Moreover, neither the frequency nor the average velocity of the plus runs is significantly reduced compared with wild type (Figure 3.2.6B, 3.2.6C). I conclude that Kinesin-2 is not the motor that drives the RNA towards the plus ends of microtubules.

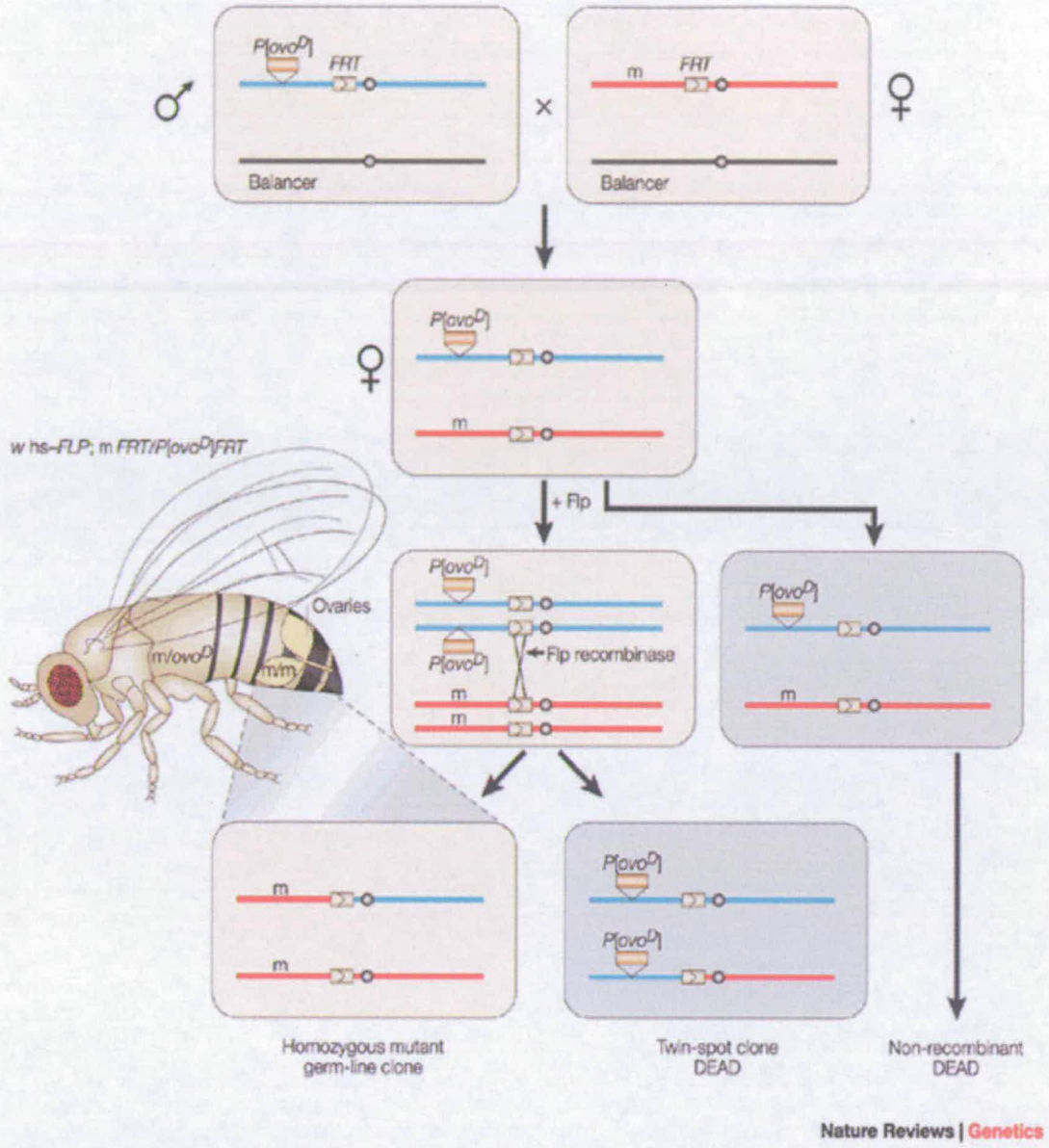


Figure 3.2.2: The DFS technique for selecting homozygous germ-line clones (picture from St Johnston, 2002)

FRT sites have been introduced close to the centromere of *Drosophila* chromosome arms, at identical positions on homologues chromosomes, so that most of the genes/mutations lie distal to them. Flp recombinase mediates site-specific mitotic recombination between FRT sites. After sister chromatid separation, clones of cells inherit two copies of the mutagenised chromosome. Temporal and spatial restriction of Flp's expression allows the identification and study of tissue and stage specific phenotypes. The DFS technique is a modification of FRT/Flp mitotic recombination approach. *OvoD* is a dominant mutation that kills female germ cells during early stages of oogenesis and is integrated into the wild type FRT chromosome arm. As a result, egg chambers than have inherited non-recombinant chromosomes arrest early in oogenesis and all the eggs laid derive from homozygous mutant germline clones.

EDINBURGH UNIV. LIBRARY

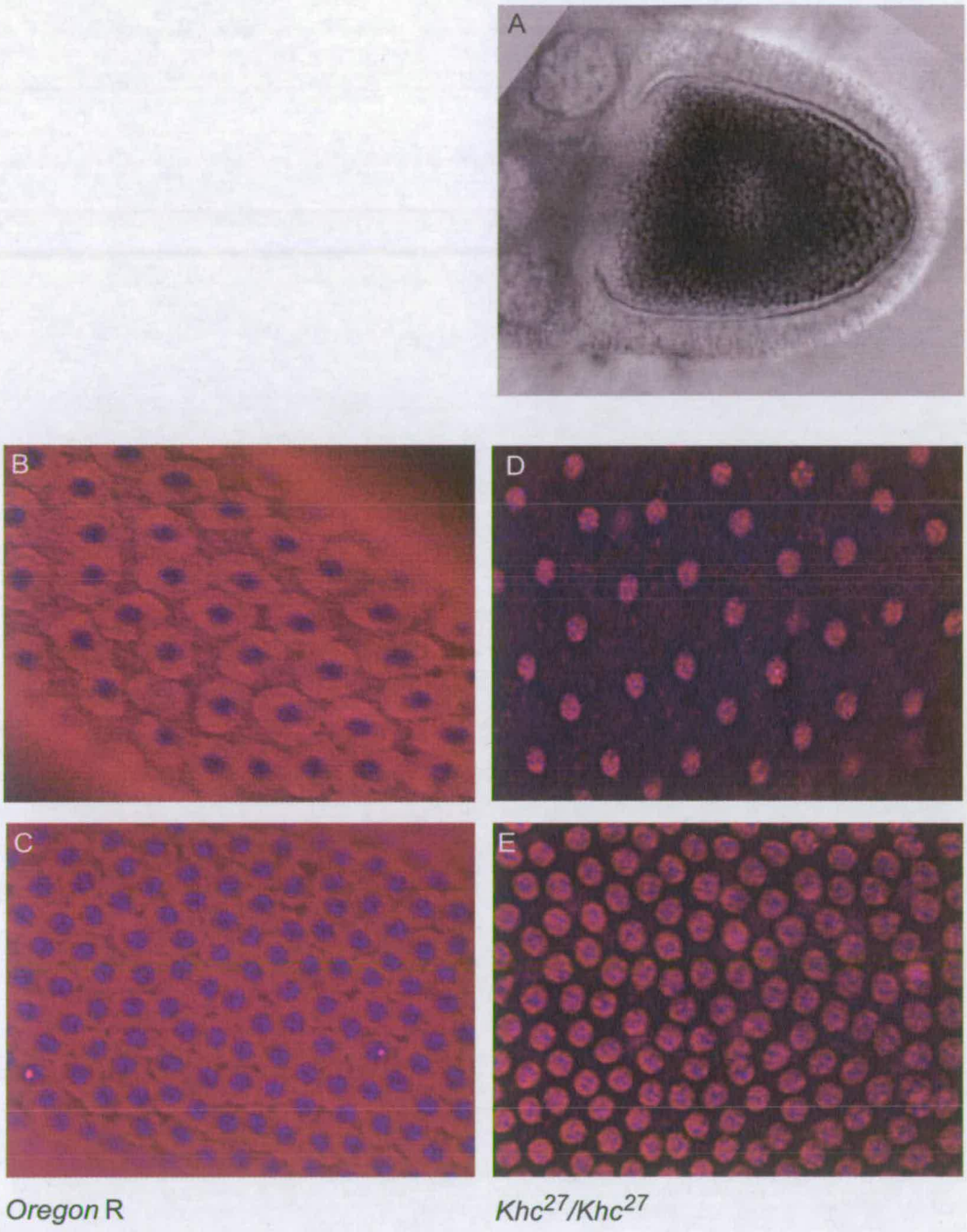


Figure 3.2.3: *Khc*^{27}/*Khc*^{27} mutant oocytes and embryos
(A) Mispositioned nucleus in *Khc*^{27}/*Khc*^{27} mutant oocytes (DIC image). (B-E) Immunostaining against Khc (Khc is shown in red, DNA in blue), (B) cycle 11 wild type embryos, (C) cycle 13 wild type embryos, (D) cycle 11 embryos laid by *Khc*^{27}/*Khc*^{27} mothers, (E) cycle 13 embryos laid by *Khc*^{27}/*Khc*^{27}mothers.

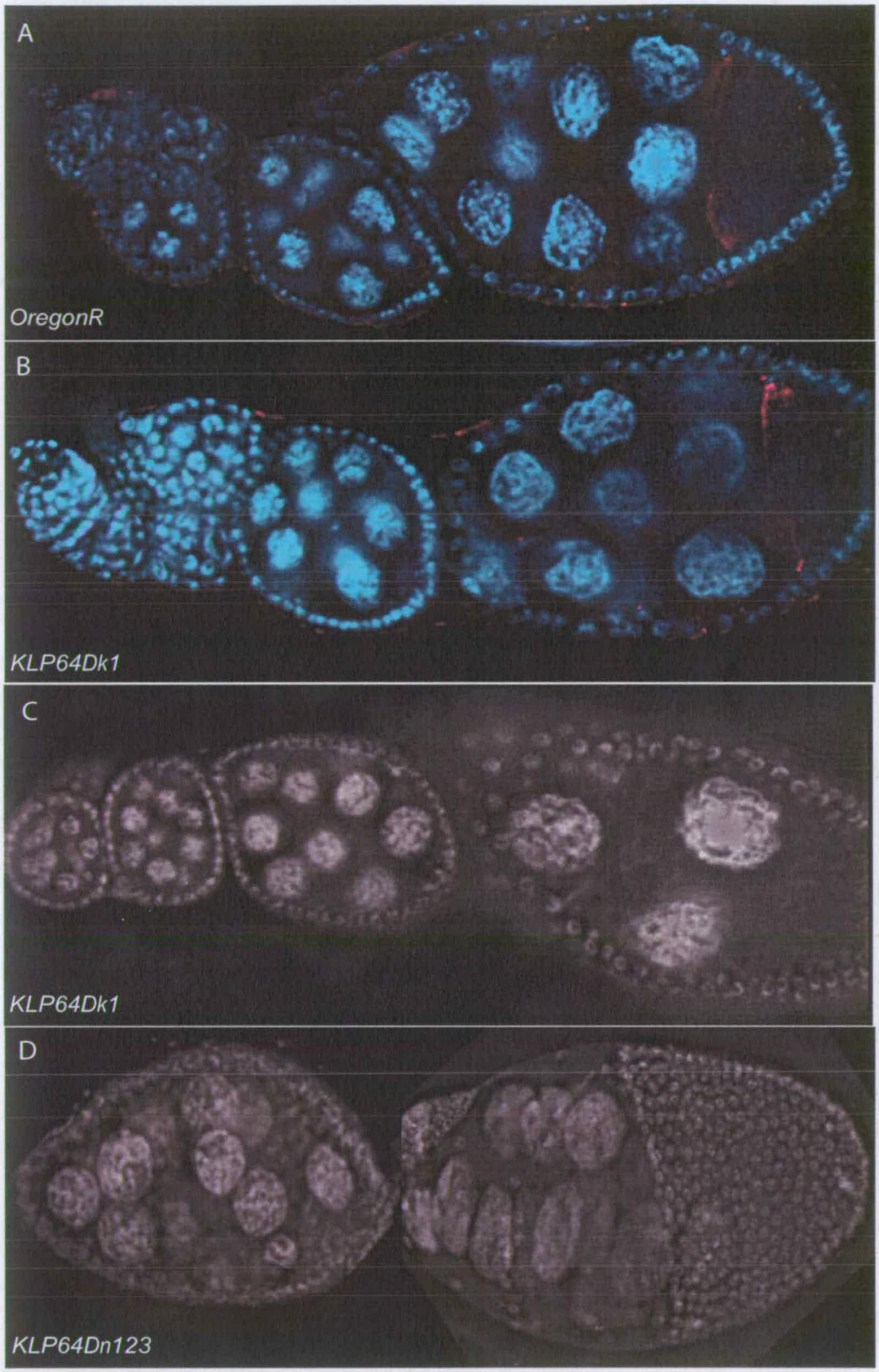


Figure 3.2.4: *KLP64D*^{k1} and *KLP64D*^{n123} egg chambers
Bcd RNA in situ hybridisation in wild type (A) and *KLP64D*^{k1} (B) egg chambers. RNA is shown in red, DNA in light blue. (C) Abnormal *KLP64D*^{k1} egg chambers. (D) *KLP64D*^{n123} egg chambers (DAPI staining).

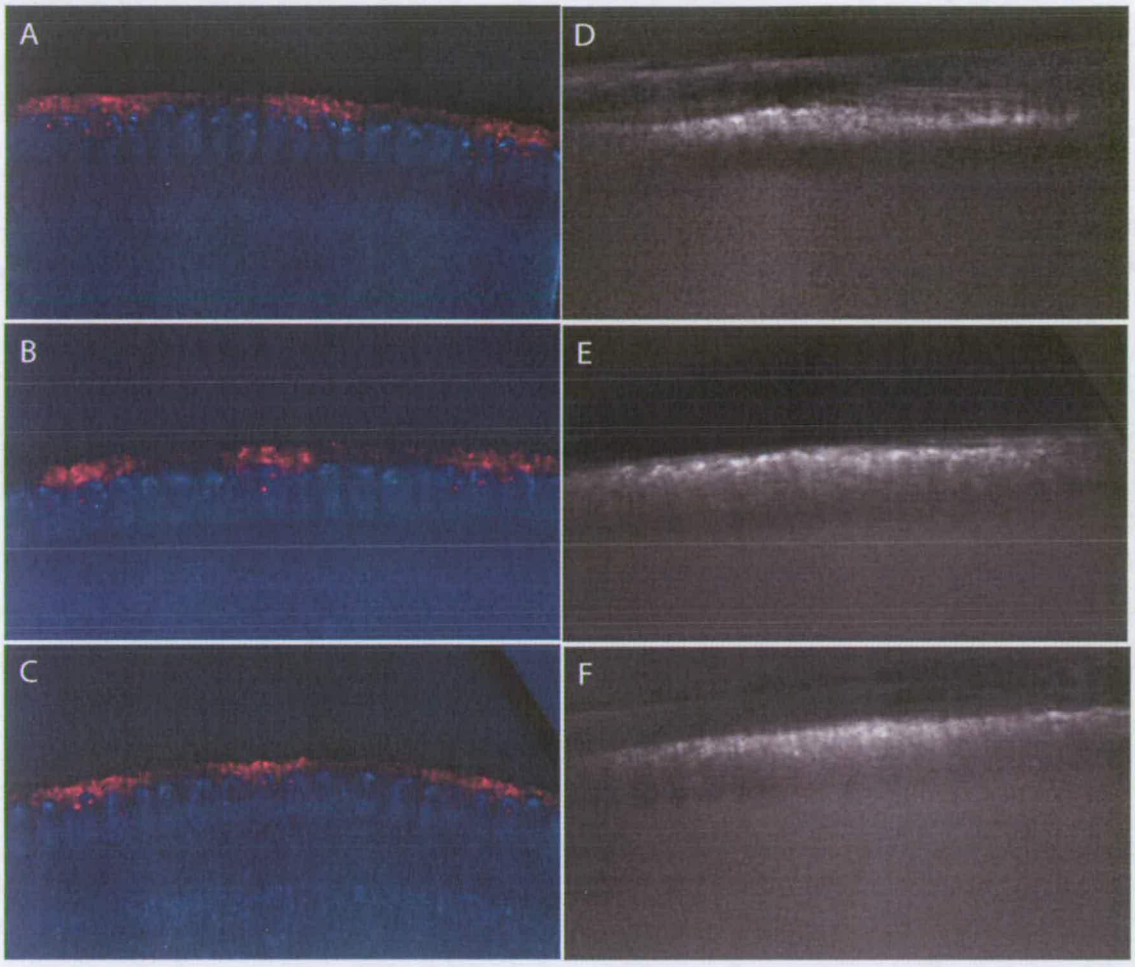


Figure 3.2.5: Wild type localisation of endogenous and injected *ftz* RNA in *KLP64D* embryos and *Khc* embryos

In situ hybridisation against endogenous *ftz* RNA (A, B, C) and injection of fluorescent *ftz* RNA (D, E, F) in wild type (A, D), Khc^{27} (B, E) and $KLP64D^{k1}$ (C, F) blastoderm syncytial embryos. Injected *ftz* is shown in white, endogenous *ftz* in red and DNA in light blue.

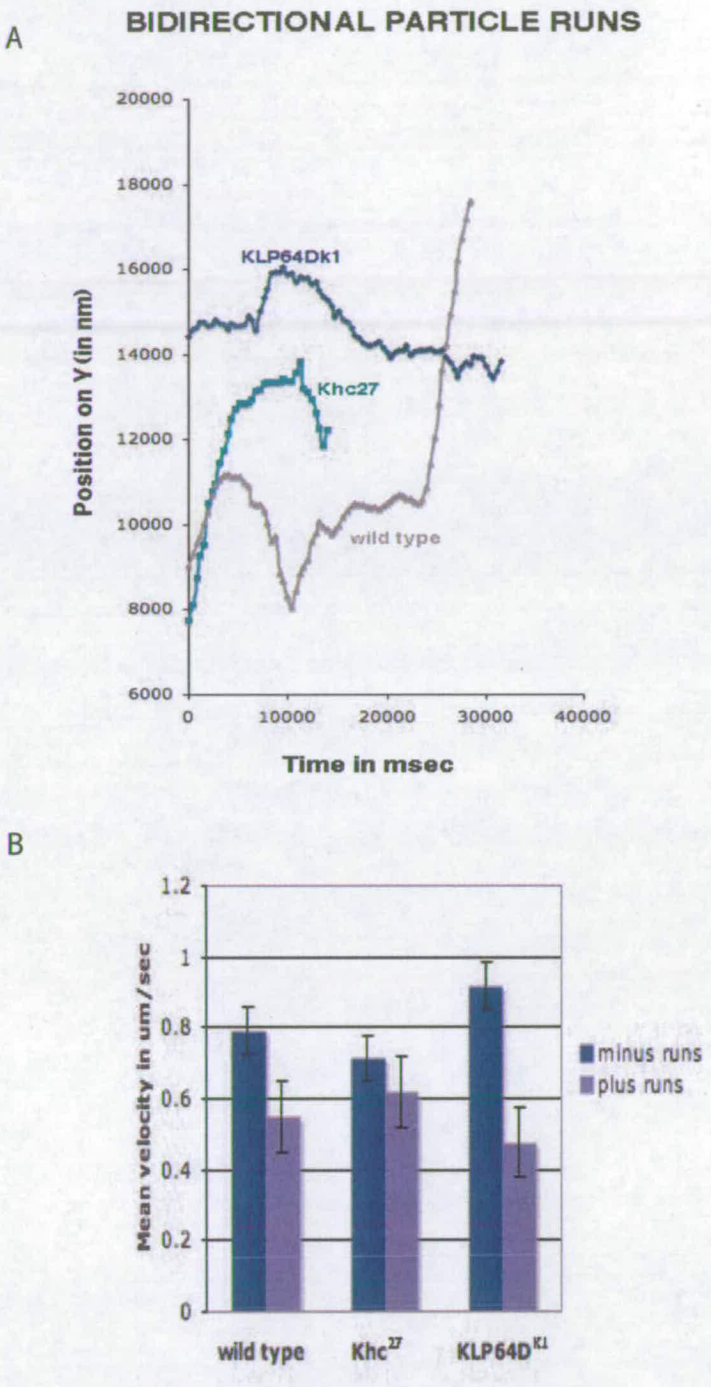


Figure 3.2.6: Bidirectional RNA motility in *Khc*^{27} and *KLP64D*^{k1} mutant embryos
ftz RNA moves bidirectionally in *Khc*^{27} and *KLP64D*^{k1} blastoderm embryos with similar kinetics to wild type. (A) Examples of bidirectional runs in wild type, *Khc*^{27} and *KLP64D*^{k1} embryos. (B) Mean velocity of minus and plus runs in wild type, *Khc*^{27} and *KLP64D*^{k1} embryos.

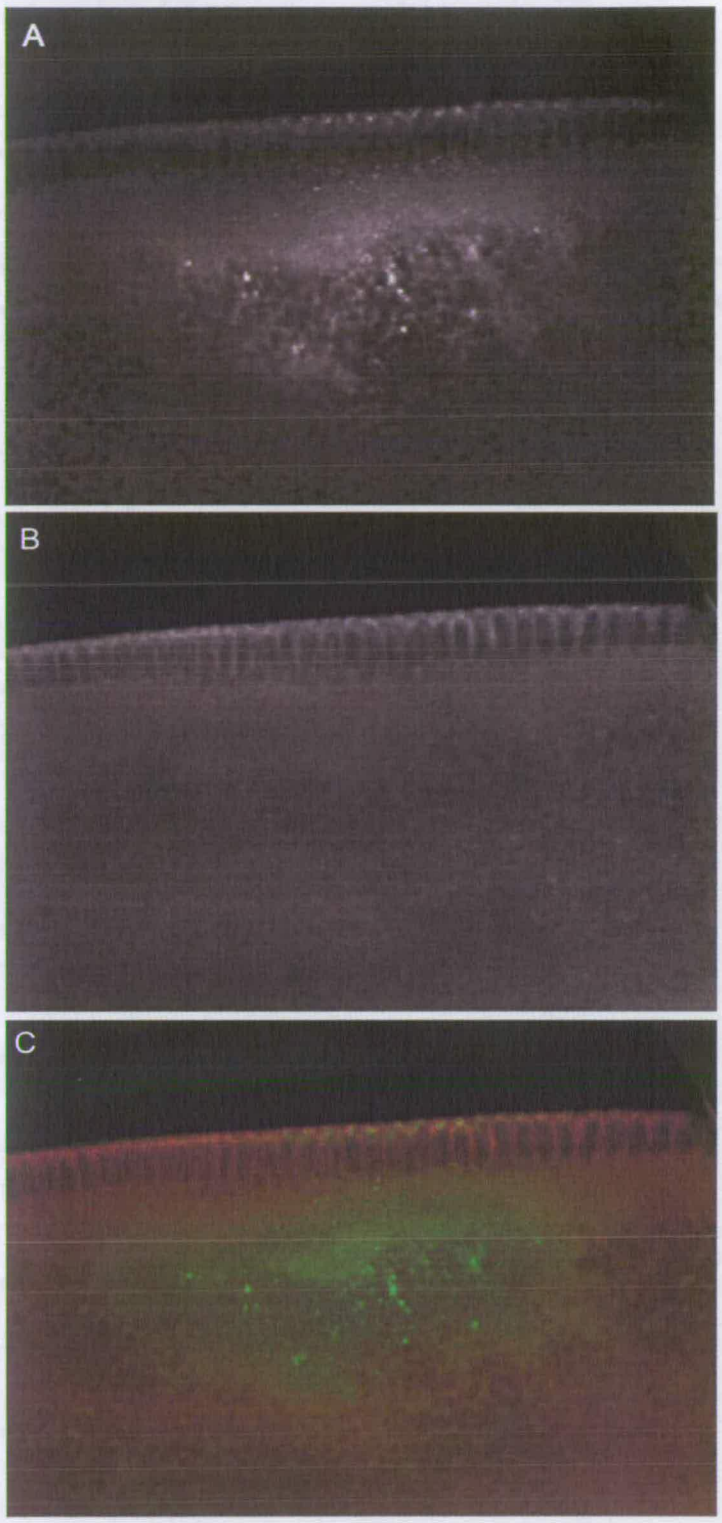


Figure 3.2.7 *ftz* RNA does not recruit Kinesin-1
(A) Injected biotinylated *ftz* RNA in *Drosophila* syncytial embryos. (B) Immunostaining against Khc in *Drosophila* syncytial embryos. (C) Merge image of (A) and (B). RNA is shown in green, Khc in red.

3.2.6 INTERFERENCE WITH DYNACTIN'S ACTIVITY INCREASES THE FREQUENCY OF PLUS RUNS AND DECREASES THE VELOCITY AND THE AVERAGE LENGTH OF MINUS END RUNS

In order to address whether dynactin regulates RNA bidirectional motility, I impaired the function of Glued. *Glued*^{1} is a spontaneous gain of function mutation (Plough and Ives, 1934) caused by the insertion of a transposable element near the 3' end of the gene (Swaroop *et al*, 1985). It codes for a truncated product, which can still associate with microtubules and dynein, but lacks the C-terminus domain that mediates its interaction with Arp-1 (McGrail *et al*, 1995). Therefore, it cannot assemble into the dynactin complex and is probably competing with the wild type product for dynein and microtubule binding sites, acting as an antimorph and poisoning dynactin's activity. The analysis of *Glued*^{1} and its genetic interaction with dynein heavy chain mutations (first shown by McGrail *et al*, 1995) has been proven a very powerful tool to study dynein/dynactin's function and has demonstrated Glued's important role in multiple processes during *Drosophila* development.

I injected *ftz* RNA into embryos laid from *Glued*^{1} heterozygous mothers (movie 3.2.6) and examined different parameters of movement, such as velocity of motion in both directions, frequency and length of plus and minus runs and frequency and duration of pauses. In the mutant embryos, particles pause and reverse direction more frequently than in wild type (Figure 3.2.8, Figure 3.2.9 and Figure 3.2.10A,C), but the average length and the velocity of the plus runs and are not severely affected (Figure 3.2.10B,D). Minus end motion is also severely disturbed, as expected. The average length, as well as the speed of minus runs is reduced compared with wild type (Figure 3.2.8, Figure 3.2.9 and Figure 3.2.10B,D). Injected RNA in *Glued*^{1} embryos localises strongly at the apical side of the nuclei. Endogenous pair rule RNAs, however, do not localise efficiently. In situ hybridization against *ftz* RNA (Delanoue and Davis, 2005) showed that some transcript fails to get transported towards the minus ends of MTs and remains

basally.

I tried to disrupt dynactin's function by injecting a large excess of p50/dynamitin in syncytial embryos. P50/dynamitin is positioned in the shoulder of dynactin and is crucial for dynactin's structure (Eckley *et al*, 1999). Overexpression of recombinant forms of dynamitin disrupts the complex and has been used as a tool to impair/abolish dynein's function and demonstrate a process's dependence on dynein. Overexpression of p50 resulted in pro-metaphase arrest in COS-7 cells (Echeverri *et al*, 1996), prophase arrest in *Drosophila* early embryos (Sharp *et al*, 2000) and impaired endocytic transport in fibroblasts (Valetti *et al*, 1999). Wilkie and Davis, 2002 showed that pair rule and *wingless* transcripts moved much slower upon injection of excess of p50/dynamitin in *Drosophila* embryos. They also observed for the first time particles displaying long backward runs after dynamitin's preinjection (Wilkie and Davis, unpublished data), but no such motility had been observed so far in wild type, so it was not tested if this observation significantly reflects increased plus motility due to dynactin's disruption.

I prepared GST-tagged and $(His)_6$ dynamitin, but preinjection of my preparation of the recombinant protein unfortunately did not severely affect RNA motility (not shown).

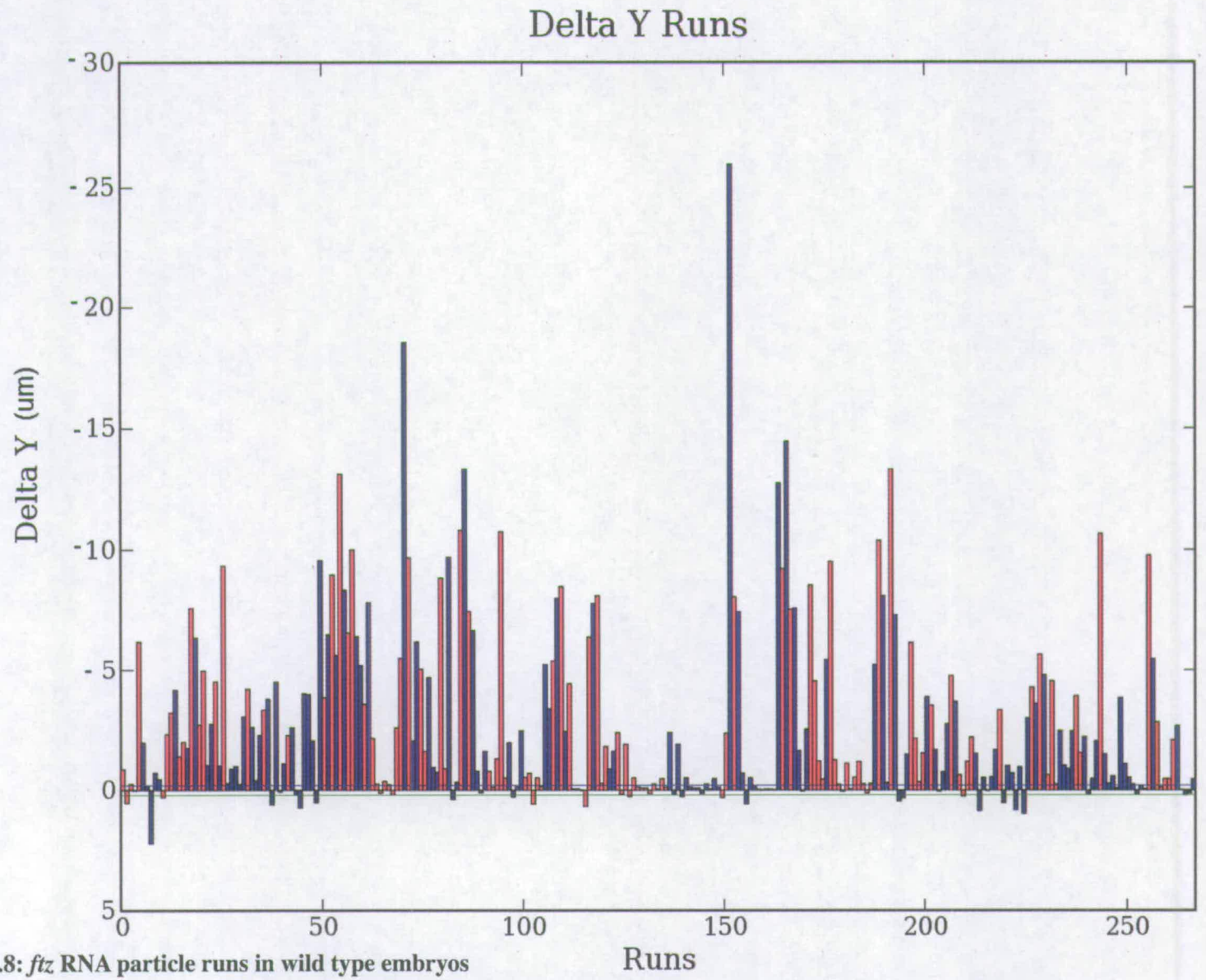


Figure 3.2.8: *ftz* RNA particle runs in wild type embryos

Change in color represents a new RNA particle analysed. The Y values of this graph represent um of distance covered in both directions, along the Y axis (data were rotated accordingly so that the Y axis was parallel to the apico-basal axis of the embryos). The values on X represent the number of particle runs analysed. Runs towards the minus ends of MTs (forward runs) are shown above the X axis and runs towards the plus ends of MTs (backward runs) are shown below the X axis.

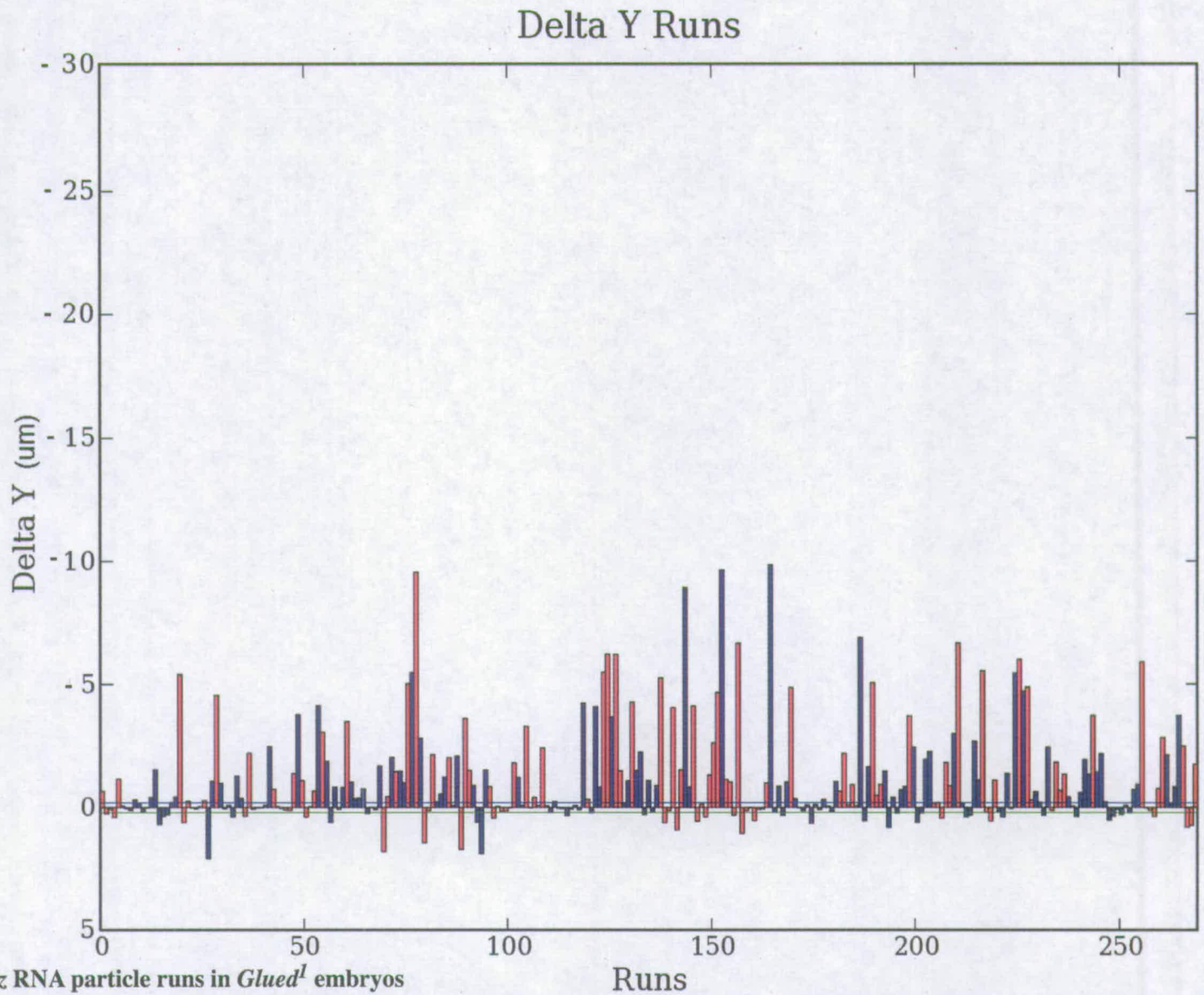


Figure 3.2.9: *ftz* RNA particle runs in *Glued*^{1} embryos

Change in color represents a new RNA particle analysed. The Y values of this graph represent um of distance covered in both directions, along the Y axis (data were rotated accordingly so that the Y axis was parallel to the apico-basal axis of the embryos). The values on X represent the number of particle runs analysed. Runs towards the minus ends of MTs (forward runs) are shown above the X axis and runs towards the plus ends of MTs (backward runs) are shown below the X axis.

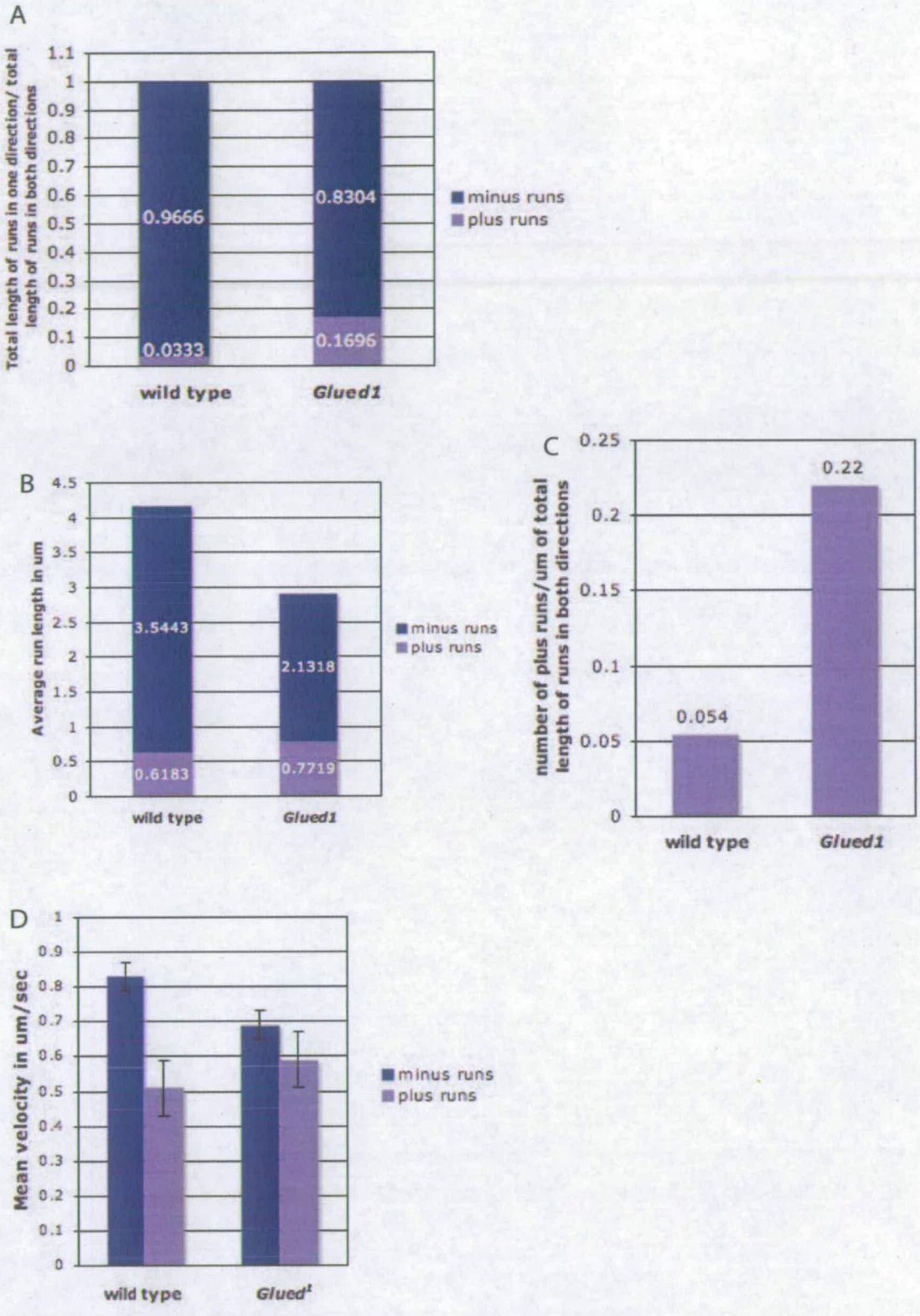


Figure 3.2.10 Glued suppresses bidirectional RNA motility

(A) Proportion of distance covered towards the minus and plus direction in wild type and *Glued*^{1} embryos. (B) Average run length of minus and plus runs in wild type and *Glued*^{1} embryos. (C) Frequency of plus runs in wild type and *Glued*^{1} embryos. (D) Mean velocity of minus and plus runs in wild type and *Glued*^{1} embryos.

3.2.7 STUDYING THE POTENTIAL ROLE OF LISSENCEPHALY-1 IN PLUS MOTILITY IN *DROSOPHILA* EMBRYOS

The *Drosophila* orthologue of the *Lissencephaly 1* disease gene, *DLis1* interacts genetically with *BicD*, *Glued* and *Dhc* (Swan *et al*, 1999, Lei and Warrior, 2000) and has well documented roles in nuclear positioning in oocytes and photoreceptor cells, in axonal transport, in nurse cell to oocyte transport, in synchronised germline cell division and oocyte determination and differentiation (Liu *et al*, 1999, Liu *et al*, 2000, Swan *et al*, 1999, Lei and Warrior, 2000). Its mode of function, however, is not clear. It could act as an adaptor, linking the dynein machinery to its cargoes, it could function as a cortical anchor for dynein and its cofactors, or it could actively regulate the motor.

Renald Delanoue in the lab (unpublished, preliminary work) observed that in syncytial blastoderm embryos preinjected with an antibody against Lis1, *ftz* RNA displayed long backward runs (not shown). In order to confirm that Lis1 indeed suppresses RNA backward motility, I used three mutant alleles, $DLis1^{11702}$ and $DLis1^{13209}$, both bearing P element insertions in the first intron of the gene and *Df(2R)JP8*, which lacks the region containing the *DLis1* gene. $DLis1^{11702}$, $DLis1^{13209}$ homozygotes lay very few eggs that are severely ventralised (Lei and Warrior, 2000) and do not develop (Delanoue, unpublished). I made $DLis1^{11702}/DLis1^{13209}$ and $DLis1^{11702}$/*Df(2R)JP8* transheterozygous females and crossed them with males of the same genotype. These females lay some apparently wildtype eggs, as reported before by Lei and Warrior, 2000, but these eggs arrest very early in embryogenesis. Only 0.3% of the eggs that I examined developed till the syncytial blastoderm stage. It was therefore difficult to perform detailed analysis of particle kinetics in these genetic backgrounds. I was only able to examine the distribution of endogenous and injected *ftz* RNA, by in situ hybridisation and injection of fluorescently labelled RNA respectively, and I found that it was indistinguishable from wild type (not shown). Due to lack of time, I did not pursue this further. It is worth testing in the future any possible

regulatory role of Lis1 in RNA motility in the embryo, by using inhibitory antibodies against the protein or generating more double heterozygotes, in order to test a satisfactory amount of syncytial embryos.

3.2.8 THE REGULATORS OF BIDIRECTIONAL MOTILITY KLARSICHT AND HALO ARE NOT INVOLVED IN RNA MOTILITY IN *DROSOPHILA* EMBRYOS

Lipid droplets in *Drosophila* embryos travel in a microtubule and dynein/dynactin dependent manner (Gross *et al*, 2000), exhibiting three distinct phases of bulk movement. In all three phases they move bidirectionally and their net displacement is determined by the amount of time they spend travelling towards each direction. At the beginning of blastoderm stages (phase I) they are found throughout the periphery of the embryo. During cellularisation (phase II) they clear the periphery and accumulate basally. The onset of gastrulation (phase III) corresponds to apical redistribution (Welte *et al*, 1998). These shifts dramatically change the opacity of the periphery of the embryo, which is opaque during phase I, transparent during phase II and becomes cloudy again during phase III.

Klarsicht mutants remain clear from gastrulation onwards, because their lipid droplets fail to redistribute throughout the periphery. However, the motion of individual droplets is slower and less frequent in all three phases. Klarsicht (Klar) is considered a central player in bidirectional transport of lipid droplets and other cargoes (Guo *et al*, 2004) and a core component of the complex that coordinates opposite polarity motors. Due to the apparent universality of Klar's function and the fact that lipid droplets and RNA utilise the same basic machinery for their transport, I investigated the role of Klar in RNA motility. I used $Klar^{A}$, $Klar^{B}$, $Klar^{1}$ and $Klar^{L}$ alleles. $Klar^{A}$ and $Klar^{B}$ are EMS alleles with a premature termination codon in the third exon of the gene, whereas $Klar^{1}$ (generated by Wieschaus and Nusslein-Volhart, 1986) bears a point mutation that introduces a stop codon at exon 14 (Guo *et al*, 2004). All three alleles have aberrant Klar staining and impair lipid droplets' transport. There is no molecular or functional information about $Klar^{L}$. I injected fluorescently labelled *ftz* RNA in embryos laid by $Klar^{A}$, $Klar^{B}$, $Klar^{1}$ and $Klar^{L}$ homozygous females and analysed the velocity

velocity of RNA particles. I did not detect any significant differences in the speed of transport of the RNA between wild type and mutant backgrounds (Fig 3.2.11A). We conclude that Klarsicht does not regulate RNA motility in *Drosophila* embryos.

Halo upregulates plus-end and downregulates minus-end motion of lipid droplets, functioning as a directionality determinant (Gross *et al*, 2003). As a result, *Halo* mutant embryos remain cloudy during cellularisation. I injected fluorescently labelled *ftz* RNA in *Halo* embryos and I was unable to visualise any RNA particles. Similar observations were previously made by Alejandra Clark in the lab. This is probably due to the opacity of the periphery of the embryo that disturbs imaging, rather than a lack of formation of particles, since injected and endogenous transcripts localise normally in the mutant embryos (Figure 3.2.11B,C).

We conclude that although RNA and lipid droplets share the same core localisation machinery (dynein and microtubules), their transport in the embryo is controlled by different regulatory factors.

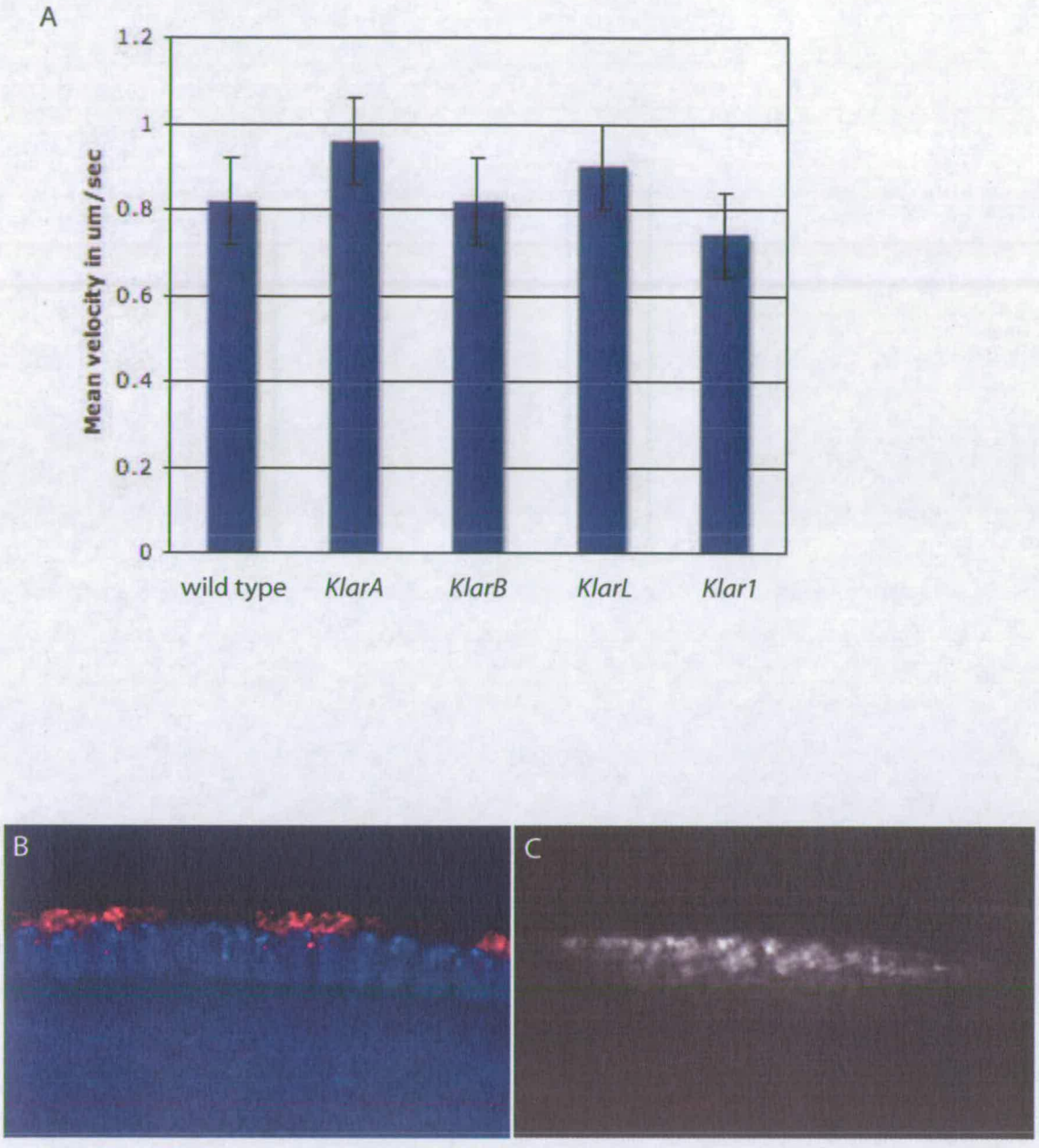


Figure 3.2.11: Wild type localisation of endogenous and injected *ftz* RNA in *Klar* mutant embryos

(A) Mean velocity of injected *ftz* RNA particles in wild type and *Klar* embryos. (B) In situ hybridisation against endogenous *ftz* RNA in *Halo* embryos. RNA is shown in red, DAPI staining in blue. (C) Apical localisation of injected *ftz* RNA in *Halo* embryos.

3.3 DISCUSSION

I improved our imaging and analysis and identified that pair rule RNAs, which are predominately transported towards the minus ends of microtubules, also display plus end directed runs. I tested various tracking softwares which allow us to track RNA particles in automated or semi-automated manner, with improved spatial resolution. I also designed together with Russell Hamilton (Davis lab) a new programme, ParticleStats, to analyse their motion more efficiently and in more detail.

I have shown that dynactin affects various physical properties of bidirectional motion of RNA in *Drosophila* embryos. Dynactin has been demonstrated to regulate bidirectional motility in diverse systems, although in the majority of the reported cases, there is no evidence suggesting which aspects of motility it affects. Both anterograde and retrograde endocytic transport in fibroblasts was affected by dynamitin overexpression (Valetti *et al*, 1999). In *Xenopus* melanophores, the Glued/p150 subunit of dynactin can bind the KAP (Kinesin associated protein) subunit of heterotrimeric Kinesin-2 (Deacon *et al*, 2003) and DIC, but not simultaneously, because the two motors compete for a common binding site on Glued. Antibodies against Glued blocked the movement of squid axoplasm organelles in either plus or minus direction (Waterman-Storer *et al*, 1997) and the *Glued*^{1} dominant negative mutation interfered with *Drosophila* lipid droplets' motility (Gross *et al*, 2002) and axonal transport of mitochondria (Martin *et al*, 1999) in both directions.

The observation that RNA particles move more frequently towards the plus ends of microtubules is also in agreement with other data (Delanoue and Davis, 2005), showing a slight basal shift in the distribution of the endogenous transcript in syncytial embryos. Gross *et al*, 2002 showed that *Glued*^{1} impairs, rather than enhancing plus motion. The differences between their results and ours could reflect different regulatory mechanisms between lipid droplets and RNA transport. Although both lipid droplets' and RNA motion are MT/dynein mediated, their

transport is likely to be controlled independently, as their destination during cellularisation is different. RNA localizes apically and lipid droplets accumulate basally. Indeed, Klar and Halo, which are key players in lipid droplet transport, are not involved in RNA motility. Moreover, *Klar* and *Halo* defects appear specific to lipid droplets in the mutant embryos, since the distribution of other organelles is normal (Welte *et al*, 1998, Gross *et al*, 2003).

In order to identify the motor that drives the RNA towards the plus ends of MTs in syncytial embryos, I made germline clones of Kinesin-1 and Kinesin-2 lethal, null mutations. The lack of significant effects on RNA motility in embryos laid by the mutant mothers suggests that neither Kinesin I nor Kinesin II mediate the observed plus motility.

I also tried to inhibit Kinesin-1 by preinjecting an antibody against Khc. I did not detect any effect on RNA motility upon injection of the antibody, however this experiment is not conclusive, since we had no positive control that the antibody could indeed block kinesin's function. Control injections in oocytes performed by myself and Renald Delanoue in the lab, did not impair ooplasmic streaming, as it had been previously reported by Serbus *et al*, 2005. In order to abolish the function of Kinesin II, I took a dominant-negative approach established by Tuma *et al*, 1998. The authors generated a headless Xklp3 (motor subunit of Xenopus Kinesin-2), in which the motor domain was replaced by EGFP. Overexpression of the fusion protein inhibited pigment dispersion and ER to Golgi transport in melanophores (Tuma *et al*, 1998, Le Bot *et al*, 1998). I cloned the headless Xklp3-EGFP fusion in a vector containing T7 promoter site, polyadenylation signals and a translation initiation sites and tried to abolish the function of Kinesin-2 in *Drosophila* embryos, by injecting in vitro transcribed RNA or in vitro translated protein. No significant effects in RNA transport were observed, but there is no evidence that the *Xenopus* protein can incorporate in the *Drosophila* complex and impair its activity.

Among all the members of the Kinesin superfamily, Kinesin-1, heterotrimeric Kinesin-2 and Kinesin-3 (see Chapter 1) are considered as the major or perhaps the only cargo transporters in the cell (Vale, 2004). I did not test the involvement of Kinesin-3 in RNA motility, because there are no available mutants or nearby transposable element insertions that could be used to create deletions by imprecise excision. Nevertheless, I consider its involvement very unlikely. The reason is that although Kinesin-3 has a well documented general role in membrane trafficking in lower eukaryotes, its metazoan orthologs are less abundant than Kinesin-1 and Kinesin-2 and are considered to be specialised in the transport of synaptic vehicles in neurons, rather than having a general function in cargo transport (Vale, 2004). The *Drosophila* ortholog, also known as Kinesin-73, has not been implicated in cellular transport so far.

I cannot categorically exclude the possibility that the RNA in our case is transported towards the plus ends of MTs with another kinesin related protein. I therefore searched the *Drosophila* genome for kinesin related proteins and I indeed found some, namely KLP3A, KLP67A, KLP61F, KLP59C, KLP38B and pavarroti, that are expressed in early embryos and have a reported motor activity. I do not consider any of these proteins good candidates for RNA motility. None of them has a documented role in cargo transport and their role is most likely limited to their already known functions in spindle assembly, chromosome motility, cytokinesis or microtubule depolymerisation, as it has also been suggested for their orthologs in other organisms. Moreover, most of the available mutants are lethals and in order to test if these motors mediate RNA transport, I would have to make germline clones or create new hypomorphic alleles. For the above reasons and due to lack of time, I decided not to pursue this further. The remaining kinesin-like proteins that were found in our searches are either not expressed in early embryos or it not known whether they have motor activity or only show homology with kinesin.

If RNA is directed towards the plus ends by a kinesin related protein, then dynactin's role could be to balance the power between the opposite polarity motors (dynein and

kinesin) or, more likely, to regulate their coordination. The observed increase of the frequency of plus runs in *Glued*[1] embryos could reflect a lack of regulation or shift of balance resulting from the interference with dynactin's activity.

It is interesting to consider whether the plus end motility we observe could be due to the dynein motor itself. The rule that a superfamily of motors moves only towards one direction and that a given motor is unidirectional was first challenged with the discovery of Myosin VI and ncd. Myosin VI, unlike other members of the myosin superfamily, moves towards the polymerising end of actin (Wells *et al*, 1999). In contrast with other kinesins that have their motor head at the N-terminus of their heavy chain, Ncd has its motor domain at the C-terminus (Sablin *et al*, 1998) and moves towards the minus ends of MTs (MacDonald *et al*, 1990). A mutant form of ncd, with only one amino acid different in the motor neck, switches stochastically between plus and minus directed motion (Endow *et al*, 2000).

The dynein family of motors includes axonemal and cytoplasmic dyneins. Both types move towards the minus ends of MTs. However, it has been shown that flagellar dynein undergoes thermal driven one-dimensional bidirectional diffusion along MTs *in vitro* (Vale *et al*, 1989). More recently, cytoplasmic dynein was shown to bind MTs with low affinity and slide back, towards the plus ends (Wang and Sheetz, 1999). The weak, electrostatic interaction and the random walk of flagellar and cytoplasmic dynein along the microtubule axis are ATP dependent, but distinct from the strong binding that is responsible for active motility by ATP hydrolysis. Its significance could lie in preventing the motor from "falling off" when it dissociates. In an in vitro study, Mallik *et al*, 2005 showed that single molecules of cytoplasmic dynein frequently undergo a transition to an unproductive state, when the motor pauses or reverses course. The backward segments can be up to 0.8μm and account for almost 20% of the net distance covered by the motor. The backward slippage increases with load and is dramatically suppressed (frequency and length of plus runs are reduced) with the employment of multiple dyneins.

Our short plus end directed episodes, that interrupt the predominant minus runs, could simply represent this kind of "off pathway" unproductive intervals. Dynein loses its strong contact with the MT and cannot generate power strokes, but stays bound weakly and passively diffuses back. We cannot easily compare the detailed properties of our in vivo plus motion with dynein's slippage in vitro. Mallik *et al* have no dynactin or other cytoplasmic determinants-dynein cofactors in their assay and they use beads as cargoes. They also employ imaging, tracking and analysis methods that are very different to ours. The characteristics of our plus runs, though, are quite similar to what they observe in vitro. Our runs are not much longer than 0.8μm, which is their maximum plus run length and they do not represent more than 20% of the net distance covered in any genetic background tested.

I injected RNA in embryos laid by mothers heterozygous for the *DHC64C6-6*, a strong, recessive lethal allele, to test if the decrease of the amount of functional dynein would affect the frequency or the physical aspects of our plus runs. In almost half of the injected embryos, I observed more frequent backward runs. Due to lack of time and the difficulty of these experiments, I did not perform further injections and systematic analysis of the data, which would be necessary to confirm this preliminary observation.

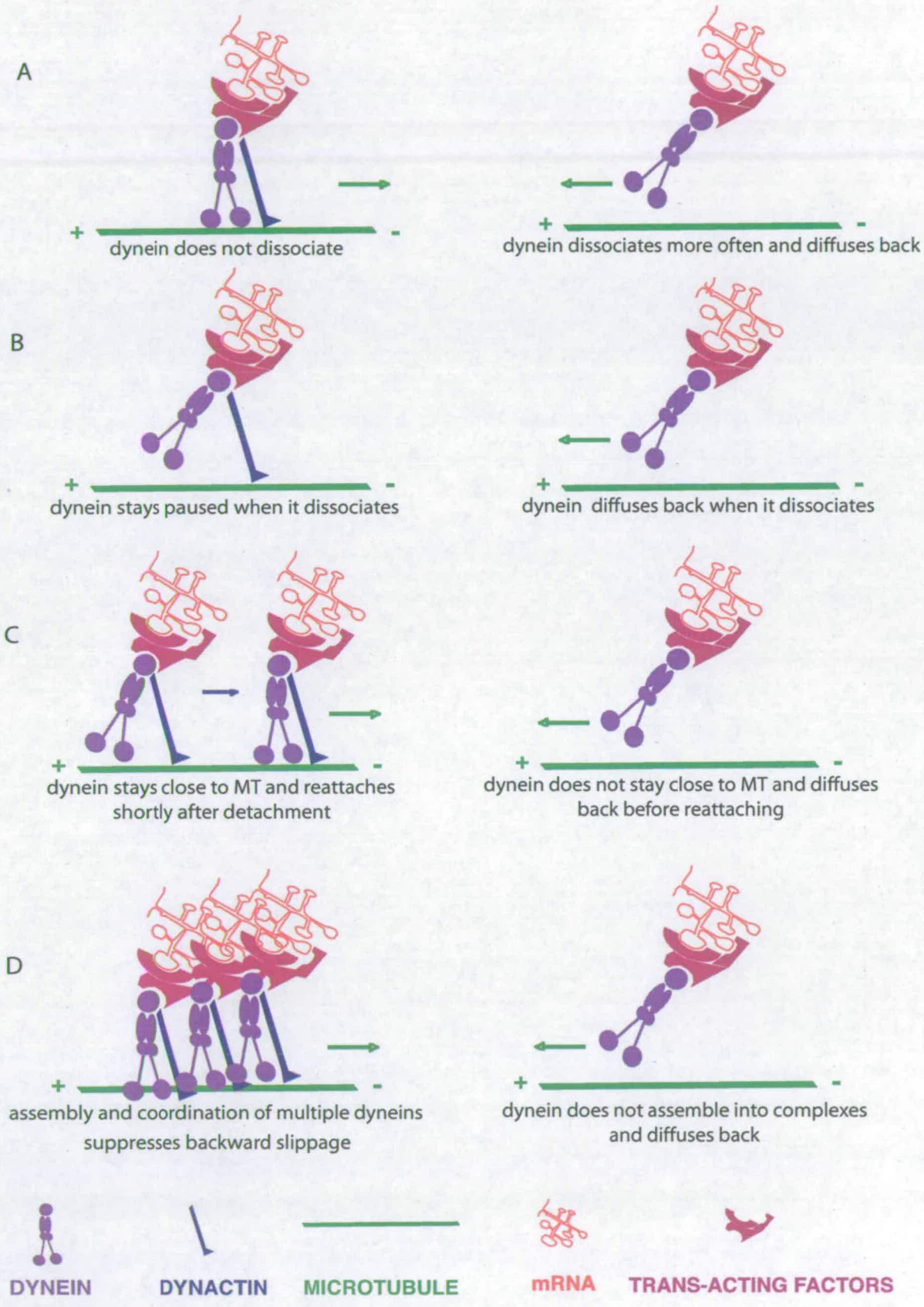
Although our data do not demonstrate that dynein itself is responsible for the plus end RNA motility, this seems like a plausible explanation. If dynein can move towards the plus ends of MTs, then there is not need for the RNA to recruit and employ kinesin. It has been shown or suggested for various bidirectional cargoes that they utilize both motors. In all these cases, however, the plus motion is not just interrupting occasionally the minus motion, but is actually the dominant motion at some phase of the cargo's journey. For instance, mitochondria in *Drosophila* axons move towards the growth cones with Kinesin-1 when the axon is growing and later return to the centre of the cell with dynein when growth cone activity stops. Frog melanophores disperse with Kinesin-2 at high levels of cAMP and aggregate with dynein when the levels of cAMP drop. In *Drosophila* embryos, lipid droplets move

towards the plus ends of MTs, to clear the peripheral cytoplasm, before moving apically, in order to accumulate into the forming cells. Apical RNA, unlike all these cargoes, does not accumulate basally, so it does not necessarily require kinesin mediated transport at any phase of its life.

If dynein is indeed the motor that "drags" the RNA particles towards the plus ends of MTs, then there are different models that could explain dynactin's involvement in the process. Given that dynein's strong binding has a probability to fail at each step and that dynactin, via its p150/Glued arm, can provide an additional interaction between dynein and the microtubule, then dynactin could eliminate dynein's backward slippage by various means (Figure 3.3.1):

1) stabilising dynein onto MTs, so that it does not detach that often,
2) stabilising dynein onto MTs, so that when it dissociates, it stays paused or flunctuates, instead of diffusing back,
3) holding the motor close to and with the right orientation along the MT track, when it dissociates, so that it can immediately reengage before slipping back or
4) assemble and/or coordinate multiple dyneins together, thus suppressing backwards slippage. Dynactin is not required for the assembly and the coordination of the multi-motor complex *in vitro*, but it could have such a regulatory role *in vivo*.

Figure 3.3.1: Dynactin could suppress dynein's backward slippage by various means
Note that dynein has two MT binding domains, one that mediates strong binding and is responsible for the generation of power strokes and active motility and one that mediates a weak electrostatic interaction with the MT and is implicated in one-dimentional diffusion.
In this cartoon, the term "dissociates" refers to the failure of dynein's strong binding and dynein is shown detached from the MT when this binding has failed. The weak interaction that mediates the shown backwards sliding, is not illustrated.


FUNCTIONAL DYNACTIN
NO FUNCTIONAL DYNACTIN
A
+
-
dynein does not dissociate
dynein dissociates more often and diffuses back
B
dynein stays paused when it dissociates
dynein diffuses back when it dissociates
C
dynein stays close to MT and reattaches shortly after detachment
dynein does not stay close to MT and diffuses back before reattaching
D
assembly and coordination of multiple dyneins suppresses backward slippage
dynein does not assemble into complexes and diffuses back
DYNEIN
DYNACTIN
MICROTUBULE
mRNA
TRANS-ACTING FACTORS

A recent study by Culver-Hanlon *et al*, 2006 reveals a highly basic microtubule binding domain in chicken Glued that lies downstream of the previously known (Vaughan and Vale, 1995, Waterman-Storer *et al*, 1995) CAP-Gly microtubule binding site. The authors show that this domain can "skate" along MT tracks in the absence of molecular motors. It is worth mentioning here that this skating is almost an order of magnitude slower and much shorter in length than our plus runs and even if the *Drosophila* homolog can undergo skating events, these could not account for our observed backward motility. Culver-Hanlon *et al* also demonstrated that the identified basic domain is sufficient to increase dynein's processivity in vitro, in contrast to the CAP-Gly domain that acts as a brake, abolishing dynein-driven motility. The N-terminus of bovine brain Glued that contains both MT binding sites has been shown to be required in vitro for the enhancement of dynein's processivity (King and Shroer, 2000). It is not known, however, if it is also sufficient for this enhancement or if other domains of the polypeptide function as processivity cofactors. *Drosophila* Glued lacks the basic domain that is the skating-processivity factor in the chichen polypeptide. It does contain the CAP-Gly microtubule binding site, but this site has not been demonstrated to be necessary or sufficient to increase dynein's processivity.

It is clear that the C-terminus of Glued or the other components of the dynactin complex, whose association with dynein it mediates, have a direct effect on dynein motility or at least they are important for Glued to fold properly, so that its NH2-terminus can bind both MTs and dynein and function as a processivity factor. There is evidence that the Glued[1] truncated product (which we used to interfere with dynactin's activity), that lacks the C-terminus, alters physical parameters of lipid droplets' motion in *Drosophila* embryos (Gross *et al*, 2000). This effect is similar to our results and distinct from a possible indirect role of Glued's C-terminus in recruiting dynein to its cargoes through its interaction with Arp-1 (see introduction of this Chapter).

It is interesting to cite here a recent report by Ross *et al*. The authors suggest that the

plus runs of dynein result from active steps taken by the motor and not from backward slippage, as it has been suggested by Wang and Sheetz, 1999 and Mallik *et al*, 2005. Their model is supported by the dependence of the speed of the plus runs on ATP concentration and by the flexibility of dynein heavy chain, which could allow the motor to rotate and stroke towards the opposite direction.

Despite being apparently inefficient and potentially energy wasteful, bidirectional transport of cargoes by molecular motors is widespread. While the significance of bidirectional motility is still not entirely clear, it has been discussed that it allows more flexible regulation of cargo destination by adjusting quickly the net transport in response to signals. It could also correct errors, provide a means to randomly distribute cargo within a cell or enable stuck cargoes to circumvent obstructions (Welte, 2004).

In the case of apical transport of RNA, the plus motility of apical RNA particles is short and infrequent, and does not significantly interfere with the overall net apical displacement. We propose that by reversing their course, the RNA particles are able to avoid locked-up motors, stuck organelles or other cytoplasmic barriers. By stepping back, RNA cargo-motor complexes maybe able to navigate the space and switch MT tracks, in order to avoid traffic jams. Indeed, I frequently observe *ftz* RNA particles hesitating in a given position for some time and then displaying backward movement for a short time, followed by a further reversal and apical movement on the same path leading to motility directly past the original stalled site. In such cases, we occasionally observe, a little later, other particles pausing or changing direction at the exact same position, suggesting that an obstacle exists at that location.

CHAPTER 4

Identification of novel localising transcripts during *Drosophila* oogenesis and embryogenesis:

Experimental validation of novel bioinformatics approaches for the identification of genes containing RNA localisation signals

4.1 INTRODUCTION

4.1.1 *GURKEN* AND THE *I* FACTOR TRANSCRIPTS SHARE A CONSENSUS LOCALISATION SIGNAL

Grk encodes a TGFα signal that establishes both the antero-posterior and dorso-ventral axes during early *Drosophila* oogenesis. *Grk* RNA first localises at the posterior, where the translated protein induces the reorganisation of the microtubule cytoskeleton and later at the dorso-anterior corner, at a crescent near the oocyte nucleus, where Grk protein determines dorsal embryonic fates and defines eggshell structures (Gonzalez-Reyes, 1995, Roth *et al*, 1995, Neuman-Silberberg *et al*, 1993, Sen *et al*, 1998).

The *I* factor is a non-LTR retrotransposon, similar to human LINE1 elements, which constitute a substantial proportion of the human genome. It encodes a nucleic acid binding protein (Dawson *et al*, 1997) and a protein with putative endonuclease, reverse transcriptase and RNaseH domains (Fawcett *et al*, 1986). The *I* factor, like other retrotransposons, transposes via an RNA intermediate. *I* factor RNA localises at the dorso-anterior corner, as well as the anterior margin of the oocyte (Seleme Mdel *et al*, 2005). It is thought that the localisation of the transcript near the oocyte nucleus facilitates nuclear entry of the *I* factor RNA intermediate, that is crucial for transposition and transmission into the next generation.

When *gurken* or *I* factor RNA are injected into the oocyte, they localise in two microtubule and dynein dependent steps, first at the anterior and then to a dorso-anterior crescent, reproducing the localisation pattern of the endogenous *grk* transcript (MacDougall *et al*, 2004, Van de Bor *et al*, 2005). *grk* and the *I* factor show limited sequence similarity, but share a consensus RNA stem loop of defined predicted secondary structure (Van de Bor *et al*, 2005, Figure 4.1.1). These motifs, named *GLS* (*grk* localisation signal) and *ILS* (*I* factor localisation signal), are necessary for localisation, since their deletion abolishes it. Moreover, they are both

sufficient to utilise the dynein/MT machinery and target themselves or heterologous, non-localising RNAs to the dorso-anterior cap, near the oocyte nucleus. Interestingly, *grk* and the *I* factor, as well as the *GLS* and *ILS* alone, not only recruit the same transport machinery, but also compete for at least some of its components. This has been demonstated by co-injection competition experiments and more importantly by the mislocalisation of the endogenous *grk* transcript, when *I* factor transposition is active (Van de Bor *et al*, 2005).

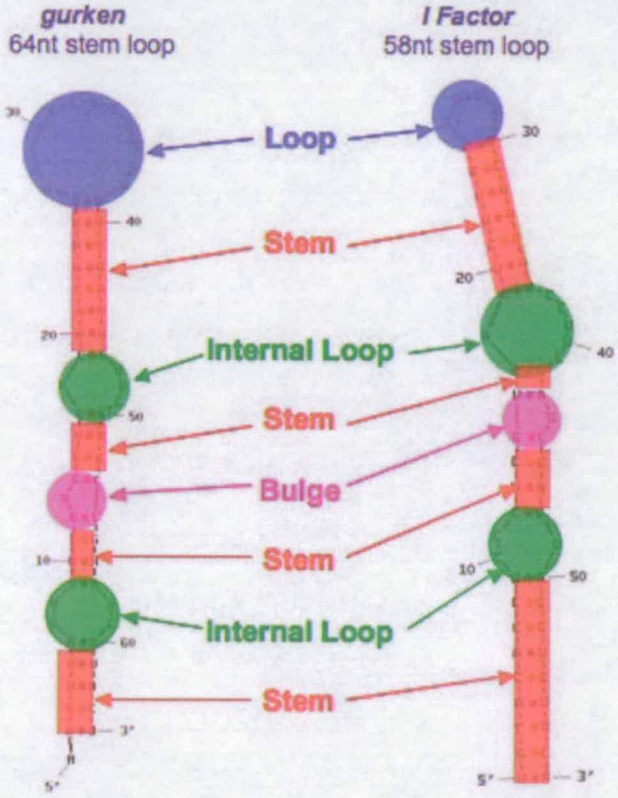


Figure 4.1.1: *GLS* and *ILS* share a similar predicted secondary structure (courtesy of Russell Hamilton).

4.1.2 GENOME-WIDE SEARCHES FOR LOCALISATION MOTIFS SIMILAR TO *GLS* AND *ILS*

Among all the localisation elements that have been characterised so far in detail in *Drosophila* (see Chapter 1), there is only one case, other than *grk* and the *I* factor, where a consensus destination signal between different transcripts has been defined. *K10* and *orb* anterior sorting is mediated by signals that are very similar at primary sequence and secondary structure level (Serano and Cohen, 1995, Cohen *et al*, 2005). In the other reported cases, no sequence or structure similarity has been observed even between localisation elements of transcripts that employ the same transport mechanism and share common temporal and spatial localisation patterns. For instance, *hairy* and *wingless* transcripts localise apically in *Drosophila* syncytial blastoderm embryos, in a MT and dynein/dynactin dependent manner, but no obvious similarity arises by comparing their localisation signals. Moreover, other *Drosophila* apically localised transcripts, such as *ftz* and *eve* share no homology among their 3'UTRs, the regions within which their localisation elements have been crudely mapped.

It is currently unclear whether *grk* and the *I* factor are the only RNAs that localise at the dorso-anterior corner of the *Drosophila* oocyte, as no systematic genome-wide in situ hybridisations have been so far performed in oocytes. We set out to test the hypothesis that other gene transcripts contain related motifs and localise in a similar manner, to restrict or enrich their products near the nucleus. Furthermore, we wanted to address whether other transposable elements recruit the host machinery to target transposition into the oocyte genome and ensure transmission to the next generation. We also wondered whether the concensus between the *ILS* and *GLS* could in some way provide insight into identifying a concensus for embryonic apical localisation of RNA.

GLS and *ILS* share very little primary sequence similarity, pointing against sequence based methods to identify other similar localisation elements. Indeed, even advanced bioinformatics algorithms for primary sequence searches have proven unfruitful in

this respect (Hamilton and Davis, unpublished observations). A novel bioinformatics tool to search the *Drosophila* genome using *grk* and *I* factor secondary structure consensus as a template was developed in the Davis lab by Russell Hamilton. An outline of the method is shown in Figure 4.1.2 and a more detailed explanation in Figure 4.1.3.

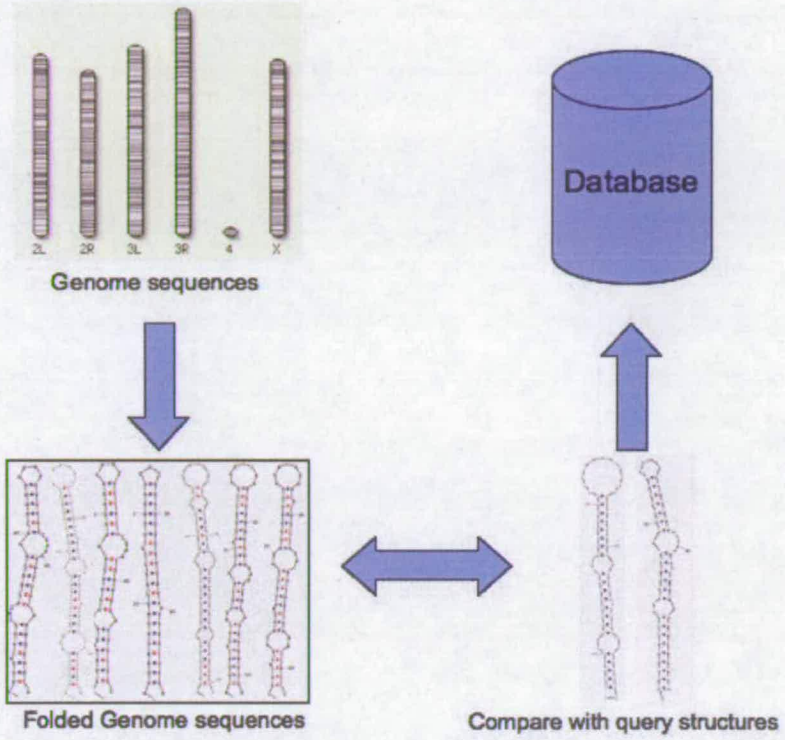


Figure 4.1.2: An outline of the Bioinformatics approach (courtesy of Russell Hamilton).

The method (Figure 4.1.3) uses RNALfold (Hofacker *et al*, 2004) to fold large RNA sequences from various *Drosophila* sequence databases (whole genes, CDSs, 5'UTRs, 3'UTRs, transposable elements) and output stable secondary structures of a given size, window lengths of 58 and 64nt in our case, which is the length of *GLS* and *ILS* respectively. The predicted stable structures are then compared to *GLS* and *ILS*, using RNAdistance (Hofacker *et al*, 2003) and RNAMotif (Macke *et al*, 2001). RNAdistance calculates similarity between the predicted structures and the template and outputs a score. RNAMotif pattern matches the predicted structures against a

structure description. The structure definition that was used in our case is flexible enough to match both *GLS* and *ILS* (see 4.2.4). The putative localisation elements identified by the searches are stored in a web-based database found at http://129.215.14.55/cgi-rna/RNASearch.pl or http://wcbweb.icmb.ed.ac.uk/~ilan/bioinformatics.html.

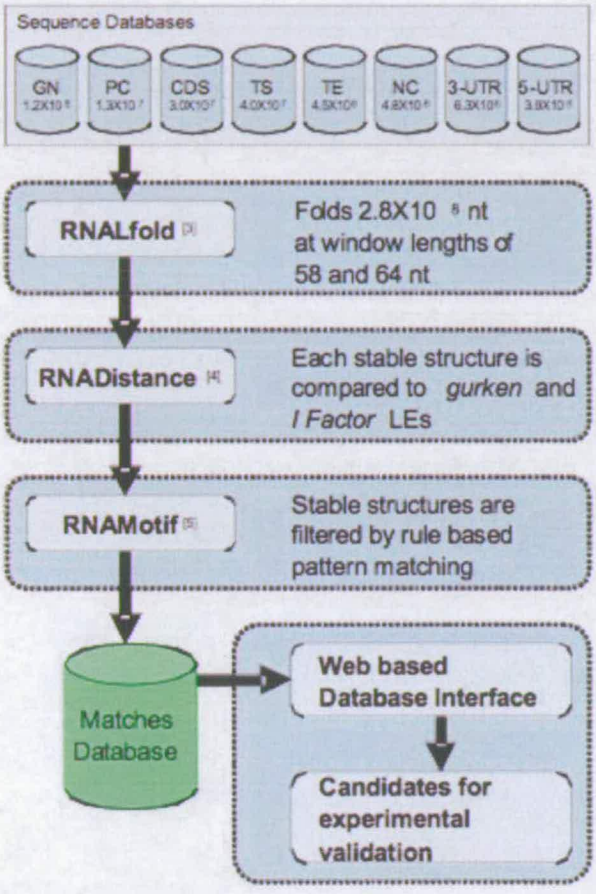


Figure 4.1.3: A detailed description of the bioinformatics tool (courtesy of Russell Hamilton). RNALfold, RNAdistance and RNAMotif are employed to find secondary structures similar to *GLS* and *ILS*. The data are then stored in a database with a web interface.

4.1.3 AIM OF THIS CHAPTER

The aim of this chapter was the genome-wide identification of *Drosophila* localisation elements and localising transcripts. To achieve this, we determined experimentally the localisation potential of RNAs that contain putative localisation motifs similar to the *GLS* and *ILS*. Furthermore, we addressed whether the predicted localisation elements are the signals responsible for the localisation of these transcripts. This project was performed by an interdisciplinary team of people in Ilan Davis's and David Finnegan's labs and includes two independent screens, the "gene screen" and the "transposable element screen", which test transcripts expressed from *Drosophila* genes and transcripts expressed from *Drosophila* transposable elements respectively. My work described in this chapter focused primarily on the "gene screen", but I made some important contributions to the transposable element screen and worked closely within this collaborative team in providing feedback and discussion to the development and revision of the bioinformatics approaches.

This chapter focuses mostly on the gene screen, although the transposable element screen is also described briefly to provide context. Section 4.2.1 presents the experimental assay. Section 4.2.2 describes a pilot screen, which assesses the localisation success of bioinformatics candidates that have been previously classified as localising by in situ hybridisation data (Tomancak *et al*, 2002). Sections 4.2.3, 4.2.4 and 4.2.5 present the experimental validation of two subclasses of RNAdistance and RNAMotif candidates: transcripts that contain at least one RNAdistance or RNAMotif hit in their 3'UTR and transcripts that contain hit(s) only in their 5'UTR or CDS. The localisation potential of a random pool of transcripts is tested in 4.2.6. The experiments described in 4.2.1 and 4.2.2 were designed and performed by myself. The work presented in 4.2.3, 4.2.4, 4.2.5 and 4.2.6 was designed and performed independently by myself and Veronique Van de Bor. Veronique's contribution is stated clearly in the results section. Her results are not always shown in full detail, but are discussed and have been taken into account in the

conclusions. Daniel Maskell, an undergraduate student in the Davis lab, performed, under my guidance and supervision, some of the work presented in 4.2.4B2.

The transposable element screen was mainly carried out by Eve Hartswood, Cheryl Jones and David Finnegan. I performed a few experiments presented in 4.2.7 and I also contributed to the design and the interpretation of some of their work. Their results are not shown, but are summarised and have been taken into account in the conclusions. Finally, in 4.2.8, 4.2.9 and 4.2.10, I describe some other interesting observations that we made while carrying out these screens and we consider worth of further investigation.

The main goal of this project was to evaluate experimentally our bioinformatics approach and explore whether and how bioinformatics tools can be used for the identification of RNA localisation signals in a genome-wide scale. The results section of this chapter mainly focuses on this theme. However, our work inevitably lead to the discovery of sequence and structural elements required for localisation and provided useful biological information for future improved bioinformatics screening approaches. The identification of novel localising transcripts during *Drosophila* oogenesis and embryogenesis was also inseparably linked to this screen. These aspects of the project and the importance of our findings are highlighted in the discussion of this chapter.

4.2 RESULTS

4.2.1 EXPERIMENTAL ASSAY

We assessed the localisation potential of the bioinformatics candidates mainly by injection of fluorescently labelled RNAs that we transcribed in vitro from full-length cDNA clones. We used cDNA clones, rather than genomic DNA as a template and we performed the injections in the cytoplasm, assuming that intronic sequences and nuclear history of our candidate transcripts are not essential for localisation. With the exception of *oskar*, whose posterior localisation in the oocyte is dependent on components of the exon-exon junction complex and requires splicing in the nucleus (Hachet and Ephrussi, 2004), all maternal and early embryonic RNAs, whose mechanism of localisation has been studied so far, do not require any nuclear processing for their localisation in the cytoplasm. Transcripts lacking introns localise correctly, reproducing the pattern of the endogenous messages, upon injection into the cytoplasm of oocytes, nurse cells or blastoderms. In any case, it is unlikely that signals related to *GLS* and *ILS*, would, unlike *GLS* and *ILS*, require nuclear determinants in order to be transported within the cytoplasm. Even if nuclear history is nevertheless fundamental for the cytoplasmic destination of some of these transcripts, we chose to ignore it, in order to bypass cloning of genomic sequences, preincubation of the RNAs with nuclear extracts or nuclear injections, which would be technically challenging and would make the screen impractical.

We performed the screen primarily in syncytial blastoderm embryos. *grk* and the *I* factor are not expressed in embryos. However, both transcripts, as well as *GLS* and *ILS*, localise apically upon injection into embryos (Van de Bor *et al*, 2005, MacDougall *et al*, 2003), utilising the same core transport machinery (dynein/MTs) that they use in the oocyte. It is known that other ectopic transcripts, like *K10* and *inscuteable* that localise in oocytes and neuroblasts respectively, also localise after injection into blastoderms (Bullock *et al*, 2001, Hughes *et al*, 2004). It seems that the embryonic transport system is quite promiscuous and can drive various ectopically

provided cargoes. We chose embryos over oocytes because embryo injections are simpler, less time consuming and more efficient than injections in the oocyte and thus more appropriate for a high-throughput screen. The transcripts that localised in embryos were further injected into oocytes, to test whether they localise like *grk* and the *I* factor.

In the Davis lab, we have been routinely using linearised plasmids as templates for in vitro transcription. Because the cDNA clones used in this screen are all inserted in only four different types of plasmids, we thought it would be more rapid to PCR them out from their vectors with common sets of primers and use the PCR products, rather than the linearised vectors, as templates. I tested the efficiency of the assay by testing 19 candidate RNAs made from PCR product templates. None of these transcripts localised upon injection into blastoderm embryos.

I performed some control injections of *runt/GH02614* transcript prepared from PCR products or linearised plasmid. Although two different preparations of *runt* RNA transcribed from the linearised plasmid localised strongly and efficiently, as expected, RNA prepared from four different PCR products failed to localise or localised very poorly in the vast majority of the injected embryos. We do not know if the inefficiency of the transcripts to localise is due to mutations introduced to the cDNA clone by the polymerase during amplification or due to other factors, but this phenomenon was also observed later for other transcripts, like *CG1841/HL07962* (mentioned later in this chapter) and transposable element RNAs (Eve Hartswood and Cheryl Jones, personal communication), which only localise when prepared from plasmid templates. We thus decided to perform the screen using linearised plasmids as templates for the in vitro transcription reaction and do not take into account the results of the injection of the 19 candidate RNAs prepared from PCR products.

4.2.2 PILOT SCREEN – DETERMINATION OF THE LOCALISATION POTENTIAL OF TRANSCRIPTS THAT CONTAIN RNADistance HITS AND ARE KNOWN TO LOCALISE DURING EMBRYOGENESIS

In order to perform a pilot screen, I biased the selection of candidates by choosing transcripts that are considered as localising during embryogenesis, based on in situ hybridisation data. This selection was aiming at identifying rapidly some localising transcripts using the injection assay and providing me with new RNA localisation signals, whose requirement for localisation could be tested.

4.2.2.1 Selection of candidates and assessing their localisation potential

I searched the BDGP expression pattern site at http://www.fruitfly.org/cgi-bin/ex/basic.pl for transcripts documented as localised during embryogenesis (Tomancak *et al*, 2002). The ones whose subcellular distribution was clearly asymmetrical, as judged by examining digital images, were selected for injection, whereas the ones which rather or only showed localised expression in particular tissues or broad regions of the embryos were ignored. All of the selected transcripts contained at least one RNAdistance hit and are listed in Table 4.2.1. *fat-spondin/CG6953/HL01082* is asymmetrically distributed in macrophages. The expression pattern of *CG10917/RE18087* is characteristic of pair rule genes and *slmb/CG3412/LD08669* is apically localised in syncytial embryos and invaginating cells (Figure 4.2.1B,C). *Bsg25A/CG12205/RE24665* shows a punctuate localisation in early embryo epithelials, *CG1962/LD41224* is centrosomic (Figure 4.2.2B,C) and *GUK-h/CG31043/GM06978* is concentrated basally, underneath the nuclei of syncytial embryos. *pxb/CG33207/RE16319* is expressed in pair rule stripes early in embryogenesis, in segment polarity stripes in gastrulating embryos and also shows an apical enrichment. Finally, *Dcp-1/CG5370/LD13945* is basally localised during early gastrulation and apically localised in later invaginating structures. Two of these transcripts, *slmb/CG3412/LD08669* and *GUK-h/CG1962/LD41224*, localised apically upon injection into embryos (Figure 4.2.1D, 4.2.2D).

Slmb/CG3412/LD08669 is most likely actively transported towards the embryo periphery, since the RNA particles move on directed paths (Figure 4.2.1E, movie 4.2.1), with kinetics similar to that of other dynein driven transcripts. *GUK-h/CG1962/LD41224*, on the contrary, is very slow and its apical accumulation is probably mediated by diffusion followed by apical entrapment or anchoring.

4.2.2.2 The predicted localisation elements of *CG3412* are not sufficient for its apical targeting

The predicted motifs of *slmb/CG3412/LD08669* are shown in Figure 4.2.1A. A truncated transcript that contains all the putative elements fails to localise, demonstrating that they are not sufficient for localisation (Figure 3.2.1F).

4.2.2.3 A predicted localisation elements of *CG1962* is necessary for its apical accumulation

The putative localisation elements of *CG1962/LD41224* are shown in figure 4.2.2A. Injection of various fragments of the transcript (Figure 4.2.2E) shows that none of the predicted signals is sufficient for localisation. At least one of predicted signals, however, is apparently necessary for localisation, as a transcript lacking the last 140nt of the 3'UTR of the RNA does not localise.

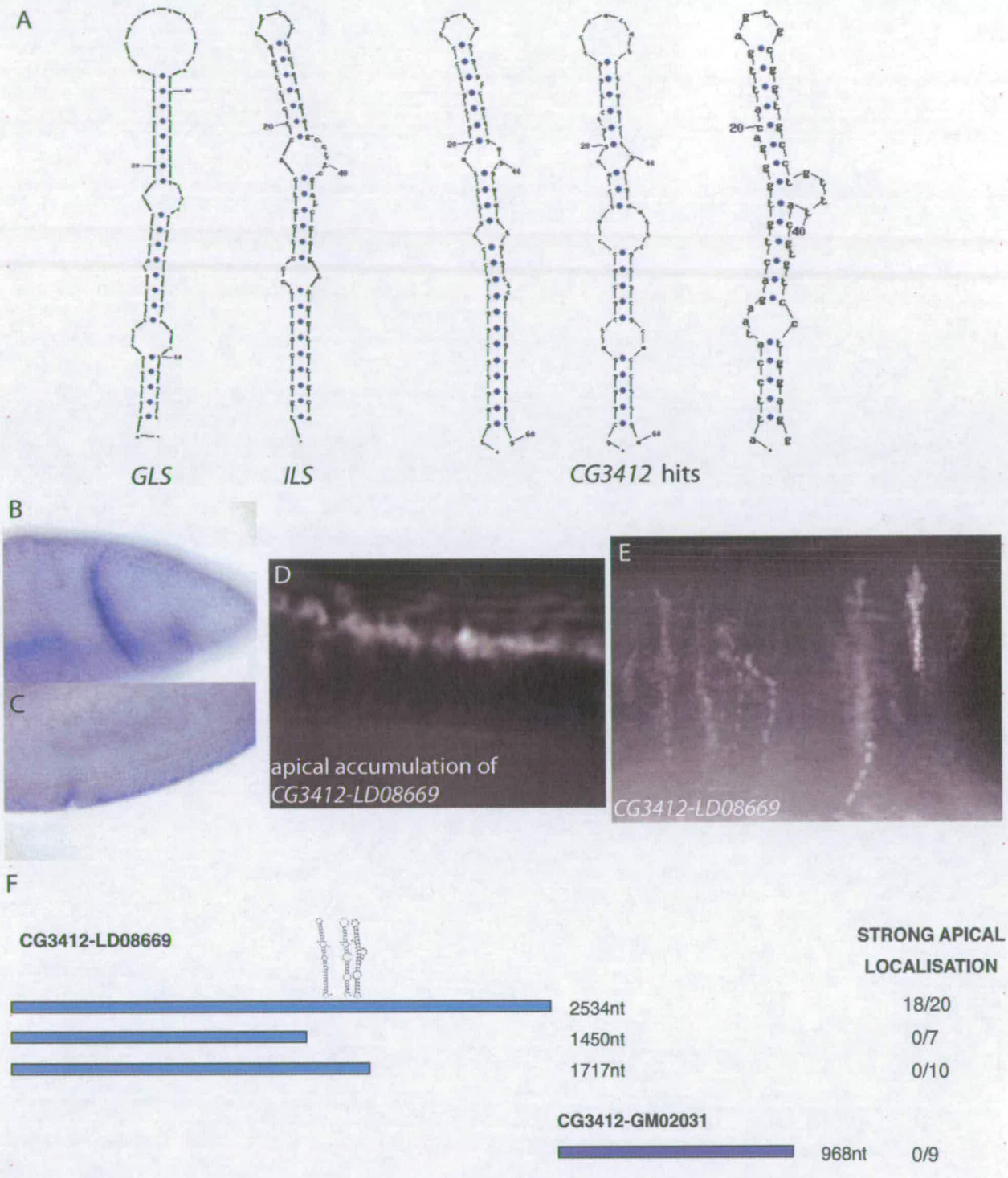


Figure 4.2.1: Apical localisation of *slmb/CG3412/LD08669* in blastoderm embryos
(A) *GLS*, *ILS* and putative localisation elements of *CG3412/LD08669*. (B-C) Endogenous *CG3412* localises apically in epithelial cells of syncytial blastoderm embryos and in invaginating cells in gatrulating embryos (Tomancak *et al*, 2002). (D) Apical accumulation of injected *CG3412/LD08669* in syncytial blastoderm embryos (15 min after injection). (E) Particles of injected *CG3412/LD08669* move on directed paths towards the periphery of embryos (time projection). (F) The putative localisation elements of *CG3412/LD08669* are not sufficient for its apical targeting. A truncated transcript that contains all three elements fails to localise. A maternal isoform of *CG3412*, *CG3412/GM02031*, does not localise upon injection into embryos.

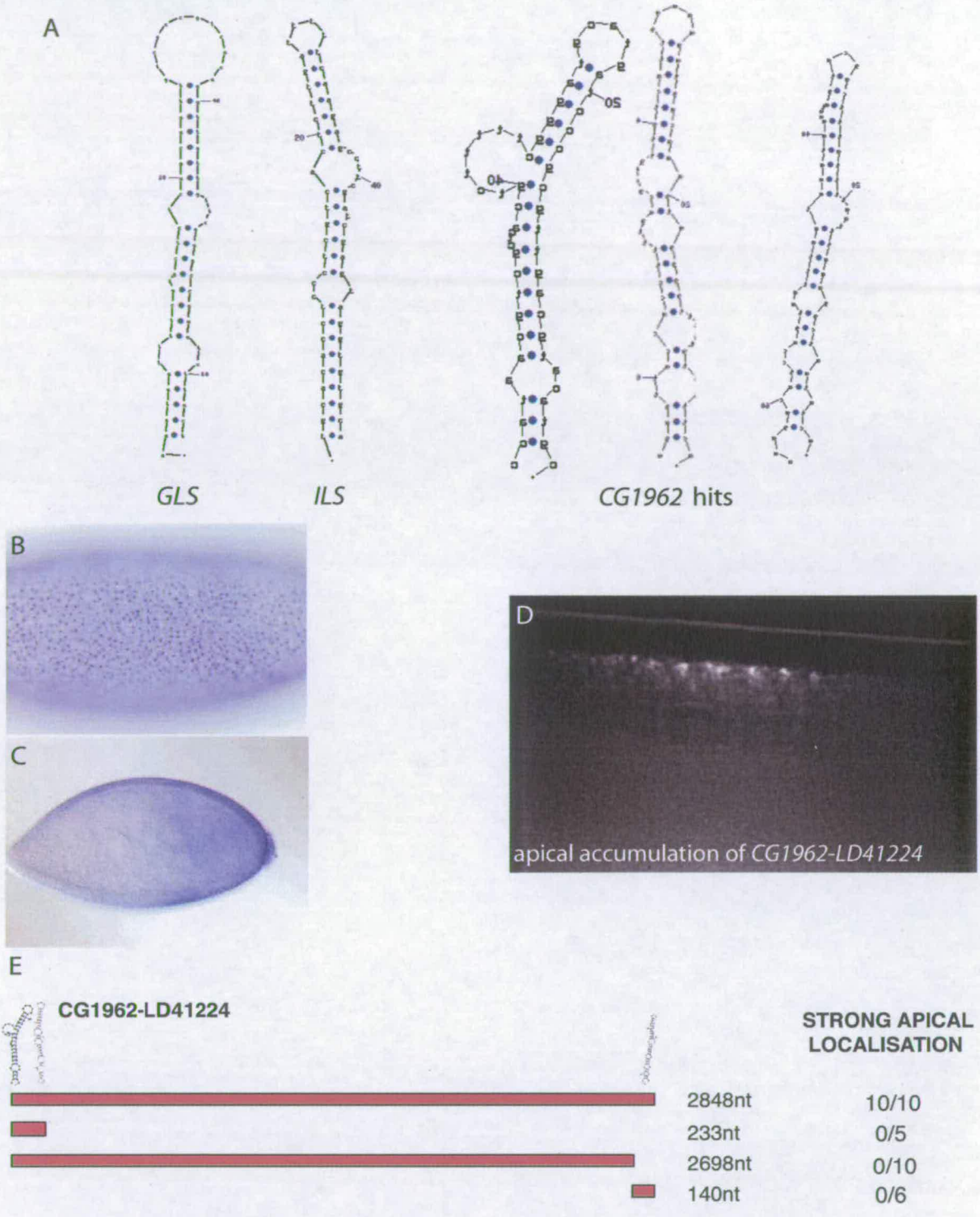


Figure 4.2.2: Apical localisation of *CG1962/LD41224* in Drosophila embryos
(A) *GLS*, *ILS* and putative localisation elements of *CG1962/LD41224*. (B-C) Endogenous *CG1962* localises at the cenrosomes of syncytial blastoderm embryos (Tomancak *et al*, 2002). (D) Apical accumulation of injected *CG1962/LD41224* in syncytial blastoderm embryos (25 min after injection). (E) Two putative localisation elements of *CG1962/LD41224* are not sufficient for its apical localisation. A short fragment that contains both elements fails to localise. A third predicted localisation element is necessary but not sufficient for apical accumulation. A truncated transcript that lacks this element does not localise. A short fragment that contains this element also fails to localise upon injection into embryos.

4.2.3 ASSESSING THE LOCALISATION POTENTIAL OF TRANSCRIPTS CONTAINING PUTATIVE LOCALISATION SIGNALS PREDICTED BY RNAdistance

4.2.3.1 Selection of candidates for injection

At the initial stage of the method, RNAdistance was used to calculate the similarity between the stable structures folded by RNALfold and *GLS* or *ILS*. The method predicted a large number of putative localisation signals in more than 3000 genes and intergenic regions, which were sorted in the database by their given score of similarity with the template structures. Unfortunately, this similarity was not always successfully represented by the output score, therefore we decided to scan through the predicted structures and evaluate their degree of similarity with *GLS* or *ILS* by eye. This narrowed the number of candidate genes down to about 400. The visual evaluation was shared between myself and Veronique van de Bor and the results are stored in the database.

The number of the structures that we found very similar with *GLS* and *ILS* was still high, so we employed additional criteria in the selection of the candidates for injection. First, we only selected the hits included in the 5'UTR, 3'UTR and protein coding sequences of the genes, and dismissed the ones lying in introns, as we were injecting transcripts made from cDNA templates (see 4.2.1). Then we tested if their sequence and secondary structure was conserved in *Drosophila pseudobscura*, by searching the *Drosophila pseudobscura* genome at http://www.hgsc.bcm.tmc.edu/projects/drosophila/ for orthologue sequences, folding them and comparing them with the *D. melanogaster* predicted structures. Finally, we were limited by the availability of full length, high quality clones that we used as templates for transcription. We obtained clones from the GOLD collection, a subset of the DGC collection, comprised of highly validated clones, verified as full-length and identical in their sequence with the genome (Stapleton *et al*, 2002). The GOLD collection represented 38% of the genome at the time these experiments were carried

out. This selection procedure was done by myself and Veronique Van de Bor and narrowed down the candidates for injection to 50.

4.2.3.2 Assessing the localisation potential of the selected candidate RNAs

We sequenced the 5' and 3' ends of the 50 selected cDNA clones to confirm their identity. We made restriction maps of the plasmids and digested them with enzymes that linearise the vector leaving the inserted clone intact. The size of the inserts was determined, to confirm that they were full length. Finally, we made RNA from the full- length clones and checked its quality. Due to difficulties in growing some of the clones and synthesising enough, good quality RNA from some others, we obtained in total 34 transcripts for injection.

We first tested 11 transcripts (shown in Table 4.2.1) that contained RNAdistance hit(s) in their 3'UTR. One of these, namely *CG15095/GH07529* (Veronique's data, not shown), localised efficiently and strongly, at the apical cytoplasm of all the injected embryos. We then examined the other 23 transcripts (Table 4.2.1) that contained RNAdistance hit(s) in their 5'UTR or protein coding sequence. One of these transcripts, *CG1841/HL07962* (Figure 4.2.3B) showed strong, apical accumulation in the vast majority of the injected embryos. *The term "efficient localisation" is used throughout this chapter to indicate that a tested transcript localised in more than 75% of the injected embryos. The terms "strong localisation" or "weak localisation" indicate the amount of the transcript that localised in each embryo.*

4.2.3.3 The predicted localisation elements of *CG1841* are not responsible for the apical localisation of the transcript

CG1841/HL07962 was sequenced to confirm that it did not bear any mutations in its predicted signals. The putative localisation signals of *CG1841* are shown in Figure 4.2.3A. In order to test whether they are necessary for localisation, I made a

transcript lacking both of them. The truncated transcript localised as efficiently as the full-length one, upon injections in embryos (Figure 4.2.3C), showing that the *GLS-like* motifs that *CG1841/HL07962* contains are not essential for its localisation. Veronique van de Bor injected short fragments, consisting of the hits and some flanking sequence and showed that each of these structures is not sufficient for localisation either. We therefore conclude that *CG1841/HL07962* is not directed towards the apical side of the embryo by the predicted by RNAdistance localisation elements.

4.2.3.4 A predicted localisation elements of *CG15095* is sufficient for apical localisation

CG15095 contains 3 RNAdistance hits, one of which is lying in its 3'UTR and is sufficient for weak localisation, as shown by injections performed by Veronique Van de Bor (not shown). We conclude that the localisation of *CG15095* is partially mediated by this signal, but other parts of the transcript are also necessary for strong, efficient apical enrichment.

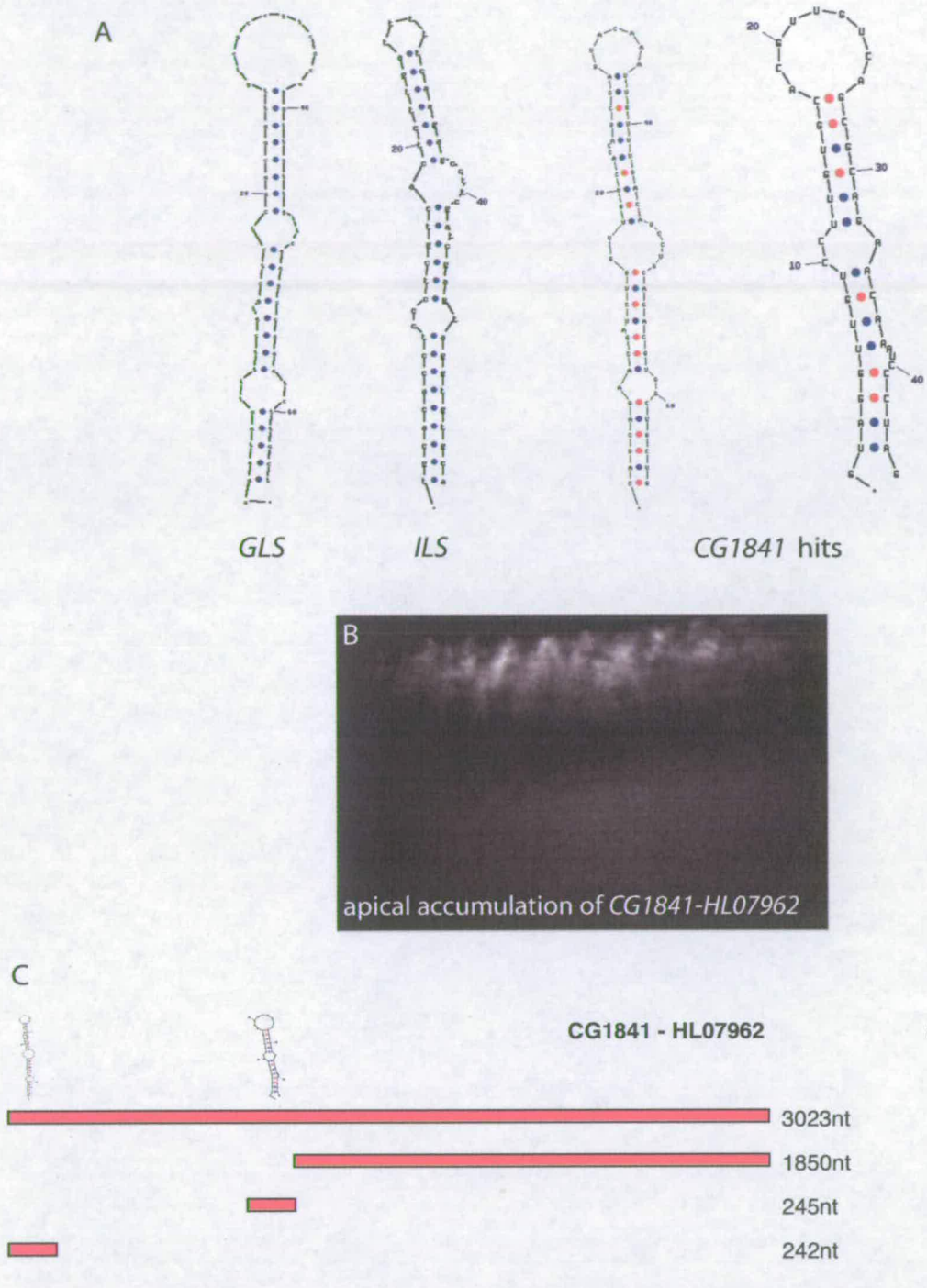


Figure 4.2.3: Apical targeting of *CG1841/HL07962* in blastoderm embryos
(A) *GLS*, *ILS* and putative localisation elements of *CG1841/HL07962*. (B) Apical accumulation of injected *CG1841/HL07962* in syncytial blastoderm embryos (15 min after injection). (C) The putative localisation elements of *CG1841/HL07962* are neither necessary nor sufficient for its apical targeting. A fragment lacking both elements localises as efficiently as the full length transcript. Short fragments (experiment performed by Veronique) containing each of the elements fail to localise.

4.2.4 ASSESSING THE LOCALISATION POTENTIAL OF TRANSCRIPTS CONTAINING PUTATIVE LOCALISATION SIGNALS PREDICTED BY RNAMotif

RNAMotif pattern matches the stable structures folded by RNALfold against a structure definition. In our case, the programme used flexible rules that could find structures matching both *GLS* and *ILS*. Two sets of hits were tested experimentally: A) structures with at least one 4-12nt loop, at least one 7-8nt stem and at least one bulge, with the top bulge bearing a UU sequence constraint, shown before (Van de Bor and Davis, unpublished work) by mutagenesis experiments to be essential for the localisation of *GLS* and *ILS* and B) structures that contained at least one 4-12nt loop and one 7-8nt stem. I am referring to these predicted signals as RNAMotif UU hits and RNAMotif basic hits respectively.

4.2.4A ASSESSING THE LOCALISATION POTENTIAL OF THE RNAMotif UU HITS

4.2.4A.1 Selection of candidates for injection

The RNAMotif hits, 140 in total, were all stored in one library, regardless of their position in the gene. For this reason, I had to select the ones that were mapped in the exons and ignore the ones that lied in the introns or the regulatory regions of the corresponding genes. This selection procedure narrowed down the number of candidate genes from about 90 to 37. At the time these experiments were performed, the DGC1 and DGC2 collections, but not the GOLD collection, became available. DGC1 and DGC2 are comprised of ESTs that have undergone 5' and 3' resequencing and although they are not as highly validated as the GOLD clones, they are identified as potentially full-length (Rubin *et al*, 2000, Stapleton *et al*, 2002). Unfortunately, they do not cover the whole genome, which limited further the number of candidate RNAs that could be easily tested.

4.2.4A.2 Assessing the localisation potential of the selected candidate RNAs

I made restriction maps of the plasmids and digested them with enzymes that linearise the vector, leaving the inserted clone intact. I further checked the size of the inserts to confirm that the clones were not truncated. Only preparations of good quality and made from full-length clones were tested. We injected 4 transcripts that contained RNAMotif UU hit(s) in their 3'UTR. One of these transcripts, *CG5876/LD08295* localised apically in 75% of the injected embryos (Figure 4.2.4B). We also tested 14 transcripts that contained hits in the rest of the transcript, none of which localised. A list of all the tested candidates and a summary of the results is shown in Table 4.2.1.

4.2.4A.3 The predicted localisation element of *CG5876* is not necessary for its apical targeting

Sequencing of CG5876/LD08295 showed that it indeed contained the predicted localisation signal without any mutations in it. I injected a *CG5876/LD08295* transcript that is transcribed from a truncated template made by SOE-PCR and lacks the predicted signal. The truncated transcript localises almost as efficiently as the full-length transcript (Figure 4.2.4.C). The predicted secondary structure motif is apparently not necessary for the apical accumulation of *CG5876/LD08295*.

4.2.4B ASSESSING THE LOCALISATION POTENTIAL OF THE RNAMotif BASIC HITS

4.2.4B.1 Selection of candidates for injection

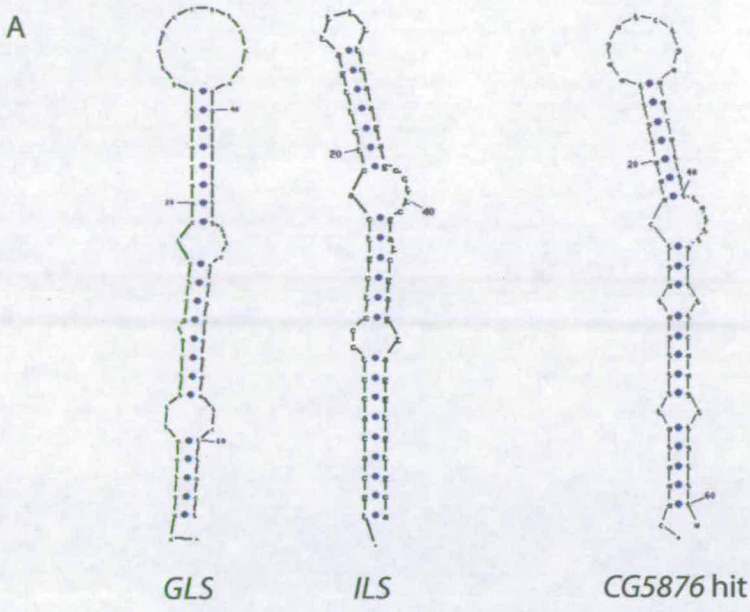
This library included 1350 hits. Because of the high number of hits, we scanned through the library and selected the ones that showed higher similarity with *GLS* and *ILS*. We then followed a selection procedure similar to the one described before for the RNAMotif UU candidates.

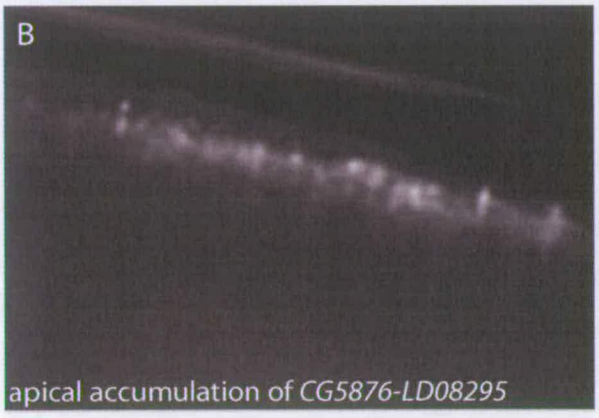
4.2.4B.2 Assessing the localisation potential of the selected candidate RNAs

Following the steps described above for the RNAMotif UU candidates, I tested 28 transcripts, 6 containing RNAMotif hits in their 3'UTR and 22 in their 5'UTR or CDS (Table 4.2.1). One of the 3'UTR candidates, *CG11448*, localised apically in 28% and showed an apical-basal distribution in another 48% of the injected embryos (Figure 4.2.5B,C). Veronique Van de Bor tested 22 more candidate RNAs (Table 4.2.1), 6 containing RNAMotif hits in their 3'UTR and 16 in their 5'UTR or CDS, none of which localised. A summary of the results is shown in Table 4.2.1.

4.2.4B.3 The predicted localisation element of *CG11448* partially mediates its asymmetric distribution

Sequencing of GH23825 showed that it contained the predicted signal with no mutations in it. The predicted localisation signal of *CG11448* is shown in Figure 4.2.5A. Injection of various truncated transcripts showed that the predicted motif is partially responsible for localisation (Figure 4.2.5D). However, other element(s) in the 3'UTR of the transcript must be essential for full efficient targeting. Veronique Van de Bor injected a short fragment containing the predicted motif and showed that it is also sufficient for weak localisation (Figure 4.2.5D).





C

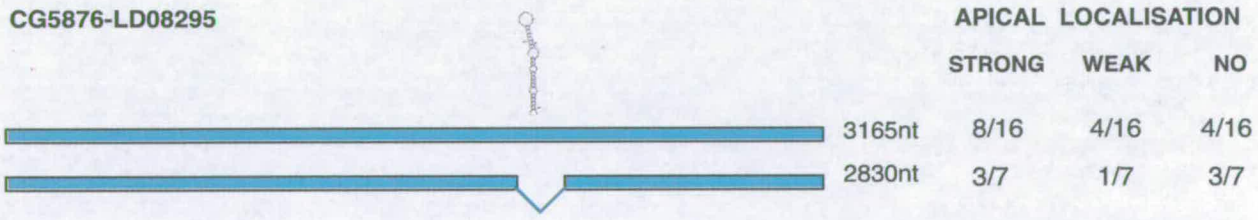


Figure 4.2.4: Apical accumulation of *CG5876/LD08295* in blastoderm embryos
(A) *GLS*, *ILS* and the putative localisation element of *CG5876/LD08295*. (B) Apical accumulation of injected *CG5876/LD08295* in syncytial blastoderm embryos (15 min after injection). (C) The putative localisation element of *CG5876/LD08295* is not necessary for its apical targeting. A fragment lacking the elements localises as efficiently as the full length transcript.

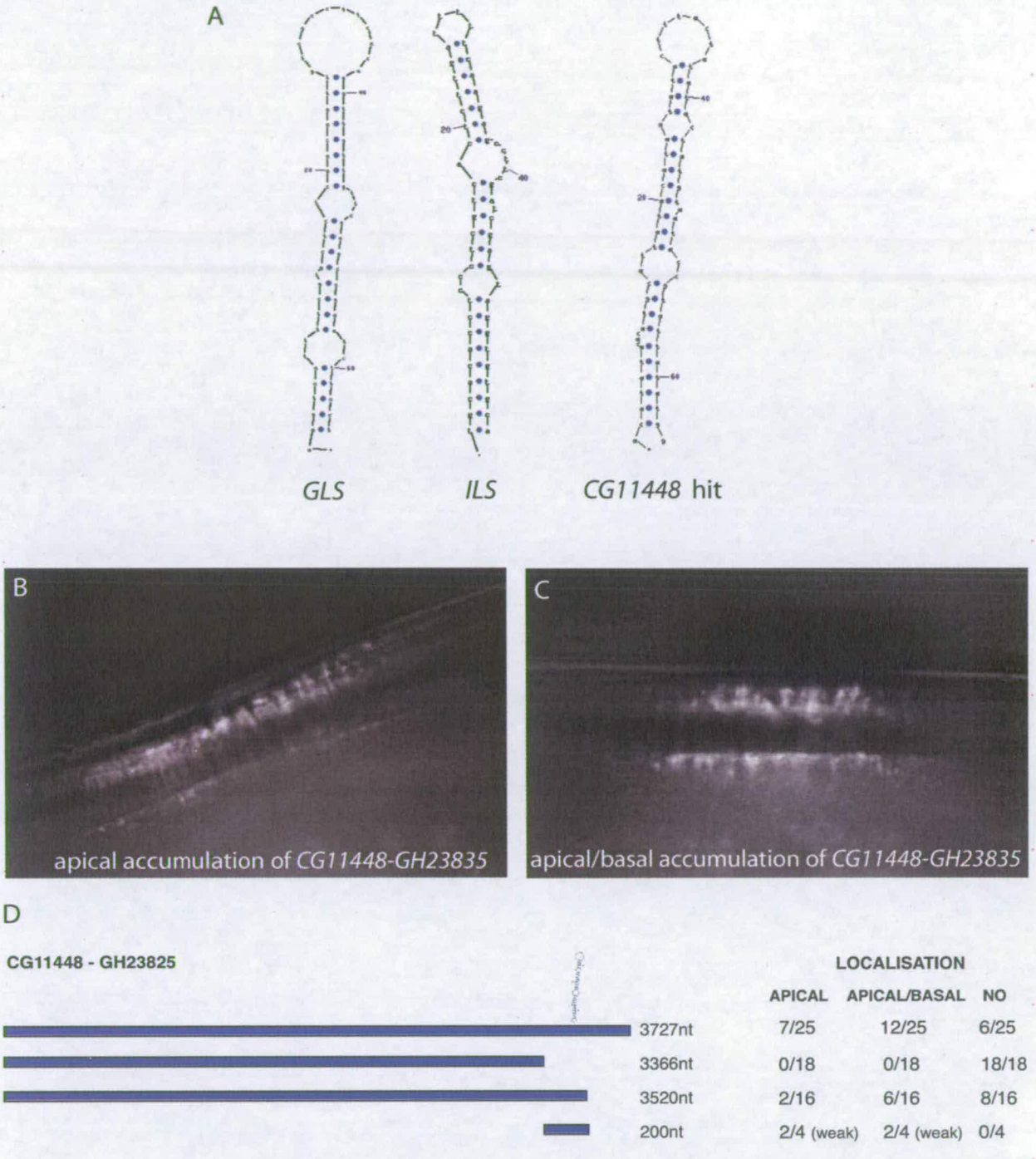


Figure 4.2.5: Localisation of *CG11448/GH23835* in blastoderm embryos
(A) *GLS*, *ILS* and the putative localisation element of *CG11448/GH23825*. (B) Apical accumulation of injected *CG11448/GH23825* in syncytial blastoderm embryos (15 min after injection). (C) Apical-basal accumulation of injected *CG11448/GH23825* in syncytial blastoderm embryos (15 min after injection). (D) The putative localisation element of *CG11448/GH23825* is necessary for its apical targeting and sufficient for weak localisation. A truncated fragment lacking most of the 3'UTR of the transcript does not localise, whereas one that lacks the part of the 3'UTR that lies downstream the element localises, although not as efficiently as the full length transcript. A short fragment (experiment carried out by Veronique Van de Bor) containing the element is sufficient for weak localisation.

4.2.5 *slmb/CG3412*, *CG1962*, *CG1841*, *CG15095*, *CG11448* AND *CG5876* ARE HOMOGENOUESLY DISTRIBUTED IN OOCYTES

All the transcripts that we identified as apically localised in embryos were further injected into oocytes by Veronique Van de Bor. None of these showed antero-dorsal or any other kind of asymmetric distribution upon injection (not shown). I performed in situ hybridisation in ovaries to test the distribution of the endogenous *CG1962*, *slmb/CG3412*, *CG1841*, *CG11448* and *CG5876*. Both *slmb*/CG3412 and *CG1962* are expressed during oogenesis, but none shows any localisation pattern (not shown). *Slmb/CG3412/GM02031*, a maternal isoform of slmb, also failed to localise in embryos (Figure 4.2.1F) or oocytes. *CG5876* is not detectable during oogenesis, whereas *CG1841* and *CG11448* are expressed but homogenouesly distributed during mid and late oogenesis (not shown).

4.2.6 TESTING THE LOCALISATION POTENTIAL OF A RANDOM POOL OF TRANSCRIPTS

The mapping experiments that we performed showed that the embryonic localisation of three out of the five localising RNAdistance or RNAMotif candidates was mediated at least partially by signals similar to *GLS* and *ILS*. These transcripts, however, are distributed homogeneously when injected into oocytes. Therefore, it is not clear if their predicted signals are indeed related to *GLS* or *ILS* but the transcripts for some reason utilise the *grk/I* factor transport machinery only in embryos, or if their ability to target the transcripts apically in embryos is unrelated to their apparent secondary structure similarity with *GLS* or *ILS* and completely incidental. Alternatively, it is possible that, although these motifs were identified due to their similarity with *GLS* or *ILS*, they actually mimick the localisation elements of other transcripts, for instance pair rule RNAs, and accumulate apically by recruiting their machinery and not that of *grk* and the *I* factor.

We could not distinguish between these possibilities directly, because the signals of most apical RNAs have not been mapped in detail. Instead, we tried to address whether our method enriches at all for localising transcripts, by injecting random RNAs and comparing their localisation success with that of the bioinformatics candidates. Following the same procedure described before for all the other candidates I chose 33 transcripts (listed in Table 4.2.1), that were selected by a random number generator, and injected them into blastoderm embryos. None of the injected RNAs localised in embryos. Veronique Van de Bor tested 17 more randomly chosen transcripts (listed in Table 4.2.1), one of which, *CG32425*, localised apically, upon injection into blastoderm embryos.

Table 4.2.2 summarises the results of the injections of the RNAdistance and RNAMotif candidates and the random transcripts. The results of the pilot screen have not been taken into account in the statistics tests, as their selection was biased. The selection of 3' UTR bioinformatics hits increased 5.5 times, from 2% to 11%, the localisation rate of transcripts. The significance of this enrichment is 88% (Fisher exact probability test), which means that the differences we observe have a 12% probability to be attributed to chance. However, the degree of enrichment correlates well with our mapping data that are mentioned above and showed that the distribution of 2 out of 27 or 7.4% of the injected RNAdistance or RNAMotif candidates is determined by the predicted signals.

GENE	Clone ID	METHOD	HIT(S) IN 3'UTR	LOCALISATION IN EMBRYOS	HIT(S) Necessary	HIT(S) sufficient
CG1962	LD41224	RNAdistance+BDGP	✓	✓	✓	✗
CG10917	RE18087	RNAdistance+BDGP	✓	✗		
CG12205	RE24665	RNAdistance+BDGP	✓	✗		
CG33207	RE16319	RNAdistance+BDGP	✗	✗		
CG31043	GM06978	RNAdistance+BDGP	✗	✗		
CG6953	HL01082	RNAdistance+BDGP	✗	✗		
CG5370	LD13945	RNAdistance+BDGP	✗	✗		
CG3412	LD08661	RNAdistance+BDGP	✗	✓	✗	✗
CG11537	LD40292	RNAdistance	✓	✗		
CG5300	LD03739	RNAdistance	✓	✗		
CG32171	LD46723	RNAdistance	✓	✗		
CG7279	RE5440	RNAdistance	✓	✗		
CG4838	GH22661	RNAdistance	✓	✗		
CG15095	GH07529	RNAdistance	✓	✓		✓
CG1725	GH01107	RNAdistance	✓	✗		
CG31761	LD19052	RNAdistance	✓	✗		
CG9401	RE14116	RNAdistance	✓	✗		
CG5575	GH12495	RNAdistance	✓	✗		
CG4385	AT04225	RNAdistance	✓	✗		
CG1841	HL07962	RNAdistance	✗	✓	✗	✗
CG7727	GH04413	RNAdistance	✗	✗		
CG3738	LD35220	RNAdistance	✗	✗		
CG7831	LD29131	RNAdistance	✗	✗		
CG32096	GH15583	RNAdistance	✗	✗		
CG1961	SD07045	RNAdistance	✗	✗		
CG9193	LD45889	RNAdistance	✗	✗		
CG4590	LD22650	RNAdistance	✗	✗		
CG8888	GH26015	RNAdistance	✗	✗		
CG6617	LD25271	RNAdistance	✗	✗		
CG8282	LD22082	RNAdistance	✗	✗		
CG31232	GH24065	RNAdistance	✗	✗		
CG5397	GH04232	RNAdistance	✗	✗		
CG3732	LD15224	RNAdistance	✗	✗		
CG11198	GH12002	RNAdistance	✗	✗		
CG8611	GH02853	RNAdistance	✗	✗		
CG1227	LD17053	RNAdistance	✗	✗		
CG2034	SD08216	RNAdistance	✗	✗		
CG7330	RE22290	RNAdistance	✗	✗		
CG8533	LD02552	RNAdistance	✗	✗		
CG1341	SD07148	RNAdistance	✗	✗		
CG15611	RE34668	RNAdistance	✗	✗		
CG9655	RE03440	RNAdistance	✗	✗		
CG10580	RE03010	RNAdistance	✗	✗		
CG8711	GM14815	RNAMotif UU	✓	✗		
CG12345	HL05903	RNAMotif UU	✓	✗		
CG5876	LD08295	RNAMotif UU	✓	✓	✗	
CG9655	RE03440	RNAMotif UU	✓	✗		
CG6772	GH16988	RNAMotif UU	✗	✗		
CG7571	GH01690	RNAMotif UU	✗	✗		
CG4899	HL08057	RNAMotif UU	✗	✗		
CG8896	GH23463	RNAMotif UU	✗	✗		
CG8942	LP05465	RNAMotif UU	✗	✗		
CG17724	LD12453	RNAMotif UU	✗	✗		
CG30055	GM14547	RNAMotif UU	✗	✗		

CG17249	LD14179	RNAMotif UU	✗	✗		
CG13850	GM07286	RNAMotif UU	✗	✗		
CG14962	AT25633	RNAMotif UU	✗	✗		
CG15727	RE13534	RNAMotif UU	✗	✗		
CG32985	SD25427	RNAMotif UU	✗	✗		
CG9648	HL03368	RNAMotif UU	✗	✗		
CG11676	GH157922	RNAMotif UU	✗	✗		
CG12345	HL05903	RNAMotif basic	✓	✗		
CG11448	GH23825	RNAMotif basic	✓	✓	✓	✓
CG14994	HL02049	RNAMotif basic	✓	✗		
CG18812	GH03014	RNAMotif basic	✓	✗		
CG9239	LD48089	RNAMotif basic	✓	✗		
CG15117	LD08118	RNAMotif basic	✓	✗		
CG5966	LD47264	RNAMotif basic	✓	✗		
CG3413	GH02310	RNAMotif basic	✓	✗		
CG3938	LD22682	RNAMotif basic	✓	✗		
CG4719	LD22548	RNAMotif basic	✓	✗		
CG6678	LD39062	RNAMotif basic	✓	✗		
CG8058	GM08242	RNAMotif basic	✓	✗		
CG5920	LD24077	RNAMotif basic	✗	✗		
CG3136	LD12677	RNAMotif basic	✗	✗		
CG31531	GH25780	RNAMotif basic	✗	✗		
CG31612	RE19601	RNAMotif basic	✗	✗		
CG6015	LD21931	RNAMotif basic	✗	✗		
CG31705	GH07269	RNAMotif basic	✗	✗		
CG32447	LP07906	RNAMotif basic	✗	✗		
CG3363	GH15647	RNAMotif basic	✗	✗		
CG3530	GH04637	RNAMotif basic	✗	✗		
CG3697	AT15210	RNAMotif basic	✗	✗		
CG4641	GH27208	RNAMotif basic	✗	✗		
CG6191	GH06193	RNAMotif basic	✗	✗		
CG5009	GH01266	RNAMotif basic	✗	✗		
CG6729	SD08609	RNAMotif basic	✗	✗		
CG7597	SD04681	RNAMotif basic	✗	✗		
CG7704	LD42828	RNAMotif basic	✗	✗		
CG1187	GM10858	RNAMotif basic	✗	✗		
CG12165	SD04909	RNAMotif basic	✗	✗		
CG12223	GM02110	RNAMotif basic	✗	✗		
CG10359	GM10015	RNAMotif basic	✗	✗		
CG10670	GM10765	RNAMotif basic	✗	✗		
CG1743	GH14412	RNAMotif basic	✗	✗		
CG15319	LD33277	RNAMotif basic	✗	✗		
CG1640	SD05601	RNAMotif basic	✗	✗		
CG1848	LD15137	RNAMotif basic	✗	✗		
CG31649	GH18470	RNAMotif basic	✗	✗		
CG14023	LD09783	RNAMotif basic	✗	✗		
CG14476	GH04962L	RNAMotif basic	✗	✗		
CG1915	GM05288	RNAMotif basic	✗	✗		
CG18654	AT10182	RNAMotif basic	✗	✗		
CG17255	SD10723	RNAMotif basic	✗	✗		
CG8709	GH19076	RNAMotif basic	✗	✗		
CG9916	SD01793	RNAMotif basic	✗	✗		
CG9856	LD13251	RNAMotif basic	✗	✗		
CG9096	LD22957	RNAMotif basic	✗	✗		
CG9311	SD03094	RNAMotif basic	✗	✗		
CG9660	LD27161	RNAMotif basic	✗	✗		

CG9709	LD22081	RNAMotif basic	✗	✗	
CG4033	GM01970	RANDOM		✗	
CG14044	LD02611	RANDOM		✗	
CG10255	LD10609	RANDOM		✗	
CG14897	GM04711	RANDOM		✗	
CG5753	LD13210	RANDOM		✗	
CG4633	LD11251	RANDOM		✗	
CG7207	GH07688	RANDOM		✗	
CG30116	GH04922	RANDOM		✗	
CG3983	LD39337	RANDOM		✗	
CG5939	GH41085	RANDOM		✗	
CG31781	GH27691	RANDOM		✗	
CG3544	GH10780	RANDOM		✗	
CG31650	LD34288	RANDOM		✗	
CG7180	GH22607	RANDOM		✗	
CG9164	GH10334	RANDOM		✗	
CG30387	SD10882	RANDOM		✗	
CG4746	SD05389	RANDOM		✗	
CG5634	LD38671	RANDOM		✗	
CG8284	LD27480	RANDOM		✗	
CG7404	GH28308	RANDOM		✗	
CG16788	LD23870	RANDOM		✗	
CG3172	LD37470	RANDOM		✗	
CG1651	LD21682	RANDOM		✗	
CG11784	LD22317	RANDOM		✗	
CG1559	LD30316	RANDOM		✗	
CG16747	GH26763	RANDOM		✗	
CG9938	LD330400	RANDOM		✗	
CG8192	LD06965	RANDOM		✗	
CG3696	GM02209	RANDOM		✗	
CG33156	LD25573	RANDOM		✗	
CG10938	LD33318	RANDOM		✗	
CG10080	SD08722	RANDOM		✗	
CG9071	GH19479	RANDOM		✗	
CG3324	GH03852	RANDOM		✗	
CG6453	LD46553	RANDOM		✗	
CG3910	GH04071	RANDOM		✗	
CG7628	GH23727	RANDOM		✗	
CG32425	SD09829	RANDOM		✓	
CG11756	AT06648	RANDOM		✗	
CG32087	AT12664	RANDOM		✗	
CG32038	SD15313	RANDOM		✗	
CG3125	SD04165	RANDOM		✗	
CG8781	RE09075	RANDOM		✗	
CG31043	RE59757	RANDOM		✗	

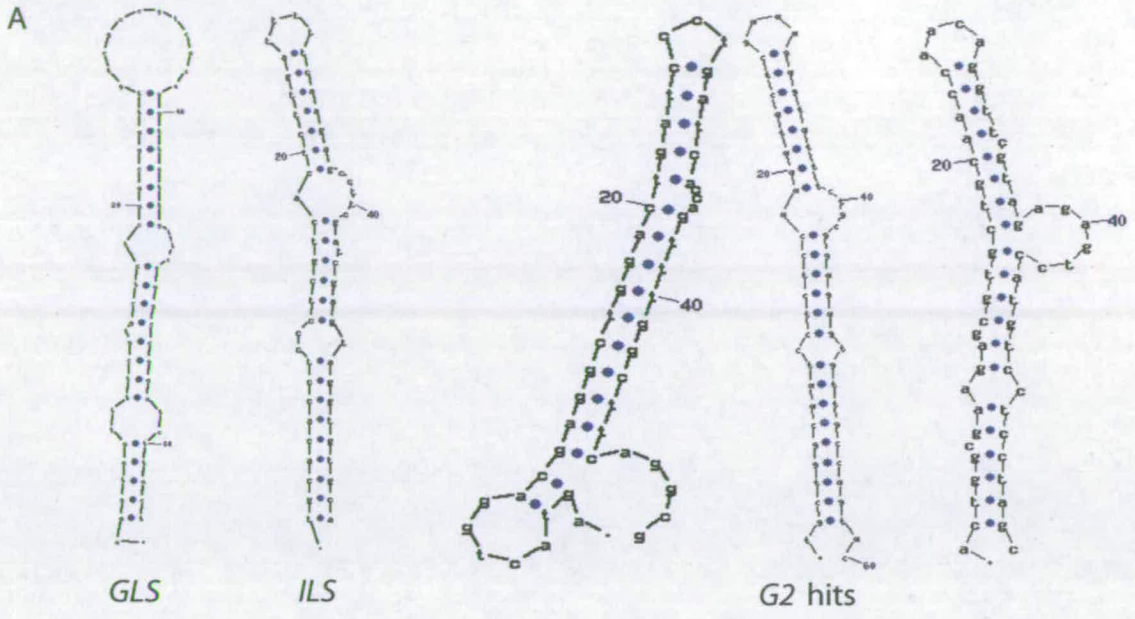
Table 4.2.1: A list of the tested bioinformatics candidates and random transcripts
The transcripts that localised ar shown in red. The transcripts that contained at least one hit in their 3'UTR are shown in gray. The ability of the predicted elements to act as localisation signals is shown in the left column of the table. The predicted localisation signals of *CG1841* are neither necessary nor sufficient for localisation. One of the predicted signals of CG15095 is sufficient for weak localisation. The predicted localisation element of CG5876 is not necessary for localisation. The predicted localisation element of CG11448 is both necessary and sufficient for localisation.

TESTED TRANSCRIPTS		LOCALISATION RATE	LOCALISATION ENRICHMENT	PROBABILITY (FISHER'S TEST)
RANDOM		1/50 or 2%		
RNAs containing HITS in their 3'UTR	RNAdistance	1/11 or 9.1%	7.1%	0.3306
	RNAMotifUU	1/4 or 25%	23%	0.3522
	RNAMotifbasic	1/12 or 8.3%	6.3%	0.143955
	TOTAL	3/27 or 11.1%	9.1%	0.121039
RNAs containing HITS in their 5'UTR or CDS	RNAdistance	1/23 or 4.35%	2.15%	0.54
	RNAMotifUU	0/14	NO	
	RNAMotifbasic	0/38	NO	
	TOTAL	1/75	NO	

Table 4.2.2: Localisation success of random transcripts and RNAdistance or RNAMotif candidates

4.2.7 ASSESSING THE LOCALISATION POTENTIAL OF TRANSPOSABLE ELEMENTS THAT CONTAIN BIOINFORMATICS HITS

Eve Hartswood and Cheryl Jones, in David Finnegan's lab, have cloned and tested the localisation potential of fragments of transposable elements that contain putative localisation signals predicted by RNAdistance or RNAMotif. I synthesised, from templates cloned by Eve and Cheryl, and injected into embryos four transcripts: *G2* and *Doc2*, coded by non-LTR retrotransposons, and *S* and *1360*, coded by "cut and paste" transposons. *G2* shows a strong apical accumulation upon injection into embryos (Figure 4.2.6), whereas *Doc2*, *S* and *1360* are distributed homogeneously. Eve and Cheryl have tested 2 other transposons, 7 other non-LTR retrotransposons and 9 LTR-retrotransposons and they have identified one more non-LTR retrotransposon, *Jockey*, that localises apically in the injected embryos (not shown). Experiments also performed by Eve and Cheryl have shown that the predicted motifs of *G2* and *Jockey* are necessary and sufficient for localisation. *G2* and *Jockey*, when injected into oocytes, accumulate at the dorso-anterior cap, reproducing the localisation pattern of *grk* and *I* factor (not shown). We conclude that the bioinformatics approach was successful in identifying localisation signals that – like *ILS*- recruit the host transport machinery to target other non-LTR retrotransposons towards the oocyte nucleus.



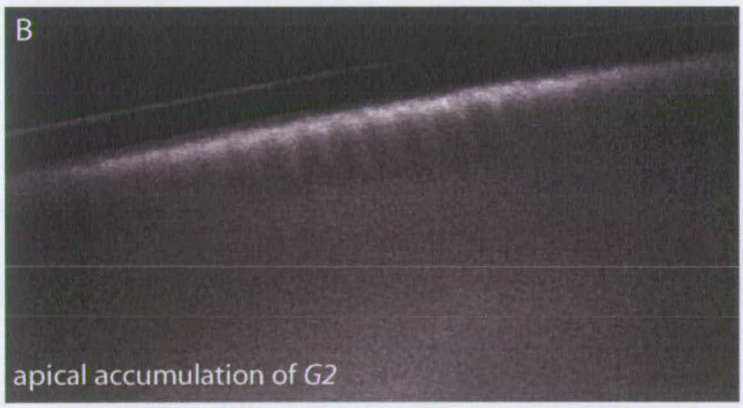


Figure 4.2.6: Apical targeting of *G2* retrotransposon in blastoderm embryos
(A) *GLS*, *ILS* and putative localisation elements of *G2*. (B) Apical accumulation of injected *G2* in syncytial blastoderm embryos (15 min after injection).

4.2.8 SOME TRANSCRIPTS ACCUMULATE BASALLY UPON INJECTION INTO BLASTODERM EMBRYOS

Some of the injected RNA preparations formed particles, which moved rapidly, in a directed way from the site of injection towards the periphery of the embryos. However, the RNA did not localise apically, but instead concentrated in a region underneath the nuclei and was usually excluded from the cells after cellularisation. Figure 4.2.7A,B and movie 4.2.2 show examples of this pattern of movement and localisation. The basal localisation of *Dcp-1/CG5370/LD13945* was not as efficient and reproducible as the localisation of apical transcripts, but it is interesting that the endogenous transcript is also found basally during early gastrulation (Tomancak *et al*, 2002). Veronique Van de Bor also identified another transcript, *CG5575* that accumulated basally after injection (not shown). Further experiments are required to dissect the mechanism of the basal localisation of these transcripts and establish whether this localisation has functional significance.

4.2.9 SOME NON-LOCALISING TRANSCRIPTS FORM PARTICLES AND MOVE DIRECTIONALLY.

We observed that a subset of non-localising transcripts can form particles and move considerable distances on directed paths. Figure 3.2.7C and movie 4.2.3 show an example of this type of transport. Our data do not address the mechanism that underlies the behaviour of these transcripts. They might contain elements with low affinity for the embryonic transport system. It is also possible that they hitchhike on other motor-driven cargoes. Neither can we exclude the possibility that this behaviour is characteristic of all transcripts and not specific to the examples we observed. The imaging of RNA particles is not always easy and straightforward and it was beyond the aim of our screen. Therefore, it is possible that we failed to identify a lot of other non-localising transcripts that undergo similar directional movements.

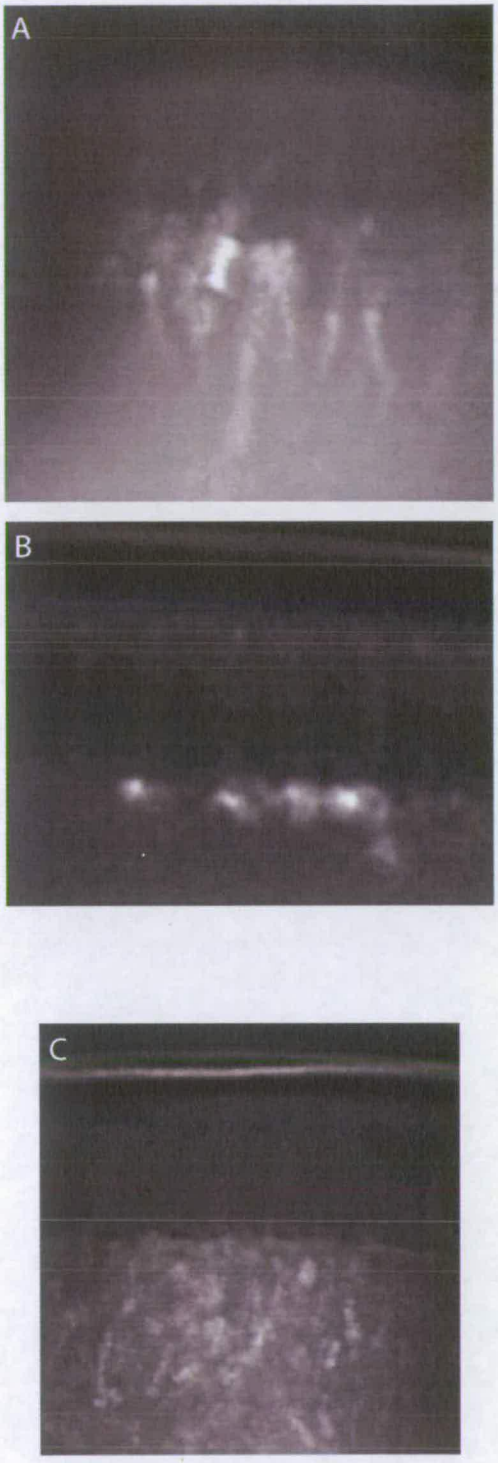


Figure 4.2.7: Novel patterns of transport and localisation
(A)CG5370/LD13945 forms particles that move rapidly and directionally towards the periphery of blastoderm embryos (time projection). (B) *CG5370/LD13945* RNA accumulates basally in blastoderm embryos. (C) Some non-localising transcripts form particles that move on directed paths in blastoderm embryos (time projection).

4.2.10 ENDOGENOUS *CG31043* IS ASYMMETRICALLY DISTRIBUTED IN OOCYTES

GUK-h/CG31043/GM06978 did not localise upon injection in embryos or oocytes. However, in situ hybridisation showed that the endogenous transcript localises anteriorly or at a cap near the oocyte nucleus, in a pattern similar to *grk* and the *I* factor (Figure 4.2.8A,B,C,D). Early in oogenesis, it is concentrated at the posterior pole of some oocytes. In a *grk* RNA null background (grk^{2B6}, Neuman-Silberberg and Schupbach, 1993, Thio *et al*, 2000), where the microtubules fail to repolarise, the transcript remains at the posterior throughout oogenesis, forming a crescent near the oocyte nucleus that has failed to migrate (Figure 4.2.8E,F). We performed control in situs in $guk\text{-}h^2$ mutant background, to confirm the specificity of the staining. $guk\text{-}h^2$ bears a P insertion in the regulatory region of the gene, which decreases dramatically the levels of expression, at least in neuromuscular junctions and the CNS (Mathew *et al*, 2002). *guk-h/CG31043* is not detectable in $guk\text{-}h^2$ oocytes (Figure 4.2.8G).

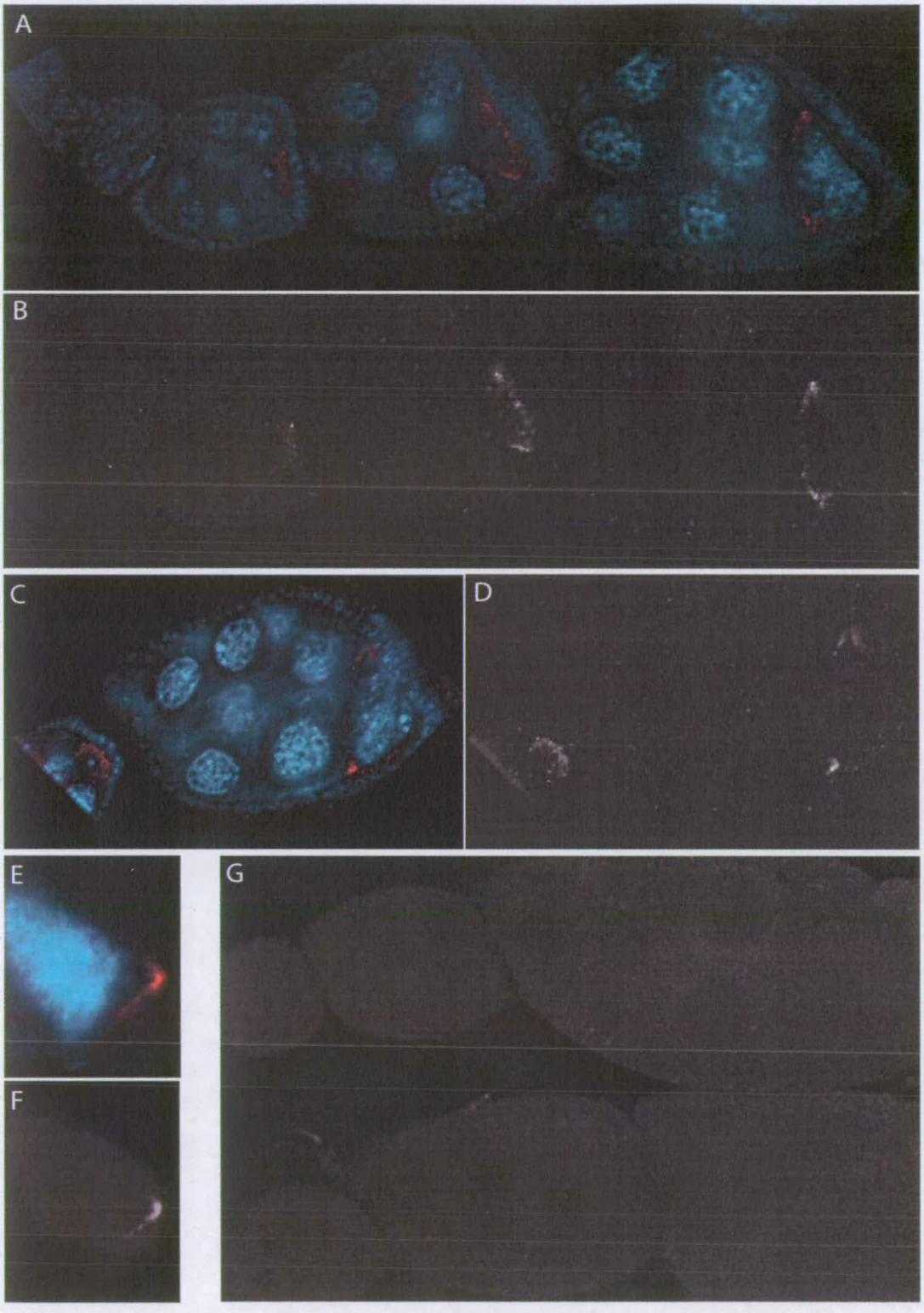


Figure 4.2.8: Asymmetric distribution of *GUK-h* RNA during oogenesis
GUK-h RNA accumulates first at the posterior (C,D) and later at the anterior (A, B) or anterodorsal corner (C,D) of the wild type oocytes during mid-oogenesis. *GUK-h* RNA remains concentrated at the posterior of *grk*2B6 mutant oocytes (E,F). *GUK-h* RNA is not detectable in *guk-h*2 mutant egg chambers. RNA is shown in red (A,C,E) or white (B,D,F,G), DAPI staining in light blue (A,C,E).

4.3 DISCUSSION

We validated experimentally a novel, genome-wide bioinformatics tool for the identification of localisation signals and localising transcripts. We showed that the method identified localisation elements lying in the 3'UTR of *Drosophila* transcripts and increased 5.5 times the localisation rate, when compared with randomly chosen RNAs. Although our data indicate that the bioinformatics predictions were successful to a degree, the observed enrichment is definitely not all we were aiming at when we initiated the screen. Moreover, the statistical significance of this enrichment is 88%, it is therefore essential to test further candidates, in order to confirm the degree and significance of the enrichment and the validity of the bioinformatics approach as a tool for the systematic identification of localisation elements.

Our method did not identify localisation signals in 5'UTRs or protein coding regions of genes, possibly because of the relatively low number of genes that contain localisation signals in these regions when compared with the high number of the ones that incidentally contain elements with similar secondary structure to *GLS* and *ILS*.

The signals we identified by their similarity with *GLS* and *ILS* mediate localisation into embryos, but fail to target the corresponding transcripts at the antero-dorsal cap of the oocyte. This could reflect the ability of the predicted structures to actually mimick the localisation elements of embryonic apical transcripts, rather than *GLS* or *ILS*, and utilise their machinery to get transported in the embryos. An alternative explanation could be that these predicted motifs, indeed mimick the localisation elements of *grk* and the *I* factor, but the corresponding transcripts are not expressed or required during oogenesis, thus they have not been subjected to the selective pressure that would be necessary to develop the fine elements essential for localisation into this system. It is possible to improve the bioinformatics searches by taking into account mutagenesis experiments that have revealed finer structure and sequence requirements for the localisation of *ILS* and *GLS*. For instance, it is now

thought (Van de Bor and Davis, unpublished work) that the some sequence information in the upper loop could be important, as well as the sequence and structure of the upper stem of *GLS* and *ILS,* whereas their lower internal loop and stem are dispensable for localisation. Susanne McDermott in the lab is currently carrying out more mutagenesis experiments to unravel more detailed structure and sequence requirements of the signals. Besides, the experimental validation that we carried out has provided us with biological information that highlights sequence and structural properties required for localisation in embryos and oocytes. This data can be used to train a machine learning algorithm to separate localising from non localising transcripts and predict the localisation fate of other transcripts. Assigning the 3D structure of *GLS* and *ILS* and non localising mutants, using NMR methods (Ball, McDermott and Davis, ongoing work) in combination with prediction of the tertiary structure of the putative signals that share secondary structure similarities with *GLS* and *ILS* will give us more insight into how similar to *GLS* or *ILS* the bioinformatics hits are and narrow down considerably the number of good candidates for a future screen.

The bioinformatics approach was succesfull in identifying other non-LTR retrotransposons that use the host machinery for their transport towards the oocyte nucleus, a step that facilitates import into the nucleus, transposition and passage to the next generation. These retrotransposons could have been, in principle, identified by testing systematically the localisation potential of a large number of transposable elements. Practically, though, this approach would be very laborious and slow, due to the high number of mutated copies of each element in the genome and their large size. The outcome of the gene screen is not contradictory to the success of the transposable element screen. It rather reflects the fact that the latter focused mainly on retrotransposons, a subcategory of candidates that are by nature more likely/expected to localise near the oocyte nucleus and have probably undergone a high selective pressure to do so, in order to be transmitted into the germline and consequently to the next generation. Instead, the gene screen involved the blind selection of a pool of candidates for which we have no evidence that are expressed in

oocytes or code for proteins that are known or thought to be distributed asymmetrically in oocytes or other cell types. The transposable element screen was aiming at identifying, with the help of bioinformatics, other transposable elements, which use the host transport system, in a manner similar to the *I* factor. The gene screen was aiming at a non-biased validation of our bioinformatics approach, as a tool to identify localisation signals in a genome-wide scale.

We identified in total 7 transcripts that localise apically upon injection into blastoderm embryos. The apical enrichment of the endogenous *slmb/CG3412* and *CG1962* has been previously shown by in situ hybridisation data (Tomancak *et al*, 2002), but their mechanism of localisation was not known. Our data show that *slmb/CG3412* is actively transported towards the periphery of the embryos, whereas *CG1962* probably reaches the periphery by diffusion. Further experiments are required to elucidate the factors that mediate the localisation of these transcripts. CG3412/slmb is an F-box protein that targets proteins to the SCF complex for degradation. It is involved in diverse processes, from egg chamber development and chorion structures formation (Muzopappa and Wappner, 2003) to Wingless, Dpp and Hedgehog signalling (Jiang and Struhl, 1998), axis specification in imaginal disks and centrosome duplication in larval neuroblasts (Wojcik *et al*, 2000). It would be interesting to address if slmb RNA or protein are distributed asymmetrically in these tissues and if their distribution is implicated in slmb's multiple tasks. Endogenous *CG1962* RNA is centrosomic, but there is no evidence about CG1962 protein distribution or function. CG5876/heix is a putative membrane transferase, whose loss of function results in the formation of melanotic tumors, overproliferation of hemocytes, overgrowth of imaginal disks and extra-differentiation of wing veins (Ashburner *et al*, 1999). The expression patterns of *heix* RNA or heix protein are not known. *CG11448* and *CG1841* are uncharacterised genes. Tomancak *et al*, 2002 have shown that *CG11448* is expressed in the CNS and *CG1841* in embryonic epidermal stripes, in the antennal sense organ and posterior spiracle, but their hybridization technique and imaging are not sensitive enough to reveal any potential subcellular compartmentalisation of the transcripts. *CG32425* is homogeneous in

very early embryos, but is later found concentrated at the pole plasm and migrating pole cells (Tomancak *et al*, 2002), its role, though, remains unknown. *CG15095* has been identified as a target of hairy transcriptional repressor (Bianchi-Frias *et al*, 2004), but there is no information about its expression pattern.

We discovered that endogenous *GUK-h* RNA localises first at the posterior and later at the anterior or the antero-dorsal corner of oocytes. In a *grk* null mutant background, where the microtubules fail to reorganise during mid oogenesis, *GUK-h* RNA is found at the posterior of stage 7-8 oocytes, concentrated near the oocyte nucleus that has also failed to migrate. This suggests that the localisation of the transcript is MT dependent, but further work is required to confirm the involvement of microtubules and dynein in this process. GUK-h contains a PDZ domain. PDZ modules are known to mediate interactions with carboxyl-terminal domains of transmembrane and other proteins. PDZ proteins usually localise at restricted regions of the cell cortex and promote the recruitment of their interacting partners, clustering them near the membrane (Bilder, 2001). Several PDZ proteins, like Bazooka, Par-6, Discs-large, Scribble and others, have a well documented role in cell shape and polarity. GUK-h interacts with Scribble and Disc-large, physically linking them at neuromuscular junctions (Mathew *et al*, 2002). The protein localises at the borders of synaptic boutons, whereas the RNA has been shown to localise in the periphery of neuroblasts (Mathew *et al*, 2002). There is no other information available about the distribution or the function of GUK-h in other tissues. It would be interesting to address the role of its anterior accumulation in oocytes. Preliminary experiments that I performed using hypomorphic mutants have failed to show any defects in the morphology of the egg chambers, the localisation of *bcd* RNA, *grk* RNA or Grk protein, the morphology of the dorsal appendages or the differentiation of the terminal follicle cells. The examination of germline clones of the available lethal alleles will be essential for the understanding of GUK-h function in oogenesis.

We demonstrated that 2% of *Drosophila* transcripts localise apically, upon injection into the cytoplasm of blastoderm syncytial embryos. These data is in agreement with

experiments performed by Bullock *et al*, 2006 that also showed that 2% of a random pool of transcripts localises apically when injected into blastoderms.

We also observed that a subset of non-localising transcripts can form particles and travel on directed paths, covering considerable distances. It is now shown by Bullock *et al*, 2006 that similar runs of other homogeneously distributed transcripts are mediated by motor activity, which is also consistent with work in mammalian cells that demonstrates that individual RNA molecules move rapidly and directionally on microtubules, regardless of their distribution in the cytoplasm (Fusco *et al.* 2003).

Some of the RNA preparations we injected travelled rapidly and directionally from the site of injection towards the periphery of the embryos, but instead of accumulating apically, they remained basally, underneath the nuclei. It would be interesting to unravel the mechanism that underlies this pattern of localisation and prevents the RNA particles from reaching the minus ends of microtubules.

CHAPTER 5

Development of an RNA localisation assay in cultured *Drosophila* cells, with a view to perform genome-wide screens for factors required for mRNA localisation

5.1 INTRODUCTION

5.1.1 TRANS-ACTING FACTORS INVOLVED IN RNA LOCALISATION

Exciting advances have been made recently towards determining the mechanistic details of RNA localisation pathways. As mentioned in Chapters 1 and 4, it is thought that mRNAs are sorted in the cytoplasm through the association of RNA localisation elements with RNA-binding proteins. These are thought to mediate the subsequent association of other factors, linking the RNA cargo to the molecular motor, thus providing specificity to the choice of transport route and final destination. Although some of these proteins have been identified by genetic screens and biochemical methods and we have now begun to build an understanding on the mechanism that underlies RNA localisation, we are still far from dissecting the RNA transport machinery down to its components or unravelling their function. The only exception to this is provided by *ASH1* mRNA localisation, where it is thought that She2 and She3 together provide the linkage between the Myosin motor and the cargo.

It is possible that some of the subunits of the RNP complexes that mediate mRNA localisation have a strictly structural role, but it is clear that at least some of them must modulate the activity of the motor or provide specificity for the cargo. Different cargoes are able to recruit different motors, but it remains unclear how exactly this is accomplished. There are also reported examples of RNA cargoes that are driven by the same motor but are targeted towards distinct destinations in the same cell. This is the case for *bcd* and *grk* transcripts. They are both thought to be transported by dynein in the *Drosophila* oocyte, but *bcd* localises at the anterior cortex, whereas *grk* concentrates at the antero-dorsal corner, near the oocyte nucleus.

Specificity of transport can arise by various means. Chemically different subsets of microtubules might exist in a cell and guide cargoes towards different paths. Bullock *et al*, 2006 have suggested that different dynein cargoes can control their sorting by

tethering a different number of the same motor complex. It is also possible that some specificity might be provided by different intermediate and light chains of motors (Vale, 2003). However, molecular motors are not thought to bind RNA directly. It is thus apparent that the ability of the transcripts to distinguish between differentially modified subclasses of microtubules, to regulate the number of motors they recruit for their transport or to utilise different motor subunits must be achieved through trans-acting factors that mediate motor-cargo interactions. How the trans-acting factors interact with the motor, the RNA or with their protein partners is poorly understood. Nor is it clear if specificity results from the employment of numerous different factors or by various combinations, numbers or post-translational modifications of a few players.

The identification and characterisation of trans-acting factors involved in RNA localisation has not been trivial for various reasons. The RNA, from its site of transcription till its final destination, becomes decorated with multiple factors implicated in various aspects of its metabolism, such as transcriptional regulation, splicing, capping, 3' end processing, polyadenylation, nuclear export, stability, translation and surveillance. RNP particles are thus typically large and highly dynamic, being repeatedly reshaped by the association-dissociation of numerous proteins (Dreyfuss *et al*, 1993, Dreyfuss *et al*, 2002, Kamma *et al*, 1995, Le Hir *et al*, 2001, Le Hir *et al*, 2000). Furthermore, some of these proteins might be present in small amounts and bind the RNA with low affinity or for a short period of time. Therefore, the biochemical purification of RNP components has been difficult and not decisive for their implication in RNA localisation.

Biochemical approaches have been successful, in some cases, in identifying key RNA localisation factors. For instance, Arn *et al*, 2003 purified a large multiprotein complex that binds the *bcd* localisation signal and demonstrated the requirement of at least one of its components for the anterior accumulation of *bcd*. A dimer of She2 binds to each of the four localisation signals of *ASH1* and is necessary for its transport towards the bud tip (Bohl *et al*, 2000, Takizawa and Vale, 2000, Niessing *et*

al, 2004). However, in most of the reported cases, it is either the interaction of a protein with a transcript or its involvement in localisation that have been demonstrated, but not both. A puzzling example is dIMP, the *Drosophila* homolog of ZBP/Vera. dIMP binds *osk* RNA and mutations in osk's dIMP binding motifs inhibit the colocalisation of *osk* and dIMP and the maintenance of *osk* at the posterior of the oocyte (Munro *et al*, 2006). It is surprising that dIMP is not required for *osk* RNA localisation (Munro *et al*, 2006).

Genetic approaches have also been only partially successful, possibly due to the early requirements of RNA localisation factors in the formation of the germarium and oocyte determination. RNAi screens in *Drosophila* oocytes or early embryos would be unfruitful, as most, if not all, of the RNA localisation determinants are synthesised in the nurse cells very early and are supplied to the developing oocytes and embryos. For instance, in aneuploid embryos that lack individual chromosome arms, pair-rule transcripts localise correctly, suggesting that all the factors required for localisation in blastoderms are maternally supplied and deposited in the egg during oogenesis (Francis-Lang *et al*, 1991).

5.1.2 AIMS OF THIS CHAPTER

The overall long term goal of the project described in this chapter was to overcome these difficulties by establishing in *Drosophila* cells, a genome wide screen for factors required for mRNA localisation. The first step towards this goal would be to develop an RNA localisation assay in cultured *Drosophila* cells. RNAi technology in cultured *Drosophila* cells has been adapted successfully for systematic, high-throughput screens and has facilitated comprehensive functional analysis and dissection of various biological processes, such as cytokinesis (Echard et al, 2004, Eggert et al, 2004), cell size control (Bjorklund et al, 2006), Hedgehog signalling (Gwack et al, 2006), Wingless signalling (DasGupta et al, 2005), splicing (Park et al, 2004) and cell morphogenesis (Kiger et al, 2003). RNAi libraries representing most

of the well annotated genes of the *Drosophila* genome are now widely available, so systematic RNA-screens are only limited by the development of an assay.

The establishment of an RNA localisation assay involves multiple steps. First, we need to identify *Drosophila* cells that look polarised in culture and then address if their microtubule network has an organisation that could support polarised transport and asymmetric cytoplasmic distribution of transcripts. Finally, we need to test the localisation success of endogenous or ectopically provided transcripts and demonstrate the dependence of their asymmetric sorting on the cytoskeleton, motors and known localisation factors. I was interested primarily in establishing an RNA localisation system that would allow us to study dynein-driven transport towards the minus ends of microtubules. This chapter presents some preliminary work I carried out and discusses some interesting ideas that arise from this work for future experiments towards developing such a system. Some of the experiments described here were performed in collaboration with Gavin Craig in the Buzz Baum lab in UCL. His contribution is stated in the results section.

5.2 RESULTS

5.2.1 MORPHOLOGY AND MICROTUBULE ORGANISATION OF S2 CELLS

I first examined S2 cells, which originate from embryos near to hatching. It is known that these cells, under routine growth conditions, adopt a spherical morphology and are small (10μm in diameter), with a thin rim of cytoplasm around the nucleus. For this reason, they have been considered very poor for cytological studies and especially for the examination of the subcellular distribution of organelles or molecules. In these cells the microtubules form a dense, crowded network with no obvious polarity.

However, the morphology of S2 cells changes dramatically when they are allowed to spread on Concanavalin A (ConA), as it is demonstrated by Rogers *et al*, 2002. In order to improve the cytology of S2 cells, the authors tested various substrates for their ability to promote cell adhesion and spreading. ConA promoted cell attachment to coverslips and caused them to adopt a flattened morphology (20μm in diameter). The cells have a radial interphase microtubule network, easy to visualise, with the plus ends extending towards the cell periphery.

In my preparations, S2 cells that were allowed to spread on ConA adopted the same discoid morphology. αtubulin staining showed that most of them had the same well organised MT network. Interestingly, some cells had a polarised MT network, with not only discernible plus tips at the periphery, but also a visible MT organisation centre near the nucleus (Figure 5.2.1). Unfortunately, these cells represented only a small percentage of the interphase cells, with the rest of them having a network of MTs with their plus ends extending radially to the periphery, but their minus ends difficult to visualise or everywhere in the main cytoplasm.

I plated the cells on coverslips treated with different concentrations of ConA (0.5mg/ml-1.5mg/ml) and I incubated them for various periods of time (1h, 2h, 4h and overnight), in an effort to increase the number of cells with the visible MTOC. Although the increase in the incubation time improved the overall MT organisation and imaging, the number of cells with polarised MTs did not obviously increase.

5.2.2 RNA DISTRIBUTION IN S2 CELLS

Using RNA *in situ* hybridisation, I tried to detect endogenous transcripts of S2 cells, but even when I could detect the transcript foci in the nucleus or the corresponding proteins in the cytoplasm, I was unable to detect any specific RNA signal in the cytoplasm (not shown).

Therefore, I transfected S2 cells that were spread on ConA with *ftz*, *runt* and *hairy* cDNA under heatshock control, as well as UbnlsGFP-hsp27-3'UTR, as a negative control of a non localising RNA. The cells were transfected overnight and were then incubated at 37^0C for 30min-1h. RNA *in situs* (Figure 5.2.2) showed that none of the tested RNAs localised in S2 cells, under these conditions. I conclude that S2 cels are not suitable for the establishment of an RNA localisation assay.

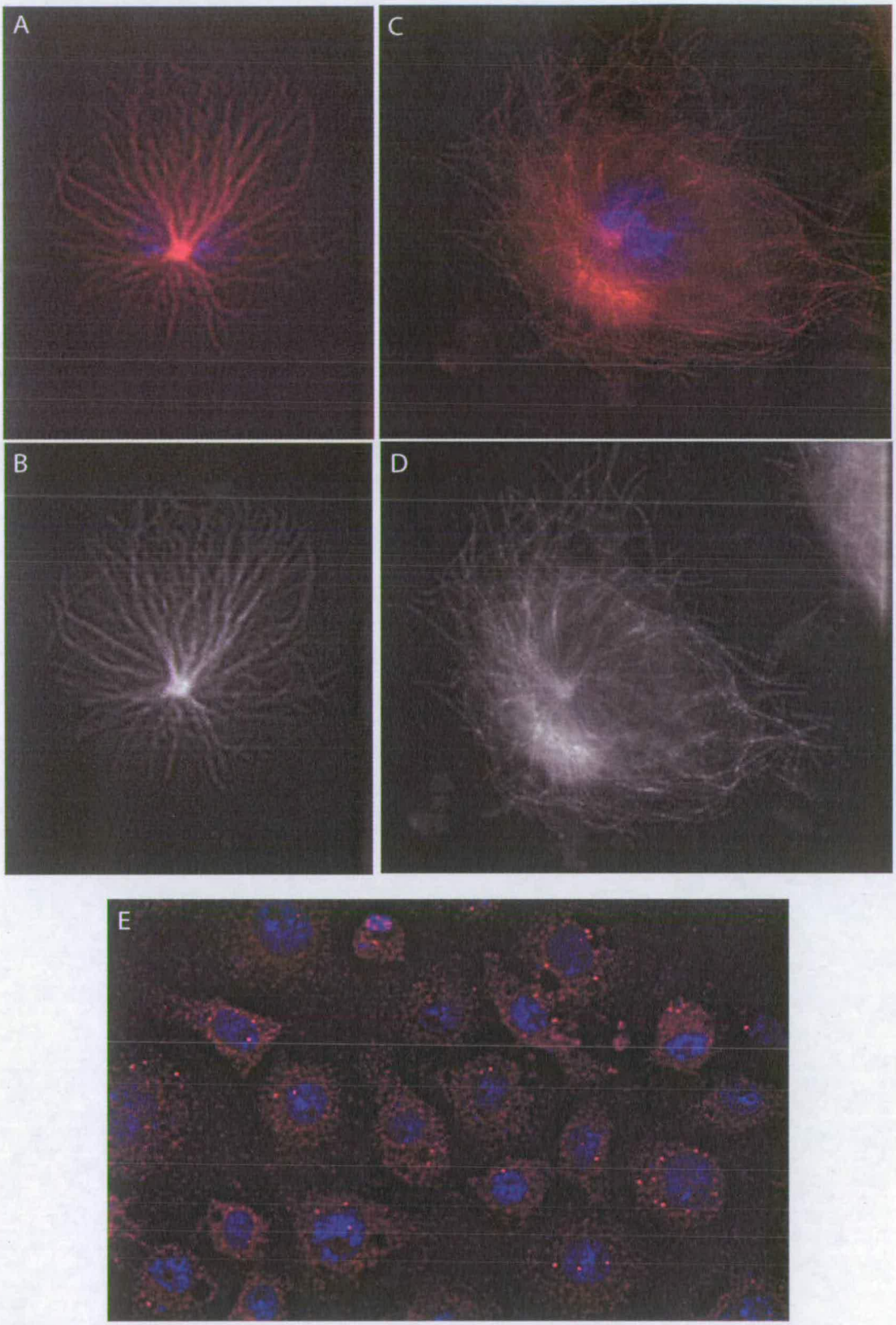


Figure 5.2.1 Morphology and microtubule organisation of S2 cells spread on ConA
αtubulin staining is shown in red (A,C) or white (B,D), γtubulin staining in red (E) and DAPI staining in blue (A,B,E).

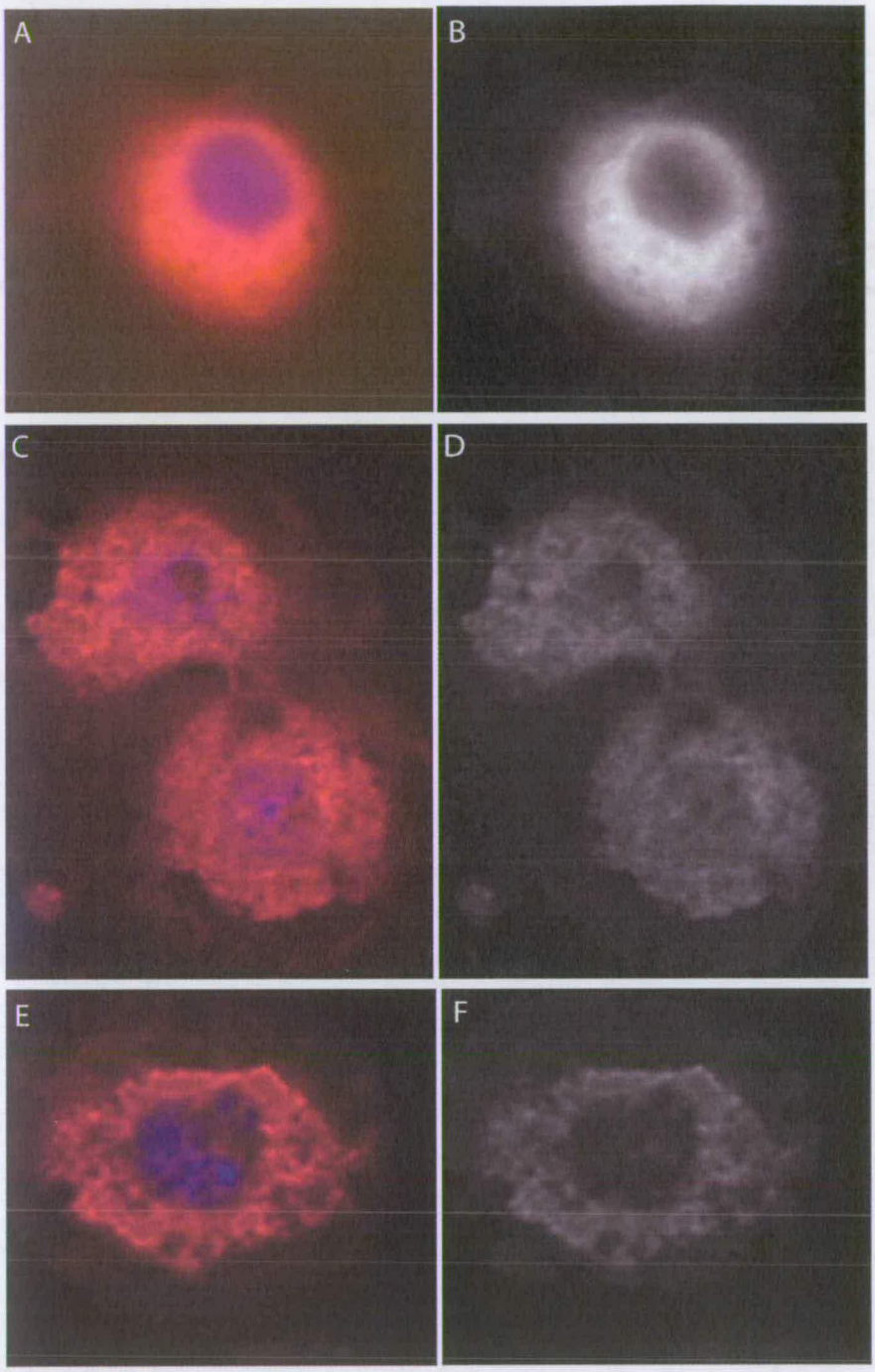


Figure 5.2.2: RNA distribution in S2 cells spread on ConA
S2 cells were transfected with UbnlsGFPhsp273'UTR (A,B), hs-runt (C,D) and hs-hairy (E,F) cDNA, were allowed to spread on ConA and then heatshocked. In situ hybridisation against *GFP* RNA (A,B), *runt* RNA (C,D) and *hairy* RNA (E,F) shows an homogeneous distribution of the transcripts. RNA is shown in red (A,C,E) or white (B,D,F), DAPI staining in blue (A,C,E).

5.2.3 MORPHOLOGY AND MICROTUBULE ORGANISATION OF KC CELLS

Kc cells, like S2 cells, are small, round cells (5-10μm in diameter), with poor cytology and limited applications for subcellular studies. However, they are very sensitive to the hormone 20-hydroxyecdysone or β-ecdysone. Kc cells treated with 20HE stop dividing and differentiate in cells with fibroblast or neuron-like appearance. They have been shown to adopt a spindle shape and emit very long, dynamic filopodia (Echalier, 1997).

I examined the organisation of microtubules in Kc cells treated with 1μg/ml 20-HE for 2 days. γtubulin staining showed that the minus ends of microtubules were ubiquitously distributed in the cytoplasm (Figure 5.2.3C). αtubulin staining detected a crowded network of microtubules in the cell body of Kc cells and microtubule tracks spanning their filopodia (Figure 5.2.3A,B). Although Kc cells do not seem to have a polarised MT network, their microtubules could mediate transport of transcripts towards and within their processes. Further work is required, however, to address their suitability for an RNA localisation assay.

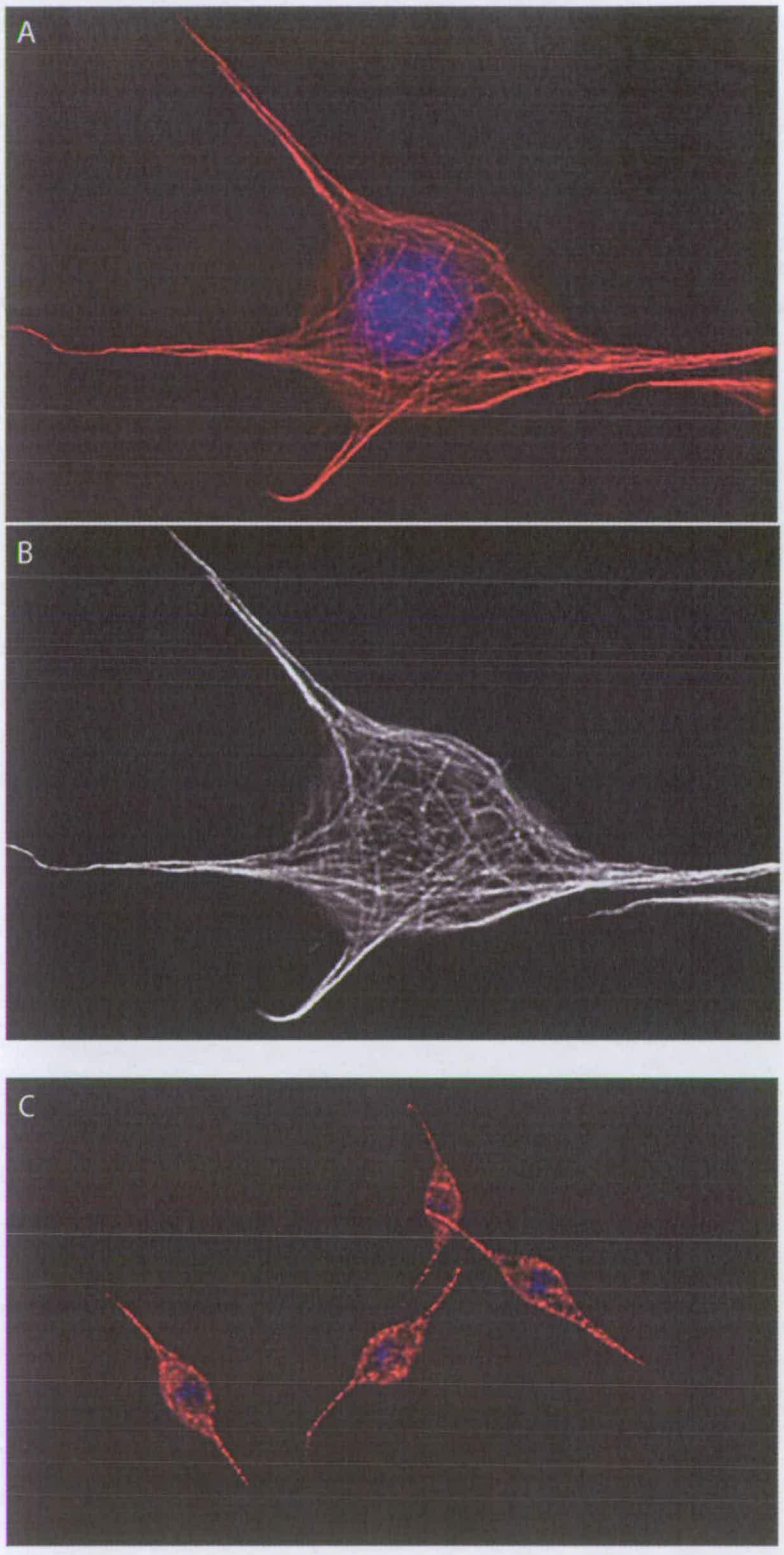


Figure 5.2.3: Morphology and microtubule organisation of Kc cells treated with 20HE
αtubulin staining is shown in red (A) or white (B), γtubulin staining in red (C) and DAPI staining in blue (A,C).

5.2.4 MORHOLOGY, MICROTUBULE ORGANISATION AND RNA DISTRIBUTION OF CLONE 8 CELLS

Cl8 cells are derived from a wing disc cell line (Peel and Milner, 1990). I chose this imaginal disc line because it is the most commonly used, it is sensitive to ecdysteroids (Peel and Milner, 1992) and it can maintain some of the properties of epithelial cells under some conditions (discussed later). Moreover, it has been shown that Cl8 cells are amenable to RNAi (Lum *et al*, 2003).

Clone 8 cells show a characteristic pattern of growth in the stages of a passage. Newly seeded cells adhere to the plastic in a monolayer and spread. After a few rounds of division they begin to pile up and form aggregates and finally these aggregates detach from the plastic and become free-floating. Adherent Cl8 cells have a fibroblast like appearance (Figure 5.2.4A,B). αtubulin staining showed that microtubules tracks span the entire cell, but they probably originate from multiple nucleating centres along the cell, as there is no visible MTOC (Figure 5.2.4C,D). *In situ* hybridisation against the endogenous *wingless* RNA, showed homogenous distribution of the RNA throughout the cytoplasm (Figure 5.2.5).

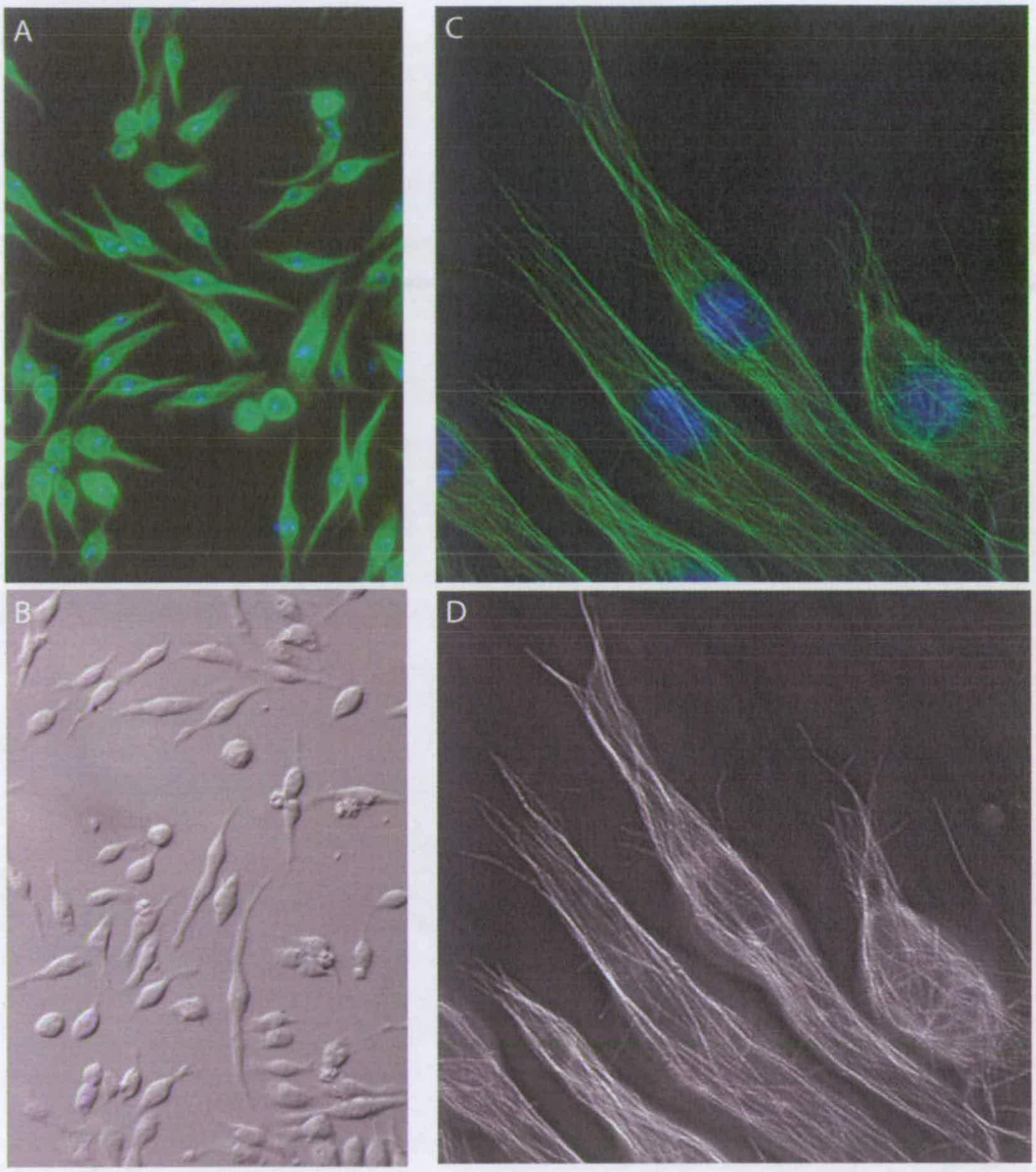


Figure 5.2.4: Morhology and microtubule organisation of clone 8 cells
αtubulin staining in clone 8 cells (A,C,D). αtubulin is shown in green (A,C), or white (D), DAPI staining in blue (A,C). (B) is a DIC image.

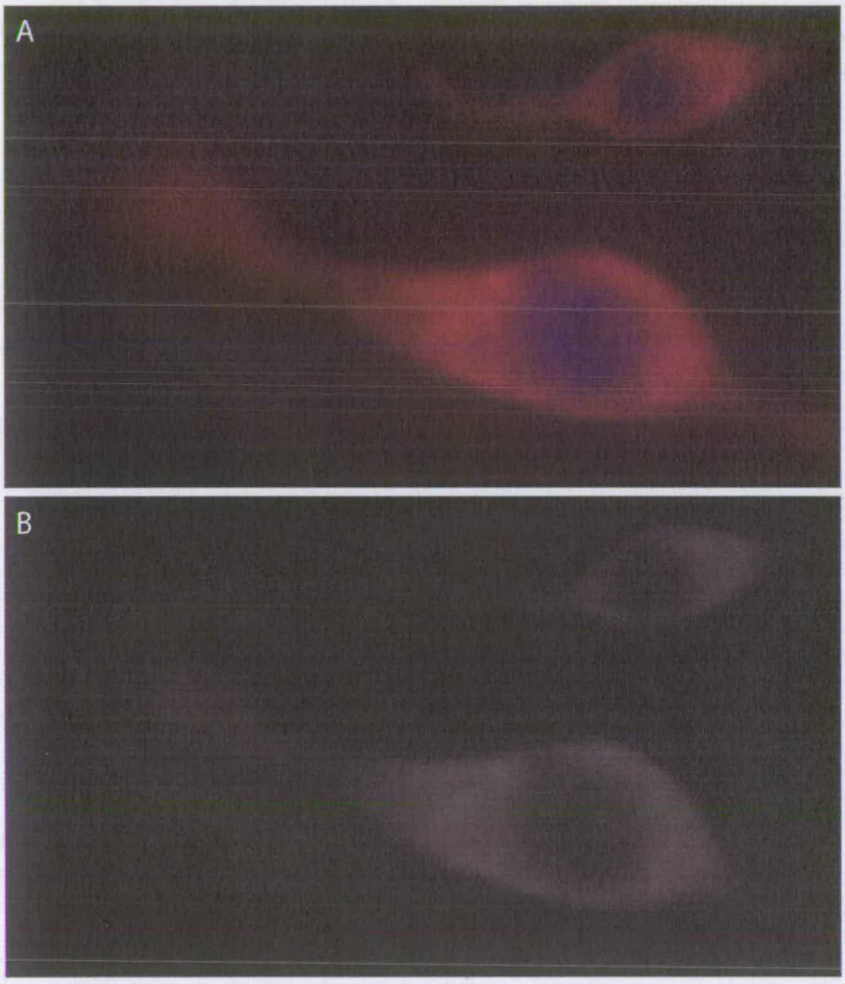


Figure 5.2.5: Distribution of *wingless* RNA in Clone 8 cells
In situ hybridisation against *wingless* RNA in Clone 8 cells. RNA is shown in red (A) or white (B), DAPI staining in blue (A).

5.2.5 MORHOLOGY AND MICROTUBULE ORGANISATION OF SR+, BG2, BG2-C2, MBN1 AND UC88 CELLS

I also examined the morphology and microtubule organisation of various less characterised cell lines. The microtubule organisation of SR+, BG2, BG2-C2, MBN1 and UC88 cells was not known when we carried out these experiments. FLIGHT (www.flight.licr.org), a new database for the integration and cross-correlation of RNAi datasets (Sims *et al*, 2005), provides some information about most of these cell lines. However, their microtubule organisation is either not shown or not clear in the images provided. The experiments described below were carried out in collaboration with Gavin Craig and Buzz Baum in UCL, who are experts in cell culture. Gavin Craig fixed the cells on slides and I performed the antibody stainings, the microscopy and image processing.

SR+ is a neuronal cell line. The cells are large, round and flat. αtubulin staining showed that some cells had a microtubule organising center close to their nucleus but the vast majority of them had a crowded network of microtubules with no obvious polarised organisation (Figure 5.2.6A,B). γtubulin staining confirmed that a small proportion of SR+ cells had a single discrete MTOC. The majority of the cells, however, had multiple MTOCs or showed ubiquitous γtubulin staining throughout the cytoplasm (Figure 5.2.6C). Therefore, I do not consider the SR+ cell line suitable for the development of an RNA localisaiton assay.

I also examined MBN cells, which are hemocytes of tumorous 3rd instar larvae and UC88 cells. MBN cells are round and small cells, whereas UC88 have a lemon-like or spindle-like shape (Figure 4.2.7).

Finally, I tested BG2 and BG2-C2 cell lines, both originating form larval CNS. BG2-C2 are round or lemon-shape cells (Figure 5.2.8A,B), whereas BG2 have long microtubule-rich axon-like processes (Figure 5.2.8C,D and 5.2.9), as shown by αtubulin staining. Single microtubules or microtubule bundles span the entire processes of BG2 cells and could support transport of transcripts from the cell body

to the axon. I thus consider the BG2 cell line a promising candidate for the development of an RNA localisation assay. Unfortunately, we obtained these cells late during my PhD work, so the lack of remaining time prevented me from following this up.

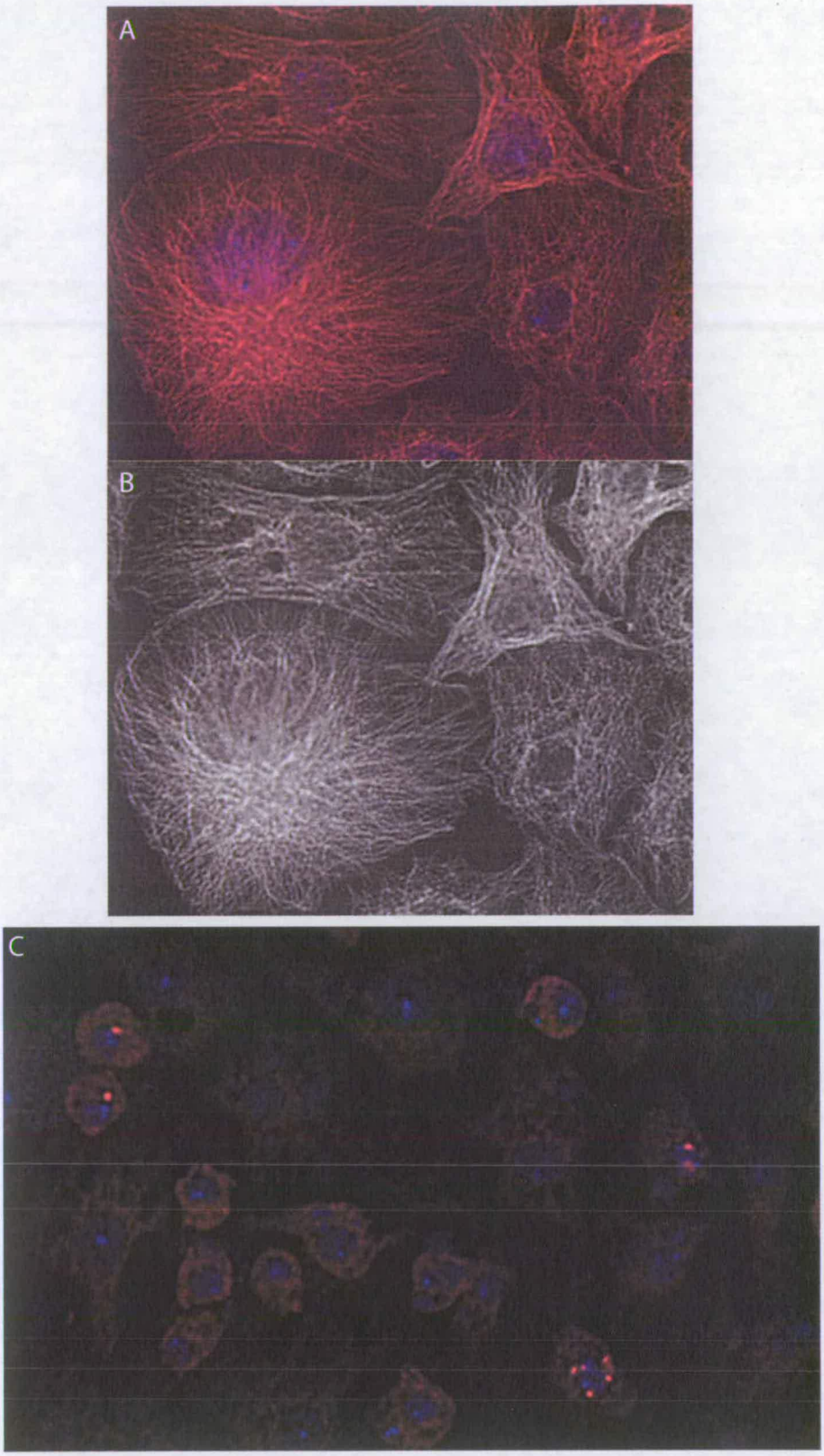


Figure 5.2.6: Morphology and microtubule organisation of SR+ cells
αtubulin staining is shown in red (A) or white (B), γtubulin staining in red (C) and DAPI staining in blue (A,C).

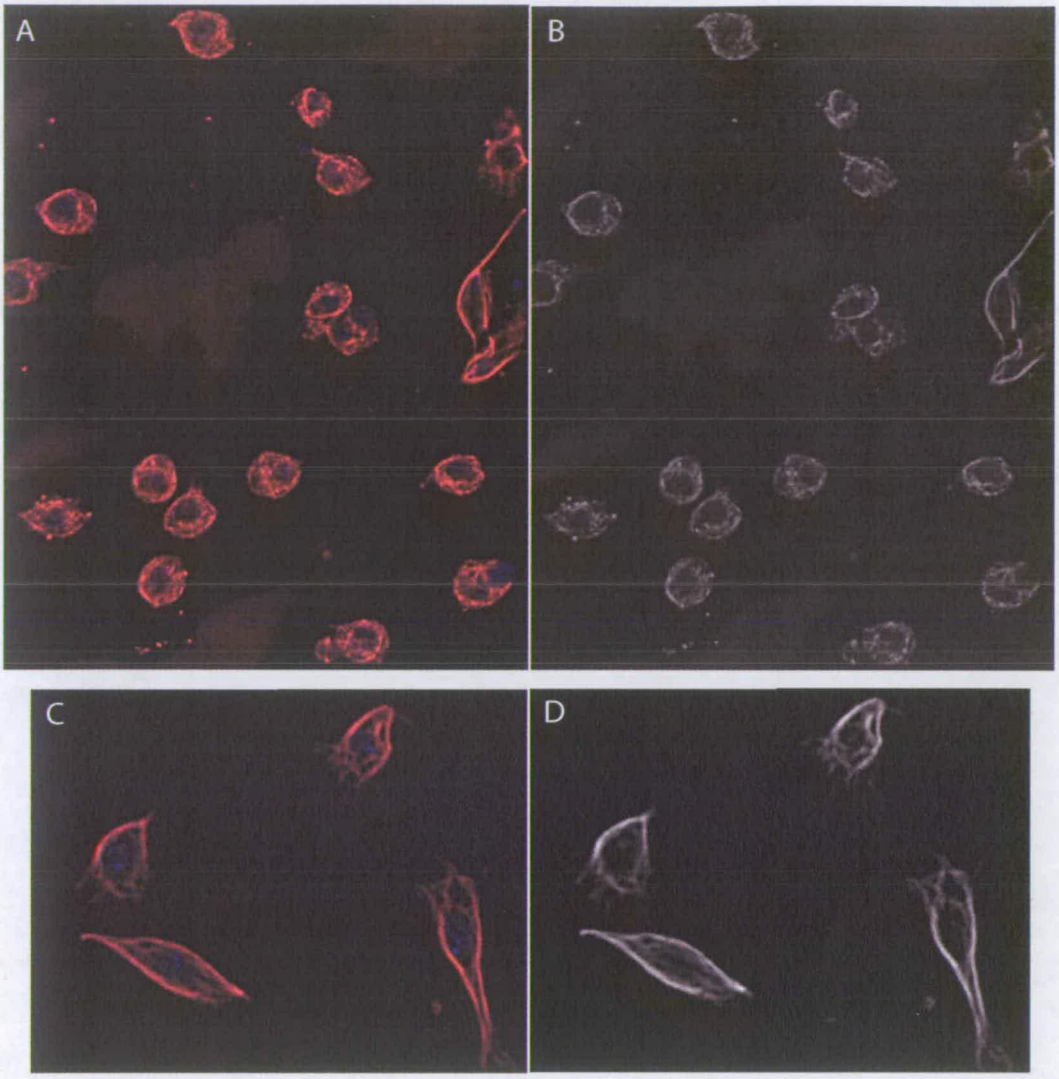


Figure 5.2.7 Morhology and microtubule organisation of MBN2 and UC88 cells
αtubulin staining in MBN2 (A,B) and UC88 cells (C,D). αtubulin is shown in red (A,C) or white (B,D), DAPI staining in blue (A,C).

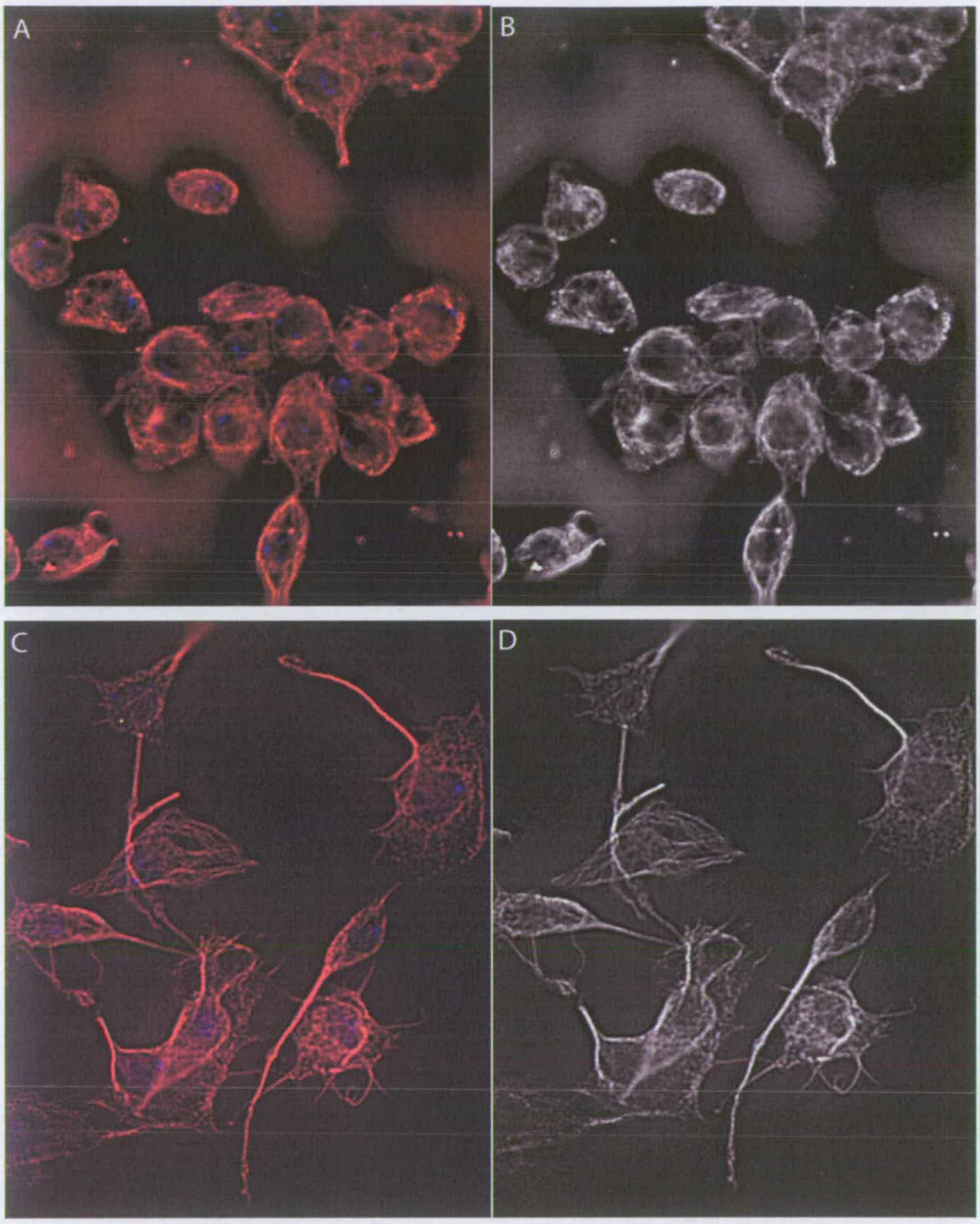


Figure 5.2.8: Morphology and microtubule organisation of BG2-C2 and BG2 cells
αtubulin staining in BG2-C2 (A,B) and BG2 cells (C,D). atubulin is shown in red (A,C) or white (B,D), DAPI staining in blue (A,C).

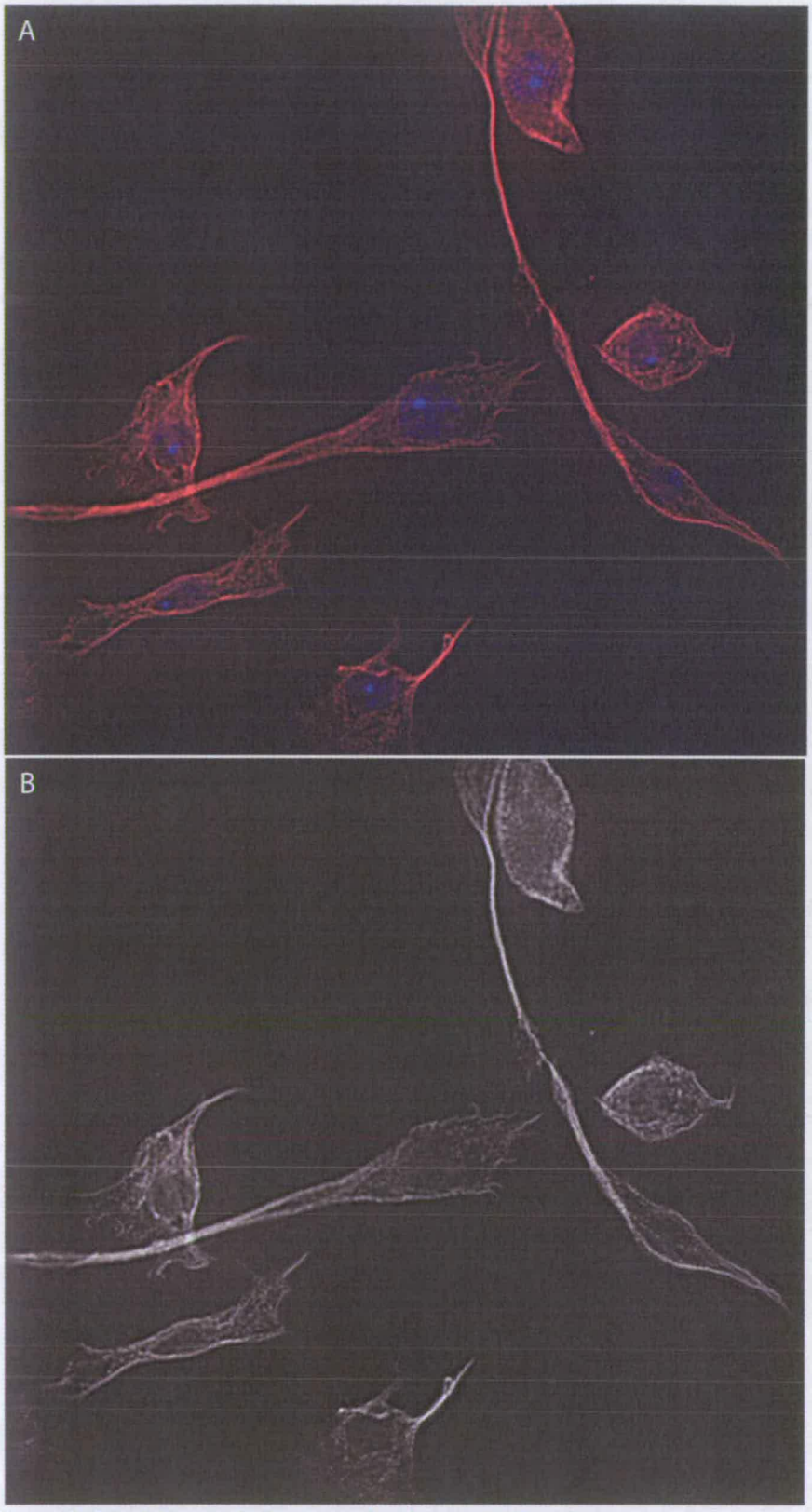


Figure 5.2.9: Microtubule organisation in BG2 cells
atubulin staining is shown in red (A) or white (B), DAPI staining in blue (A).

5.3 DISCUSSION

In this chapter, we tested the morphology and microtubule organisation of various cell lines, under various conditions. Initially, we examined Kc and S2 cells. Since both cell types are undifferentiated and show no signs of polarity, we treated them with 20HE and ConA, which dramatically changed the morphology of Kc cells and S2 cells respectively. Kc cells emitted long, dynamic processes, span by microtubule tracks, upon treatment with 20HE. However, further work is required in order to assess their suitability for an RNA localisation assay.

S2 cells spread on ConA and adopted a discoid morphology, but the examination of their microtubule organisation and in situ hybridisation experiments showed that they are not suitable for the study of dynein mediated transport. It has been reported that ectopic expression of *daughterless* promotes differentiation of S2 cells by activating the myogenic program (Wei *et al*, 2000) and converts them to elongated, flattened, binucleate or multinucleate cells. The microtubule organisation in these cells has not been examined, but it is known that human muscle cell lines have a well organised array of microtubules, extending from the nuclear periphery towards the cell periphery. It would be interesting to test the organisation of the MT network in S2 cells transfected with *daughterless*.

We further tested Clone 8 cells, which derive from imaginal disks. Clone 8 cells looked more polarised in culture than S2 and Kc cells, but they lacked any sign of apico-basal polarity. Nevertheless, it has been demonstrated that they are capable of cell-cell contact and cell-substrate adhesion (Miller *et al*, 1999, Miller *et al*, 2000). This observation suggested that some aspects of apico-basal morphology could be restored under suitable conditions. It is known, for instance, that nutrient uptake through the basement membrane induces and maintains polarity in vivo. Cells grown on coverslips or on flasks in vitro take nutrients via other surfaces. Therefore, Miller *et al*, 2000 grew Cl8 cells on human fibronectin and they discovered that they showed some characteristics of epithelial cells, such as apical microvilli, the beginnings of junctions differentiation at the lateral surfaces and basal epithelial feet.

Epithelial cells have a polarised microtubule network, where microtubules nucleate from their apical surface and extend towards the basal side. Since Cl8 cells grown on fibronectin resemble the imaginal disc cells in vivo much more than conventionally grown cells, I believe that it would be worthwhile testing the organisation of their microtubules and the distribution of candidate RNAs. It is also worth stimulating them with IDGF (Imaginal Disk Growth Factor) that was shown by Kawamura *et al*, 1999 to promote elongation, extension of pseudopodia and increased cell motility. Clone 8 cells, like several other *Drosophila* cell lines, are also sensitive to physiological concentrations of 20HE (Peel and Milner, 1992). The response of cells generally includes dramatic morphological changes, changes in the expression of cell surface glycoproteins, increase of the levels of actin and tubulin, as well as increased cell motility (Echalier, 1997). It would thus worth examining the effect of 20HE on the microtubule network of Cl8 cells in order to assess their suitability for an assay.

We also tested the morphology and microtubule organisation of SR+, UC88, MBN, BG2 and BG-2 *Drosophila* cells. These cell lines are not as well studied as S2, Kc and Cl8 cells and although some information is now available about the properties and morphology of some of them, their microtubule organisation has not been described. We consider BG2 cells good candidates for the establishment of an RNA transport assay. BG2 cells have a neuron-like appearance and emit long processes that are microtubule rich. It is not clear if we imaged single microtubules or bundles of microtubules, but it appears that the microtubule tracks run along the entire process and could support long distance directional travel of transcripts form the cell body towards the axon. We do not necessarily need to identify transcripts that are segregated in restricted regions of the axon, as the transport of transcripts from the cell body to the axon as such, even if it eventually distributes the RNA homogenouesly in the cell, could be used as an assay. Although, there are not reported examples of RNA transport in *Drosophila* axons, there is emerging evidence from other organisms that RNA is transported and translated locally to the synapses and growth cones, to regulate synaptic plasticity and axonal regulation (Martin, 2004). *βactin* RNA and *MBP* RNA are also transported towards the growth

cones and filopodia of rat cultured cells and the processes of mouse oligodendrocytes respectively (Bassell *et al*, 1998). It would be interesting to test the distribution of *actin* RNA or other transcripts in BG2 cells.

When I initiated this project, there was no information available about the expression profile of *Drosophila* cells in culture. The FLIGHT database now provides microarray data about various cell lines, which will facilitate the selection of candidate RNAs and the study of the distribution of endogenous messages, rather than ectopically provided, overexpressed transcripts.

CHAPTER 6

DISCUSSION-FUTURE PERSPECTIVES

RNA localisation is a strategy used by diverse systems to target proteins to their site of function. Asymmetric distribution of transcripts is well documented in germ cells and somatic cells of various organisms, as a means to establish or maintain polarity and initiate or elaborate specification, pattern formation and cell fate determination. In the recent years, it has emerged that RNA sorting has novel, unexpected functions in other fascinating biological processes. For instance, RNA localisation is now considered a central player in axonal navigation and synaptic plasticity, as it enables growth cones and synapses to alter instantly their protein repertoire and subsequently their structure and function, in response to local cues.

The study of the mechanism that underlies RNA localisation has absorbed increasing interest in the last decade and has benefit significantly by the development of in vivo systems susceptible to genetic manipulation or drug disruption and by the use of advanced new techniques for in vivo visualisation of RNA. Labelling of in vitro transcribed RNA with fluorescent dyes or endogenous transcripts with molecular beacons, as well as GFP-tagging of proteins that recognise endogenous or inserted elements in the RNA of interest, have been extremely advantageous for mechanistic studies and have expanded significantly our knowledge about the processes that mediate various RNA localisation pathways. These methods have revealed, for instance, that many transcripts engage molecular motors for their transport towards distinct destinations in the cell. Dynein or kinesin drive their RNA cargoes over long distances, towards the minus or plus ends of microtubule tracks respectively, whereas myosin mediates short-distance transport along actin microfilaments.

Motors have been known for a long time to transport a wide range of organelles and proteins, to power motion of cells or organisms and to mediate chromosome motility and cell division. However, their function in RNA localisation and their subsequent crucial role in fundamental developmental processes were not fully appreciated until recently. It is thus apparent that the discovery of motor-mediated RNA transport does not only further our understanding of the mechanism of RNA localisation, but also adds an exciting new function in the agenda of motor tasks. Moreover, real time

imaging of motor-driven RNA transport in living cells provides us with an assay for the investigation and disruption of motor function in vivo, the emergence of which is reinforced lately by intriguing evidence linking motor defects with neurodegenerative diseases, myopathies and other human disorders. Although the properties of motors have been demonstrated in detail in vitro, it is clear that their behaviour is different in vivo, in a crowded cellular environment, where they can act individually or synergistically in small or large groups, in the presence of their accessory co-factors, competitors and regulators and under natural load.

In the Davis lab, we study motor-driven transport of RNA cargoes by injecting fluorescently tagged transcripts in live *Drosophila* embryos and oocytes and imaging their motion in real time. In chapter 3 of this thesis, I improved the acquisition rate of our sampling, the tracking of motion of RNA particles and the analysis of the tracking data and identified that RNA moves bidirectionally along microtubules. I demonstrated that individual particles of pair rule transcripts, previously shown to travel towards the minus ends of MTs using dynein, occasionally also undergo plus end directed motion. Our data suggests that these backsteps enable the RNA to navigate the space and bypass obstacles.

Many other cargoes that achieve net displacement and asymmetric segregation in restricted regions of the cytoplasm over time are now known to move in a bidirectional manner. In most of the reported cases, the minus motor is dynein, but the plus end directed motor remains to be identified. I have shown that plus motility of RNA is not mediated by Kinesin-1 or Kinesin-2, which are the major cargo transporters towards the plus ends of MTs. Interestingly, Mallik *et al*, 2005 showed that single molecules of cytoplasmic dynein frequently pause or reverse course in vitro. The plus end runs I observe have similar properties to dynein's in vitro backward motility and therefore we suggest that they could be mediated by dynein itself. This hypothesis is not contradictory to data from other systems that have implicated opposite polarity motors in bidirectional motility. In these systems, the requirement of a kinesin-like motor is profound, as cargoes undergo various phases

of movement and the plus end directed motion is the predominant type of motion during at least one of these phases.

As dynein is not known so far to move bidirectionally in vivo, it would be interesting to address its potential role in bidirectional RNA motility. It is shown that, at least in vitro, the backwards movement of the motor is suppressed with the employment and coordination of multiple dyneins in groups. This predicts that a decrease in the dosage of functional dynein in vivo would enhance backward motility. It is worth testing this prediction in dynein mutant backgrounds or by using dynein antibodies and inhibitors. If dynein is indeed responsible for plus RNA motility, we can use our assay to move beyond the investigation of bidirectional RNA motility itself to the detailed study of dynein's bidirectional properties in vivo.

I have demonstrated that dynactin suppresses plus end directed motility of RNA. This could be achieved by various means. Dynactin could balance the power or control the coordination between dynein and a kinesin-related motor. Alternatively, dynactin could eliminate dynein's backward slippage by stabilising dynein on the microtubule or by assembling and coordinating multi-dynein complexes. Future experiments could distinguish between these possibilities by determining how many molecules of dynein are associated with the cargo in various mutant backgrounds.

Motor driven transport RNA cargoes typically requires recognition of signals present on the transcript by the motor machinery. In Chapter 4 of this thesis, we validated a novel bioinformatics approach developed in the Davis lab by Russell Hamilton, as a tool for genome-wide identification of RNA localisation signals related to *gurken* and the *I* factor retrotransposon. We demonstrate that the method can successfully identify other non-LTR retrotransposons that contain localisation signals similar in secondary structure with *GLS* and *ILS* and utilise the oocyte transport machinery for their localisation near the oocyte nucleus. Although the bioinformatics strategy did not highly or significantly enrich for localising transcripts coded by endogenous *Drosophila* genes, it did identify some localisation elements responsible for apical

targeting in blastoderm embryos and led to the identification of dorso-anterior localisation signals in two additional transposable elements.

It is apparently necessary to modify the bioinformatics searches by combining them with biological information defining finer sequence and structure requirements for the localisation of *GLS* and *ILS*. Determination of the structure of *GLS* and *ILS* by NMR, as well as mutagenesis experiments currently carried out in the Davis lab should provide us with information invaluable for future, more sophisticated searches. Moreover, the results of our screen give us some insight on sequence and structure properties responsible or dispensible for localisation and can be useful for training a machine learning algorithm to seperate localising from non localising RNAs and predict the localisation success of untested transcripts.

Motor-driven transport of RNA involves an interplay between the cargo and the transport machinery. The transport machinery recognises the signals or zipcodes of the transcript and targets it to its site of localisation, but at least in some cases the cargo itself also regulates the efficiency of the motor and the kinetics of transport. In Chapter 4 of this thesis, we discovered a novel pattern of transport. A subset of the transcripts we injected in embryos, travelled from the site of injection towards the periphery, but concentrated at the basal side of the nuclei. The speed and directionality of the motion of these transcripts indicates dynein driven transport. It would be interesting to confirm dynein's involvement and identify the signals that regulate the motor and prevent it from reaching the minus ends of MTs. Another remaining question is how many transcripts are transported in this way and how many are transported by dynein to other sites of localisation in the embyro. It would also be interesting to know whether a genuine kinesin based basal RNA transport exists in the embryo.

Our screen also identified seven apically localising transcripts. It is worth addressing in the future their endogenous distribution and the functional role of their asymmetric sorting, as well as the sequences necessary and sufficient for localisation. I showed

that endogenous *guk-h* RNA localises along the anterior margin or at the dorsal-anterior corner of *Drosophila* oocytes. GUK-h is a member of the PDZ family of proteins, which are considered key players in cell shape and polarity. It would thus be interesting to address the potential role of the anterior accumulation of *GUK-h* in maintaining the polarity of the *Drosophila* oocyte. As the spliced *GUK-h* transcript does not localise by injection, it is possible that intronic signals predetermine in the nucleus the cytoplasmic destination of the endogenous transcript.

The destination of a transcript is not specified directly by its cis-acting elements, but by trans-acting factors that interpret these signals. The trans-acting factors do not simply function as adaptors between the molecular motor and the cargo, but also regulate the motor and provide specificity for the cargo. It is surprising that a small repertoire of motors can transport a huge number of cargoes in a controlled manner, but there is relatively little known about how this is achieved. It is even more obscure how a particular motor drives various cargoes towards different destinations in the same cell. Understanding how the complement of transacting factors recruit and influence motors and their choice of transport routes, destinations and anchoring sites, may have to wait until the full composition of localising RNP complexes is determined.

The composition of the RNA localisation apparatus of different transcripts or the specific role of its subunits is still poorly understood. Their biochemical purification of RNA localisation factors is hampered by the fact that RNA molecules during their lifetime become coated with numerous proteins involved in multiple steps of their biogenesis. Genetic approaches for the identification of trans-acting factors have not been entirely straightforward either and cannot be easily performed in large scales, as the lethal phenotypes and maternal effects of the induced mutations make the generation of germline clones essential for their study. Therefore, we thought to employ an RNAi strategy for the identification of novel RNA localisation determinants.

Libraries of dsRNAs against most of the *Drosophila* genes are now available, so the development of an RNA localisation assay is the only limiting factor for the performance of high-throughput RNAi screen. RNA localisation in oocytes and early embryos of *Drosophila* cannot be used as an assay, due to the maternal supply of RNA localisation factors. Therefore, we attempted to establish an RNA localisation system in cultured *Drosophila* cells. The development of such an assay will allow us to screen systematically the genome for trans-acting factors. Genetic and biochemical approaches coupled with yeast-two-hybrid and mass spec will unravel the genetic and physical interactions of the identified candidate factors and dissect the locasome down to its components. Chapter 5 describes our work on developing an RNA localisation system. We consider two of the cell lines we tested promising candidates, but further work is required to confirm their suitability for an RNAi localisation screen.

CHAPTER 7

REFERENCES

Ainger, K., Avossa, D., Diana, A. S., Barry, C., Barbarese, E. and Carson, J. H. (1997). Transport and localization elements in myelin basic protein mRNA. *J Cell Biol* 138, 1077-87.

Allen, L., Kloc, M. and Etkin, L. D. (2003). Identification and characterization of the Xlsirt cis-acting RNA localization element. *Differentiation* 71, 311-21.

Arn, E. A., Cha, B. J., Theurkauf, W. E. and Macdonald, P. M. (2003). Recognition of a bicoid mRNA localization signal by a protein complex containing Swallow, Nod, and RNA binding proteins. *Dev Cell* 4, 41-51.

Ashburner, M., Misra, S., Roote, J., Lewis, S. E., Blazej, R., Davis, T., Doyle, C., Galle, R., George, R., Harris, N., *et al.* (1999). An exploration of the sequence of a 2.9-Mb region of the genome of Drosophila melanogaster: the Adh region. Genetics *153*, 179-219.

Ashkin, A., Schutze, K., Dziedzic, J. M., Euteneuer, U. and Schliwa, M. (1990). Force generation of organelle transport measured in vivo by an infrared laser trap. *Nature* 348, 346-8.

Barker, D. D., Wang, C., Moore, J., Dickinson, L. K. and Lehmann, R. (1992). Pumilio is essential for function but not for distribution of the Drosophila abdominal determinant Nanos. *Genes Dev* 6, 2312-26.

Bashirullah, A., Halsell, S. R., Cooperstock, R. L., Kloc, M., Karaiskakis, A., Fisher, W. W., Fu, W., Hamilton, J. K., Etkin, L. D. and Lipshitz, H. D. (1999). Joint action of two RNA degradation pathways controls the timing of maternal transcript elimination at the midblastula transition in Drosophila melanogaster. *Embo J* 18, 2610-20.

Bassell, G. J., Kao, A. C., Kislauskis, E. H., Femino, A. F., Lifshitz, L. M., Singer, R. H. and Kosik, K. S. (1995). Localization Of Beta-Actin Messenger-Rna to Growth Cones Depends On Microtubles and Cis-Acting Sequences Specific to Neurons. *Molecular Biology Of the Cell* 6, 700-700.

Bassell, G. J., Zhang, H., Byrd, A. L., Femino, A. M., Singer, R. H., Taneja, K. L., Lifshitz, L. M., Herman, I. M., and Kosik, K. S. (1998). Sorting of beta-actin mRNA and protein to neurites and growth cones in culture. J Neurosci *18*, 251-265.

Basyuk, E., Galli, T., Mougel, M., Blanchard, J. M., Sitbon, M. and Bertrand, E. (2003). Retroviral genomic RNAs are transported to the plasma membrane by endosomal vesicles. *Dev Cell* 5, 161-74.

Beckel-Mitchener, A. and Greenough, W. T. (2004). Correlates across the structural, functional, and molecular phenotypes of fragile X syndrome. *Ment Retard Dev Disabil Res Rev* 10, 53-9.

Bergsten, S. E. and Gavis, E. R. (1999). Role for mRNA localization in translational activation but not spatial restriction of nanos RNA. *Development* 126, 659-69.

Berleth, T., Burri, M., Thoma, G., Bopp, D., Richstein, S., Frigerio, G., Noll, M. and Nusslein-Volhard, C. (1988). The role of localization of bicoid RNA in organizing the anterior pattern of the Drosophila embryo. *Embo J* 7, 1749-56.

Betley, J. N., Heinrich, B., Vernos, I., Sardet, C., Prodon, F. and Deshler, J. O. (2004). Kinesin II mediates Vg1 mRNA transport in Xenopus oocytes. *Curr Biol* 14, 219-24.

Bjorklund, M., Taipale, M., Varjosalo, M., Saharinen, J., Lahdenpera, J., and Taipale, J. (2006). Identification of pathways regulating cell size and cell-cycle progression by RNAi. Nature *439*, 1009-1013.

Bobola, N., Jansen, R. P., Shin, T. H. and Nasmyth, K. (1996). Asymmetric accumulation of Ash1p in postanaphase nuclei depends on a myosin and restricts yeast mating-type switching to mother cells. *Cell* 84, 699-709.

Bohl, F., Kruse, C., Frank, A., Ferring, D. and Jansen, R. P. (2000). She2p, a novel RNA-binding protein tethers ASH1 mRNA to the Myo4p myosin motor via She3p. *Embo J* 19, 5514-24.

Bowman, A. B., Kamal, A., Ritchings, B. W., Philp, A. V., McGrail, M., Gindhart, J. G. and Goldstein, L. S. (2000). Kinesin-dependent axonal transport is mediated by the sunday driver (SYD) protein. *Cell* 103, 583-94.

Brendza, K. M., Rose, D. J., Gilbert, S. P. and Saxton, W. M. (1999). Lethal kinesin mutations reveal amino acids important for ATPase activation and structural coupling. *J Biol Chem* 274, 31506-14.

Brendza, R. P., Serbus, L. R., Duffy, J. B. and Saxton, W. M. (2000). A function for kinesin I in the posterior transport of *oskar* mRNA and Staufen protein. *Science* 289, 2120-2.

Brendza, R., Serbus, L., Saxton, W., and Duffy, J. (2002). Posterior localization of Dynein and dorsal-ventral axis formation depend on Kinesin in Drosophila oocytes. Curr Biol *12*, 1541.

Broadus, J., Fuerstenberg, S. and Doe, C. Q. (1998). Staufen-dependent localization of prospero mRNA contributes to neuroblast daughter-cell fate. *Nature* 391, 792-5.

Bullock, S. L. and Ish-Horowicz, D. (2001). Conserved signals and machinery for RNA transport in *Drosophila* oogenesis and embryogenesis. *Nature* 414, 611-616.

Bullock, S. L., Stauber, M., Prell, A., Hughes, J. R., Ish-Horowicz, D. and Schmidt-Ott, U. (2004). Differential cytoplasmic mRNA localisation adjusts pair-rule transcription factor activity to cytoarchitecture in dipteran evolution. *Development* 131, 4251-61.

Bullock, S. L., Zicha, D. and Ish-Horowicz, D. (2003). The Drosophila hairy RNA localization signal modulates the kinetics of cytoplasmic mRNA transport. *Embo J* 22, 2484-94.

Bullock, S. L., Nicol, A., Gross, S. P., and Zicha, D. (2006). Guidance of bidirectional motor complexes by mRNA cargoes through control of dynein number and activity. Curr Biol *16*, 1447-1452.

Carson, J. H., Worboys, K., Ainger, K. and Barbarese, E. (1997). Translocation of myelin basic protein mRNA in oligodendrocytes requires microtubules and kinesin. *Cell Motil Cytoskeleton* 38, 318-28.

Chabanon, H., Nury, D., Mickleburgh, I., Burtle, B. and Hesketh, J. (2004). Characterization of the cis-acting element directing perinuclear localization of the metallothionein-1 mRNA. *Biochem Soc Trans* 32, 702-4.

Chartrand, P., Meng, X. H., Singer, R. H. and Long, R. M. (1999). Structural elements required for the localization of ASH1 mRNA and of a green fluorescent protein reporter particle in vivo. *Current Biology* 9, 333-336.

Chicurel, M. E., Terrian, D. M. and Potter, H. (1993). mRNA at the synapse: analysis of a synaptosomal preparation enriched in hippocampal dendritic spines. *J Neurosci* 13, 4054-63.

Chou, T. B., Noll, E. and Perrimon, N. (1993). Autosomal P[ovoD1] dominant female-sterile insertions in Drosophila and their use in generating germ-line chimeras. *Development* 119, 1359-69.

Clark, I., Giniger, E., Ruohola-Baker, H., Jan, L. Y. and Jan, Y. N. (1994). Transient posterior localization of a kinesin fusion protein reflects anteroposterior polarity of the *Drosophila* oocyte. *Current Biology* 4, 289-300.

Clark, I. E., Jan, L. Y. and Jan, Y. N. (1997). Reciprocal localization of Nod and kinesin fusion proteins indicates microtubule polarity in the *Drosophila* oocyte, epithelium, neuron and muscle. *Development* 124, 461-470.

Cohen, R. S., Zhang, S. and Dollar, G. L. (2005). The positional, structural, and sequence requirements of the Drosophila TLS RNA localization element. *Rna* 11, 1017-29.

Cote, C. A., Gautreau, D., Denegre, J. M., Kress, T. L., Terry, N. A. and Mowry, K. L. (1999). A Xenopus protein related to hnRNP I has a role in cytoplasmic RNA localization. *Mol Cell* 4, 431-7.

Cristofanilli, M., Iacoangeli, A., Muslimov, I. A. and Tiedge, H. (2006). Neuronal BC1 RNA: microtubule-dependent dendritic delivery. *J Mol Biol* 356, 1118-23.

Culver-Hanlon, T. L., Lex, S. A., Stephens, A. D., Quintyne, N. J., and King, S. J. (2006). A microtubule-binding domain in dynactin increases dynein processivity by skating along microtubules. Nat Cell Biol *8*, 264-270.

DasGupta, R., Kaykas, A., Moon, R. T., and Perrimon, N. (2005). Functional genomic analysis of the Wnt-wingless signaling pathway. Science *308*, 826-833.

Dawson, A., Hartswood, E., Paterson, T., and Finnegan, D. J. (1997). A LINE-like transposable element in Drosophila, the I factor, encodes a protein with properties similar to those of retroviral nucleocapsids. Embo J *16*, 4448-4455.

Deacon, S. W., Serpinskaya, A. S., Vaughan, P. S., Lopez Fanarraga, M., Vernos, I., Vaughan, K. T. and Gelfand, V. I. (2003). Dynactin is required for bidirectional organelle transport. *J Cell Biol* 160, 297-301.

Deshler, J. O., Highett, M. I. and Schnapp, B. J. (1997). Localization of Xenopus Vg1 mRNA by Vera protein and the endoplasmic reticulum. *Science* 276, 1128-31.

Ding, D., Parkhurst, S. M., Halsell, S. R. and Lipshitz, H. D. (1993). Dynamic Hsp83 RNA localization during Drosophila oogenesis and embryogenesis. *Mol Cell Biol* 13, 3773-81.

Dreyfuss, G., Kim, V. N., and Kataoka, N. (2002). Messenger-RNA-binding proteins and the messages they carry. Nat Rev Mol Cell Biol *3*, 195-205.

Dreyfuss, G., Matunis, M. J., Pinol-Roma, S., and Burd, C. G. (1993). hnRNP proteins and the biogenesis of mRNA. Annu Rev Biochem *62*, 289-321.

Dubnau, J. and Struhl, G. (1996). RNA recognition and translational regulation by a homeodomain protein. *Nature* 379, 694-9.

Duchek, P. and Rorth, P. (2001). Guidance of cell migration by EGF receptor signaling during Drosophila oogenesis. *Science* 291, 131-3.

Echard, A., Hickson, G. R., Foley, E., and O'Farrell, P. H. (2004). Terminal cytokinesis events uncovered after an RNAi screen. Curr Biol *14*, 1685-1693.

Echalir, Guy, 1997. *Drosophila* cells in culture.

Echeverri, C. J., Paschal, B. M., Vaughan, K. T. and Vallee, R. B. (1996). Molecular characterization of the 50-kD subunit of dynactin reveals function for the complex in chromosome alignment and spindle organization during mitosis. *J Cell Biol* 132, 617-33.

Eckley, D. M., Gill, S. R., Melkonian, K. A., Bingham, J. B., Goodson, H. V., Heuser, J. E. and Schroer, T. A. (1999). Analysis of dynactin subcomplexes reveals a novel actin-related protein associated with the arp1 minifilament pointed end. *J Cell Biol* 147, 307-20.

Eggert, U. S., Kiger, A. A., Richter, C., Perlman, Z. E., Perrimon, N., Mitchison, T. J., and Field, C. M. (2004). Parallel chemical genetic and genome-wide RNAi screens identify cytokinesis inhibitors and targets. PLoS Biol *2*, e379.

Endow, S. A. and Higuchi, H. (2000). A mutant of the motor protein kinesin that moves in both directions on microtubules. *Nature* 406, 913-6.

Ephrussi, A., Dickinson, L. K. and Lehmann, R. (1991). Oskar organizes the germ plasm and directs localization of the posterior determinant nanos. *Cell* 66, 37-50.

Ephrussi, A. and St Johnston, D. (2004). Seeing is believing: the bicoid morphogen gradient matures. *Cell* 116, 143-52.

Fawcett, D. H., Lister, C. K., Kellett, E., and Finnegan, D. J. (1986). Transposable Elements Controlling I-R Hybrid Dysgenesis in D. melanogaster Are Similar to Mammalian LINEs. Cell *47*, 1007-1015.

Ferrandon, D., Elphick, L., Nüsslein-Volhard, C. and St Johnston, D. (1994). Staufen protein associates with the 3'UTR of bicoid mRNA to form particles that move in a microtubule-dependent manner. *Cell* 79, 1221-32.

Forrest, K. M. and Gavis, E. R. (2003). Live imaging of endogenous RNA reveals a diffusion and entrapment mechanism for nanos mRNA localization in Drosophila. *Curr Biol* 13, 1159-68.

Francis-Lang, H., Davis, I., and Ish-Horowicz, D. (1996). Asymmetric localization of *Drosophila* pair-rule rranscripts from displaced nuclei - evidence for directional nuclear export. Embo Journal *15*, 640-649.

Fusco, D., Accornero, N., Lavoie, B., Shenoy, S. M., Blanchard, J. M., Singer, R. H., and Bertrand, E. (2003). Single mRNA molecules demonstrate probabilistic movement in living mammalian cells. Curr Biol *13*, 161-167.

Gautreau, D., Cote, C. A. and Mowry, K. L. (1997). Two copies of a subelement from the Vg1 RNA localization sequence are sufficient to direct vegetal localization in Xenopus oocytes. *Development* 124, 5013-20.

Gibbons, I. R., Lee-Eiford, A., Mocz, G., Phillipson, C. A., Tang, W. J. and Gibbons, B. H. (1987). Photosensitized cleavage of dynein heavy chains. Cleavage at the "V1 site" by irradiation at 365 nm in the presence of ATP and vanadate. *J Biol Chem* 262, 2780-6.

Glotzer, J. B., Saffrich, R., Glotzer, M. and Ephrussi, A. (1997). Cytoplasmic flows localize injected oskar RNA in Drosophila oocytes. *Current Biology* 7, 326-337.

Gonzalez, I., Buonomo, S. B., Nasmyth, K. and von Ahsen, U. (1999). ASH1 mRNA localization in yeast involves multiple secondary structural elementsand ash1 protein translation. *Curr Biol* 9, 337-40.

Gonzalez-Reyes, A., Elliott, H., and St Johnston, D. (1995). Polarization of both major body axes in *Drosophila* by Gurken-Torpedo signaling. Nature *375*, 654-658.

Gross, S. P. (2004). Hither and yon: a review of bi-directional microtubule-based transport. *Phys Biol* 1, R1-11.

Gross, S. P., Welte, M. A., Block, S. M. and Wieschaus, E. F. (2000). Dynein-mediated cargo transport in vivo. A switch controls travel distance. *J Cell Biol* 148, 945-56.

Gross, S. P., Welte, M. A., Block, S. M. and Wieschaus, E. F. (2002). Coordination of opposite-polarity microtubule motors. *J Cell Biol* 156, 715-24.

Habermann, A., Schroer, T. A., Griffiths, G. and Burkhardt, J. K. (2001). Immunolocalization of cytoplasmic dynein and dynactin subunits in cultured macrophages: enrichment on early endocytic organelles. *J Cell Sci* 114, 229-240.

Hachet, O. and Ephrussi, A. (2004). Splicing of oskar RNA in the nucleus is coupled to its cytoplasmic localization. *Nature* 428, 959-63.

Hall, D. H. and Hedgecock, E. M. (1991). Kinesin-related gene unc-104 is required for axonal transport of synaptic vesicles in C. elegans. *Cell* 65, 837-47.

Han, J. W., Park, J. H., Kim, M. and Lee, J. (1997). mRNAs for microtubule proteins are specifically colocalized during the sequential formation of basal

body, flagella, and cytoskeletal microtubules in the differentiation of Naegleria gruberi. *J Cell Biol* 137, 871-9.

Haywood, V., Yu, T. S., Huang, N. C. and Lucas, W. J. (2005). Phloem long-distance trafficking of GIBBERELLIC ACID-INSENSITIVE RNA regulates leaf development. *Plant J* 42, 49-68.

Hoek, K. S., Kidd, G. J., Carson, J. H. and Smith, R. (1998). hnRNP A2 selectively binds the cytoplasmic transport sequence of myelin basic protein mRNA. *Biochemistry* 37, 7021-9.

Hofacker, I. L. (2003). Vienna RNA secondary structure server. Nucleic Acids Res *31*, 3429-3431.

Hofacker, I. L., Bernhart, S. H., and Stadler, P. F. (2004). Alignment of RNA base pairing probability matrices. Bioinformatics *20*, 2222-2227.

Holleran, E. A., Karki, S. and Holzbaur, E. L. (1998). The role of the dynactin complex in intracellular motility. *Int Rev Cytol* 182, 69-109.

Hughes, J. R., Bullock, S. L. and Ish-Horowicz, D. (2004). Inscuteable mRNA localization is dynein-dependent and regulates apicobasal polarity and spindle length in Drosophila neuroblasts. *Curr Biol* 14, 1950-6.

Hurd, D. D. and Saxton, W. M. (1996). Kinesin mutations cause motor neuron disease phenotypes by disrupting fast axonal transport in Drosophila. *Genetics* 144, 1075-85.

Ingham, P. W. (1985). Genetic control of the spatial pattern of selector gene expression in Drosophila. *Cold Spring Harb Symp Quant Biol* 50, 201-8.

Jiang, J., and Struhl, G. (1998). Regulation of the Hedgehog and Wingless signalling pathways by the F-box/WD40-repeat protein Slimb. Nature *391*, 493-496.

Kamma, H., Portman, D. S., and Dreyfuss, G. (1995). Cell type-specific expression of hnRNP proteins. Exp Cell Res *221*, 187-196.

Kanai, Y., Dohmae, N. and Hirokawa, N. (2004). Kinesin Transports RNA; Isolation and Characterization of an RNA-Transporting Granule. *Neuron* 43, 513-25.

Karlin-Mcginness, M., Serano, T. L. and Cohen, R. S. (1996). Comparative analysis of the kinetics and dynamics of K10, bicoid, and oskar mRNA localization in the Drosophila oocyte. *Dev Genet* 19, 238-48.

Karki, S. and Holzbaur, E. L. (1995). Affinity chromatography demonstrates a direct binding between cytoplasmic dynein and the dynactin complex. *J Biol Chem* 270, 28806-11.

Keene, J. D. and Tenenbaum, S. A. (2002). Eukaryotic mRNPs may represent posttranscriptional operons. *Mol Cell* 9, 1161-7

Kiger, A. A., Baum, B., Jones, S., Jones, M. R., Coulson, A., Echeverri, C., and Perrimon, N. (2003). A functional genomic analysis of cell morphology using RNA interference. J Biol *2*, 27.

King, S. J. and Schroer, T. A. (2000). Dynactin increases the processivity of the cytoplasmic dynein motor. *Nat Cell Biol* 2, 20-4.

Kohrmann, M., Luo, M., Kaether, C., DesGroseillers, L., Dotti, C. G. and Kiebler, M. A. (1999). Microtubule-dependent recruitment of Staufen-green fluorescent protein into large RNA-containing granules and subsequent dendritic transport in living hippocampal neurons. *Mol Biol Cell* 10, 2945-53.

Lakadamyali, M., Rust, M. J., Babcock, H. P. and Zhuang, X. (2003). Visualizing infection of individual influenza viruses. *Proc Natl Acad Sci U S A* 100, 9280-5.

Lambert, J. D. and Nagy, L. M. (2002). Asymmetric inheritance of centrosomally localized mRNAs during embryonic cleavages. *Nature* 420, 682-6.

Le Bot, N., Antony, C., White, J., Karsenti, E. and Vernos, I. (1998). Role of xklp3, a subunit of the Xenopus kinesin II heterotrimeric complex, in membrane transport between the endoplasmic reticulum and the Golgi apparatus. *J Cell Biol* 143, 1559-73.

Le Hir, H., Moore, M. J., and Maquat, L. E. (2000). Pre-mRNA splicing alters mRNP composition: evidence for stable association of proteins at exon-exon junctions. Genes Dev *14*, 1098-1108.

Leopold, P. L., Snyder, R., Bloom, G. S. and Brady, S. T. (1990). Nucleotide specificity for the bidirectional transport of membrane-bounded organelles in isolated axoplasm. *Cell Motil Cytoskeleton* 15, 210-9.

Li, P., Yang, X. H., Wasser, M., Cai, Y. and Chia, W. (1997). Inscuteable and staufen mediate asymmetric localization and segregation of prospero RNA during Drosophila neuroblast cell divisions. *Cell* 90, 437-447.

Long, R. M., Chartrand, P., Gu, W., Meng, X. H., Schaefer, M. R. and Singer, R. H. (1997a). Characterization of transport and localization of ASH1 mRNA in yeast. *Molecular Biology Of the Cell* 8, 2060-2060.

Long, R. M., Gu, W., Lorimer, E., Singer, R. H. and Chartrand, P. (2000). She2p is a novel RNA-binding protein that recruits the Myo4p-She3p complex to ASH1 mRNA. ***Embo J*** **19, 6592-601.**

Long, R. M., Singer, R. H., Meng, X. H., Gonzalez, I., Nasmyth, K. and Jansen, R. P. (1997b). Mating type switching in yeast controlled by asymmetric localization of ASH1 mRNA. ***Science*** **277, 383-387.**

Lum, L., Yao, S., Mozer, B., Rovescalli, A., Von Kessler, D., Nirenberg, M., and Beachy, P. A. (2003). Identification of Hedgehog pathway components by RNAi in Drosophila cultured cells. Science ***299*****, 2039-2045.**

Macdonald, P. M., Kerr, K., Smith, J. L. and Leask, A. (1993). RNA regulatory element BLE1 directs the early steps of bicoid mRNA localization. ***Development*** **118, 1233-43.**

MacDougall, N., Clark, A., MacDougall, E. and Davis, I. (2003). Drosophila gurken (TGFalpha) mRNA Localizes as Particles that Move within the Oocyte in Two Dynein-Dependent Steps. ***Dev Cell*** **4, 307-19.**

Macke, T. J., Ecker, D. J., Gutell, R. R., Gautheret, D., Case, D. A., and Sampath, R. (2001). RNAMotif, an RNA secondary structure definition and search algorithm. Nucleic Acids Res ***29*****, 4724-4735.**

Mallik, R., Carter, B. C., Lex, S. A., King, S. J. and Gross, S. P. (2004). Cytoplasmic dynein functions as a gear in response to load. ***Nature*** **427, 649-52.**

Mallik, R., Petrov, D., Lex, S. A., King, S. J. and Gross, S. P. (2005). Building complexity: an in vitro study of cytoplasmic dynein with in vivo implications. ***Curr Biol*** **15, 2075-85.**

Martin, K. C. (2004). Local protein synthesis during axon guidance and synaptic plasticity. Curr Opin Neurobiol ***14*****, 305-310.**

Martin, M., Iyadurai, S. J., Gassman, A., Gindhart, J. G., Jr., Hays, T. S. and Saxton, W. M. (1999). Cytoplasmic dynein, the dynactin complex, and kinesin are interdependent and essential for fast axonal transport. ***Mol Biol Cell*** **10, 3717-28.**

Matanis, T., Akhmanova, A., Wulf, P., Del Nery, E., Weide, T., Stepanova, T., Galjart, N., Grosveld, F., Goud, B., De Zeeuw, C. I. et al. (2002). Bicaudal-D regulates COPI-independent Golgi-ER transport by recruiting the dynein-dynactin motor complex. ***Nat Cell Biol*** **4, 986-92.**

Mathew, D., Gramates, L. S., Packard, M., Thomas, U., Bilder, D., Perrimon, N., Gorczyca, M., and Budnik, V. (2002). Recruitment of scribble to the

synaptic scaffolding complex requires GUK-holder, a novel DLG binding protein. Curr Biol *12*, 531-539.

Matsuzaki, F., Ohshiro, T., Ikeshima-Kataoka, H. and Izumi, H. (1998). miranda localizes staufen and prospero asymmetrically in mitotic neuroblasts and epithelial cells in early Drosophila embryogenesis. *Development* 125, 4089-98.

McDonald, D., Vodicka, M. A., Lucero, G., Svitkina, T. M., Borisy, G. G., Emerman, M. and Hope, T. J. (2002). Visualization of the intracellular behavior of HIV in living cells. *J Cell Biol* 159, 441-52.

McDonald, H. B., Stewart, R. J. and Goldstein, L. S. (1990). The kinesin-like ncd protein of Drosophila is a minus end-directed microtubule motor. *Cell* 63, 1159-65.

McGrail, M., Gepner, J., Silvanovich, A., Ludmann, S., Serr, M. and Hays, T. S. (1995). Regulation of cytoplasmic dynein function in vivo by the *Drosophila* Glued complex. *J. Cell Biol.* 131, 411-425.

Micklem, D. R., Adams, J., Grunert, S. and St Johnston, D. (2000). Distinct roles of two conserved Staufen domains in oskar mRNA localization and translation. *Embo J* 19, 1366-77.

Miller, A. S., Cottam, D. M., and Milner, M. J. (2000a). Adhesion of Drosophila imaginal disc cells in vitro. In Vitro Cell Dev Biol Anim *36*, 174-179.

Miller, A. S., Cottam, D. M., and Milner, M. J. (2000b). Cell-cell and cell-substrate adhesion in cultured Drosophila imaginal disc cells. In Vitro Cell Dev Biol Anim *36*, 180-187.

Mingle, L. A., Okuhama, N. N., Shi, J., Singer, R. H., Condeelis, J. and Liu, G. (2005). Localization of all seven messenger RNAs for the actin-polymerization nucleator Arp2/3 complex in the protrusions of fibroblasts. *J Cell Sci* 118, 2425-33.

Morris, R. L. and Scholey, J. M. (1997). Heterotrimeric kinesin-II is required for the assembly of motile 9+2 ciliary axonemes on sea urchin embryos. *J Cell Biol* 138, 1009-22.

Morris, R. L. and Hollenbeck, P. J. (1995). Axonal transport of mitochondria along microtubules and F-actin in living vertebrate neurons. *J Cell Biol* 131, 1315-26.

Mosquera, L., Forristall, C., Zhou, Y. and King, M. L. (1993). A mRNA localized to the vegetal cortex of Xenopus oocytes encodes a protein with a nanos-like zinc finger domain. ***Development*** **117, 377-86.**

Mowry, K. L. and Melton, D. A. (1992). Vegetal messenger RNA localization directed by a 340-nt RNA sequence element in Xenopus oocytes. ***Science*** **255, 991-4.**

Munchow, S., Sauter, C. and Jansen, R. P. (1999). Association of the class V myosin Myo4p with a localised messenger RNA in budding yeast depends on She proteins. ***J Cell Sci*** **112, 1511-8.**

Ross, J. L., K. Wallace, et al. (2006). "Processive bidirectional motion of dynein-dynactin complexes in vitro." **Nat Cell Biol** **8(6): 562-70.**

Murata, Y. and Wharton, R. P. (1995). Binding of pumilio to maternal hunchback mRNA is required for posterior patterning in Drosophila embryos. ***Cell*** **80, 747-56.**

Muresan, V., Stankewich, M. C., Steffen, W., Morrow, J. S., Holzbaur, E. L. and Schnapp, B. J. (2001). Dynactin-Dependent, Dynein-Driven Vesicle Transport in the Absence of Membrane Proteins. A Role for Spectrin and Acidic Phospholipids. ***Mol Cell*** **7, 173-183.**

Murray, J. W., Bananis, E. and Wolkoff, A. W. (2000). Reconstitution of ATP-dependent movement of endocytic vesicles along microtubules in vitro: an oscillatory bidirectional process. ***Mol Biol Cell*** **11, 419-33.**

Nascimento, A. A., Roland, J. T. and Gelfand, V. I. (2003). Pigment cells: a model for the study of organelle transport. ***Annu Rev Cell Dev Biol*** **19, 469-91.**

Navarro, C., Puthalakath, H., Adams, J. M., Strasser, A. and Lehmann, R. (2004). Egalitarian binds dynein light chain to establish oocyte polarity and maintain oocyte fate. ***Nat Cell Biol*** **6, 427-35.**

Neuman-Silberberg, F. S. and Schüpbach, T. (1993). The ***Drosophila*** **dorsoventral patterning gene** ***gurken*** **produces a dorsally localized RNA and encodes a TGF alpha-like protein.** ***Cell*** **75, 165-174.**

Niessing, D., Huttelmaier, S., Zenklusen, D., Singer, R. H., and Burley, S. K. (2004). She2p is a novel RNA binding protein with a basic helical hairpin motif. Cell ***119*****, 491-502.**

Norvell, A., Kelley, R. L., Wehr, K. and Schüpbach, T. (1999). Specific isoforms of Squid, a ***Drosophila*** **hnRNP, perform distinct roles in** ***gurken*** **localization during oogenesis.** ***Genes Dev*** **13, 864-876.**

Okita, T. W. and Choi, S. B. (2002). mRNA localization in plants: targeting to the cell's cortical region and beyond. ***Curr Opin Plant Biol*** **5, 553-9.**

Palacios, I. M. and Johnston, D. S. (2001). Getting the message across: the intracellular localization of mRNAs in higher eukaryotes. ***Annu Rev Cell Dev Biol*** **17, 569-614.**

Park, J. W., Parisky, K., Celotto, A. M., Reenan, R. A., and Graveley, B. R. (2004). Identification of alternative splicing regulators by RNA interference in Drosophila. Proc Natl Acad Sci U S A ***101*****, 15974-15979.**

Peel, D. J., Johnson, S. A., and Milner, M. J. (1990). The ultrastructure of imaginal disc cells in primary cultures and during cell aggregation in continuous cell lines. Tissue Cell ***22*****, 749-758.**

Peri, F. and Roth, S. (2000). Combined activities of Gurken and decapentaplegic specify dorsal chorion structures of the Drosophila egg. ***Development*** **127, 841-50.**

Pilling, A. D., Horiuchi, D., Lively, C. M. and Saxton, W. M. (2006). Kinesin-1 and Dynein are the primary motors for fast transport of mitochondria in Drosophila motor axons. ***Mol Biol Cell*** **17, 2057-68.**

Plough, H. H. and Ives, P. T. (1934). Heat Induced Mutations in Drosophila. ***Proc Natl Acad Sci U S A*** **20, 268-273.**

Pollock, N., de Hostos, E. L., Turck, C. W. and Vale, R. D. (1999). Reconstitution of membrane transport powered by a novel dimeric kinesin motor of the Unc104/KIF1A family purified from Dictyostelium. ***J Cell Biol*** **147, 493-506.**

Prahlad, V., Helfand, B. T., Langford, G. M., Vale, R. D. and Goldman, R. D. (2000). Fast transport of neurofilament protein along microtubules in squid axoplasm. ***J Cell Sci*** **113, 3939-46.**

Prahlad, V., Yoon, M., Moir, R. D., Vale, R. D. and Goldman, R. D. (1998). Rapid movements of vimentin on microtubule tracks: kinesin-dependent assembly of intermediate filament networks. ***J Cell Biol*** **143, 159-70.**

Presley, J. F., Cole, N. B., Schroer, T. A., Hirschberg, K., Zaal, K. J. and Lippincott-Schwartz, J. (1997). ER-to-Golgi transport visualized in living cells. ***Nature*** **389, 81-5.**

Raff, J. W., Whitfield, W. G. F. and Glover, D. M. (1990). 2 Distinct Mechanisms Localize Cyclin-B Transcripts In Syncytial Drosophila Embryos. ***Development*** **110, 1249-1261.**

Ray, K., Perez, S. E., Yang, Z., Xu, J., Ritchings, B. W., Steller, H. and Goldstein, L. S. (1999). Kinesin-II is required for axonal transport of choline acetyltransferase in Drosophila. *J Cell Biol* 147, 507-18.

Reck-Peterson, S. L., Provance, D. W., Jr., Mooseker, M. S. and Mercer, J. A. (2000). Class V myosins. *Biochim Biophys Acta* 1496, 36-51.

Riechmann, V. and Ephrussi, A. (2001). Axis formation during Drosophila oogenesis. *Curr Opin Genet Dev* 11, 374-83.

Rogers, S. L., Tint, I. S., Fanapour, P. C. and Gelfand, V. I. (1997). Regulated bidirectional motility of melanophore pigment granules along microtubules in vitro. *Proc Natl Acad Sci U S A* 94, 3720-5.

Rogers, S. L., Rogers, G. C., Sharp, D. J., and Vale, R. D. (2002). Drosophila EB1 is important for proper assembly, dynamics, and positioning of the mitotic spindle. J Cell Biol *158*, 873-884.

Ross, A. F., Oleynikov, Y., Kislauskis, E. H., Taneja, K. L. and Singer, R. H. (1997). Characterization of a beta-actin mRNA zipcode-binding protein. *Molecular and Cellular Biology* 17, 2158-2165.

Ross, J. L., Wallace, K., Shuman, H., Goldman, Y. E., and Holzbaur, E. L. (2006). Processive bidirectional motion of dynein-dynactin complexes in vitro. Nat Cell Biol *8*, 562-570.

Roth, S., Neuman-Silberberg, F. S., and Schüpbach, T. (1995). Dorsoventral signaling in *Drosophila* oogenesis. J Cell Biochem *19A*, 326.

Rubin, G. M., Hong, L., Brokstein, P., Evans-Holm, M., Frise, E., Stapleton, M., and Harvey, D. A. (2000). A Drosophila complementary DNA resource. Science *287*, 2222--2224.

Sablin, E. P., Case, R. B., Dai, S. C., Hart, C. L., Ruby, A., Vale, R. D. and Fletterick, R. J. (1998). Direction determination in the minus-end-directed kinesin motor ncd. *Nature* 395, 813-6.

Sanson, B. (2001). Generating patterns from fields of cells. Examples from Drosophila segmentation. *EMBO Rep* 2, 1083-8.

Schliwa, M. and Woehlke, G. (2003). Molecular motors. *Nature* 422, 759-65.

Schuldt, A. J., Adams, J. H., Davidson, C. M., Micklem, D. R., Haseloff, J., St Johnston, D. and Brand, A. H. (1998). Miranda mediates asymmetric protein and RNA localization in the developing nervous system. *Genes Dev* 12, 1847-57.

Seleme Mdel, C., Disson, O., Robin, S., Brun, C., Teninges, D., and Bucheton, A. (2005). In vivo RNA localization of I factor, a non-LTR retrotransposon, requires a cis-acting signal in ORF2 and ORF1 protein. Nucleic Acids Res *33*, 776-785.

Semotok, J. L., Cooperstock, R. L., Pinder, B. D., Vari, H. K., Lipshitz, H. D. and Smibert, C. A. (2005). Smaug recruits the CCR4/POP2/NOT deadenylase complex to trigger maternal transcript localization in the early Drosophila embryo. *Curr Biol* 15, 284-94.

Sen, J., Goltz, J. S., Stevens, L., and Stein, D. (1998). Spatially restricted expression of pipe in the Drosophila egg chamber defines embryonic dorsal-ventral polarity. Cell *95*, 471-481.

Serano, T. L., and Cohen, R. S. (1995). A small predicted stem-loop structure mediates oocyte localization of Drosophila K10 mRNA. Development *121*, 3809-3818.

Serbus, L. R., Cha, B. J., Theurkauf, W. E. and Saxton, W. M. (2005). Dynein and the actin cytoskeleton control kinesin-driven cytoplasmic streaming in Drosophila oocytes. *Development* 132, 3743-52.

Shakir, M. A., Fukushige, T., Yasuda, H., Miwa, J. and Siddiqui, S. S. (1993). C. elegans osm-3 gene mediating osmotic avoidance behaviour encodes a kinesin-like protein. *Neuroreport* 4, 891-4.

Shen, C. P., Knoblich, J. A., Chan, Y. M., Jiang, M. M., Jan, L. Y. and Jan, Y. N. (1998). Miranda as a multidomain adapter linking apically localized inscuteable and basally localized Staufen and Prospero during asymmetric cell division in Drosophila. *Genes & Development* 12, 1837-1846.

Simmonds, A. J., dosSantos, G., Livne-Bar, I. and Krause, H. M. (2001). Apical Localization of *wingless* Transcripts is Required for Wingless Signaling. *Cell* 105, 197–207.

Sims, D., B. Bursteinas, et al. (2006). "FLIGHT: database and tools for the integration and cross-correlation of large-scale RNAi phenotypic datasets." Nucleic Acids Res 34(Database issue): D479-83.

Smith, G. A., Gross, S. P. and Enquist, L. W. (2001). Herpesviruses use bidirectional fast-axonal transport to spread in sensory neurons. *Proc Natl Acad Sci U S A* 98, 3466-70.

Stapleton, M., Liao, G., Brokstein, P., Hong, L., Carninci, P., Shiraki, T., Hayashizaki, Y., Champe, M., Pacleb, J., Wan, K., *et al.* (2002). The Drosophila gene collection: identification of putative full-length cDNAs for 70% of D. melanogaster genes. Genome Res *12*, 1294-1300.

St Johnston, D., Beuchle, D. and Nüsslein-Volhard, C. (1991). Staufen, a Gene Required to Localize Maternal Rnas In the Drosophila Egg. ***Cell*** **66, 51-63.**

Suh, M. R., Han, J. W., No, Y. R. and Lee, J. (2002). Transient concentration of a gamma-tubulin-related protein with a pericentrin-related protein in the formation of basal bodies and flagella during the differentiation of Naegleria gruberi. ***Cell Motil Cytoskeleton*** **52, 66-81.**

Suomalainen, M., Nakano, M. Y., Keller, S., Boucke, K., Stidwill, R. P. and Greber, U. F. (1999). Microtubule-dependent plus- and minus end-directed motilities are competing processes for nuclear targeting of adenovirus. ***J Cell Biol*** **144, 657-72.**

Swaroop, A., Paco-Larson, M. L. and Garen, A. (1985). Molecular genetics of a transposon-induced dominant mutation in the Drosophila locus Glued. ***Proc Natl Acad Sci U S A*** **82, 1751-5.**

Takeda, S., Yamazaki, H., Seog, D. H., Kanai, Y., Terada, S. and Hirokawa, N. (2000). Kinesin superfamily protein 3 (KIF3) motor transports fodrin-associating vesicles important for neurite building. ***J Cell Biol*** **148, 1255-65.**

Takizawa, P. A., and Vale, R. D. (2000). The myosin motor, Myo4p, binds Ash1 mRNA via the adapter protein, She3p. Proc Natl Acad Sci U S A ***97*****, 5273-5278.**

Takizawa, P. A., Sil, A., Swedlow, J. R., Herskowitz, I. and Vale, R. D. (1997). Actin-dependent localization of an RNA encoding a cell-fate determinant in yeast. ***Nature*** **389, 90-3.**

Tanaka, Y., Kanai, Y., Okada, Y., Nonaka, S., Takeda, S., Harada, A. and Hirokawa, N. (1998). Targeted disruption of mouse conventional kinesin heavy chain, kif5B, results in abnormal perinuclear clustering of mitochondria. ***Cell*** **93, 1147-58.**

Tekotte, H. and Davis, I. (2002). Intracellular mRNA localization: motors move messages. ***Trends Genet*** **18, 636-42.**

Theurkauf, W. E., Smiley, S., Wong, M. L. and Alberts, B. M. (1992). Reorganization of the cytoskeleton during ***Drosophila*** **oogenesis - implications for axis specification and intercellular transport.** ***Development*** **115, 923-936.**

Thio, G. L., Ray, R. P., Barcelo, G., and Schupbach, T. (2000). Localization of gurken RNA in Drosophila oogenesis requires elements in the 5' and 3' regions of the transcript. Dev Biol ***221*****, 435-446.**

Tiedge, H., Fremeau, R. T., Jr., Weinstock, P. H., Arancio, O. and Brosius, J. (1991). Dendritic location of neural BC1 RNA. ***Proc Natl Acad Sci U S A*** **88, 2093-7.**

Tomancak, P., Beaton, A., Weiszmann, R., Kwan, E., Shu, S., Lewis, S. E., Richards, S., Ashburner, M., Hartenstein, V., Celniker, S. E., and Rubin, G. M. (2002). Systematic determination of patterns of gene expression during Drosophila embryogenesis. Genome Biol *3*, RESEARCH0088.

Tomishige, M., Klopfenstein, D. R. and Vale, R. D. (2002). Conversion of Unc104/KIF1A kinesin into a processive motor after dimerization. ***Science*** **297, 2263-7.**

Trapp, B. D., Moench, T., Pulley, M., Barbosa, E., Tennekoon, G. and Griffin, J. (1987). Spatial segregation of mRNA encoding myelin-specific proteins. ***Proc Natl Acad Sci U S A*** **84, 7773-7.**
Vale, R. D. (2003). The molecular motor toolbox for intracellular transport. ***Cell*** **112, 467-80.**

Vale, R. D. and Milligan, R. A. (2000). The way things move: looking under the hood of molecular motor proteins. ***Science*** **288, 88-95.**

Vale, R. D., Soll, D. R. and Gibbons, I. R. (1989). One-dimensional diffusion of microtubules bound to flagellar dynein. ***Cell*** **59, 915-25.**

Valetti, C., Wetzel, D. M., Schrader, M., Hasbani, M. J., Gill, S. R., Kreis, T. E. and Schroer, T. A. (1999). Role of dynactin in endocytic traffic: effects of dynamitin overexpression and colocalization with CLIP-170. ***Mol Biol Cell*** **10, 4107-20.**

Vallee, R. B., Williams, J. C., Varma, D. and Barnhart, L. E. (2004). Dynein: An ancient motor protein involved in multiple modes of transport. ***J Neurobiol*** **58, 189-200.**

Van De Bor, V., Hartswood, E., Jones, C., Finnegan, D. and Davis, I. (2005). gurken and the I factor retrotransposon RNAs share common localization signals and machinery. ***Dev Cell*** **9, 51-62.**

Vaughan, K. T., Holzbaur, E. L. and Vallee, R. B. (1995). Subcellular targeting of the retrograde motor cytoplasmic dynein. ***Biochem Soc Trans*** **23, 50-4.**

Wacker, I., Kaether, C., Kromer, A., Migala, A., Almers, W. and Gerdes, H. H. (1997). Microtubule-dependent transport of secretory vesicles visualized in real time with a GFP-tagged secretory protein. ***J Cell Sci*** **110 (Pt 13), 1453-63.**

Wang, Z., Khan, S. and Sheetz, M. P. (1995). Single cytoplasmic dynein molecule movements: characterization and comparison with kinesin. *Biophys J* 69, 2011-23.

Wang, Z. and Sheetz, M. P. (1999). One-dimensional diffusion on microtubules of particles coated with cytoplasmic dynein and immunoglobulins. *Cell Struct Funct* 24, 373-83.

Waterman-Storer, C. M., Karki, S. and Holzbaur, E. L. (1995). The p150/Glued component of the dynactin complex binds to both microtubules and the actin-related protein centractin (Arp-1). *Proc Natl Acad Sci U S A* 92, 1634-8.

Waterman-Storer, C. M., Karki, S. B., Kuznetsov, S. A., Tabb, J. S., Weiss, D. G., Langford, G. M. and Holzbaur, E. L. (1997). The interaction between cytoplasmic dynein and dynactin is required for fast axonal transport. *Proc Natl Acad Sci U S A* 94, 12180-5.

Wei, Q., Marchler, G., Edington, K., Karsch-Mizrachi, I., and Paterson, B. M. (2000). RNA interference demonstrates a role for nautilus in the myogenic conversion of Schneider cells by daughterless. Dev Biol *228*, 239-255.

Wells, A. L., Lin, A. W., Chen, L. Q., Safer, D., Cain, S. M., Hasson, T., Carragher, B. O., Milligan, R. A. and Sweeney, H. L. (1999). Myosin VI is an actin-based motor that moves backwards. *Nature* 401, 505-8.

Welte, M. A., Gross, S. P., Postner, M., Block, S. M. and Wieschaus, E. F. (1998). Developmental regulation of vesicle transport in Drosophila embryos: forces and kinetics. *Cell* 92, 547-57.

Wharton, R. P. and Struhl, G. (1991). RNA regulatory elements mediate control of Drosophila body pattern by the posterior morphogen nanos. *Cell* 67, 955-67.

Wilkie, G. S. and Davis, I. (2001). *Drosophila wingless* and pair-rule transcripts localize apically by dynein-mediated transport of RNA particles. *Cell* 105, 209-219.

Wojcik, E. J., Glover, D. M., and Hays, T. S. (2000). The SCF ubiquitin ligase protein slimb regulates centrosome duplication in Drosophila. Curr Biol *10*, 1131-1134.

Wu, X. and Hammer, J. A., 3rd. (2000). Making sense of melanosome dynamics in mouse melanocytes. *Pigment Cell Res* 13, 241-7.

Zhang, J., Houston, D. W., King, M. L., Payne, C., Wylie, C. and Heasman, J. (1998). The role of maternal VegT in establishing the primary germ layers in Xenopus embryos. *Cell* 94, 515-24.

MOVIE LEGENTS

Movie 3.2.1: in vitro transcribed, fluorescently labelled *ftz* RNA moves bidirectionally in wild type syncytial blastoderm embryos. The apical side of the embryo is up and the basal is down. A relatively smooth minus run is marked in red and another minus run, interrupted by pauses and shorter or longer backsteps is marked in green. Movie is speeded up approximately 2.8 times and represents 80sec.

Movie 3.2.2: trail movie of a selected region of movie 1. Most of the *ftz* RNA particles shown move towards the minus ends of MTs. Two particles display plus runs. Movie is speeded up approximately 2.8 times.

Movie 3.2.3: Another example of bidirectional runs in wid type embryos. The apical side of the embryo is up and the basal is down. A smooth minus run is marked in red and another minus run, interrupted by pauses and shorter or longer backsteps is marked in green. Movie is speeded up approximately 1.5 times.

Movie 3.2.4: in vitro transcribed, fluorescently labelled *ftz* RNA moves bidirectionally in Khc^{27} syncytial blastoderm embryos. The apical side of the embryo is up and the basal is down.

Movie 3.2.5: in vitro transcribed, fluorescently labelled *ftz* RNA moves bidirectionally in $KLP64D^{k1}$ syncytial blastoderm embryos. The apical side of the embryo is up and the basal is down. Movie is speeded up approximately 1.5 times.

Movie 3.2.6: : in vitro transcribed, fluorescently labelled *ftz* RNA moves more frequently towards the plus end of MTs in $Glued^{1}$ syncytial blastoderm embryos. The apical side of the embryo is up and the basal is down.

Movie 4.1.1: in vitro transcribed, fluorescently labelled *slmb* RNA forms particles and moves on directed paths towards the apical cytoplasm of blastoderm embryos. The apical side of the embryo is up and the basal is down.

Movie 4.2.2: in vitro transcribed, fluorescently labelled *Dcp-1* RNA forms particles and displays long, directed runs from the site of injection towards the apical cytoplasm of blastoderm embryos, but accumulates at the basal side of the nuclei. The apical side of the embryo is up and the basal is down.

Movie 4.2.3: in vitro transcribed, fluorescently labelled non-localising transcripts form particles and move in a directed way. The apical side of the embryo is up and the basal is down.